NASA Technical Paper 1227

A Numerical Solution of the Navier-Stokes Equations for Chemically Nonequilibrium, Merged Stagnation Shock Layers on Spheres and Two-Dimensional Cylinders in Air

Kenneth D. Johnston and William L. Hendricks

MAY 1978

NASA

NASA Technical Paper 1227

A Numerical Solution of the Navier-Stokes Equations for Chemically Nonequilibrium, Merged Stagnation Shock Layers on Spheres and Two-Dimensional Cylinders in Air

Kenneth D. Johnston
George C. Marshall Space Flight Center
Marshall Space Flight Center, Alabama

and

William L. Hendricks
Lockheed Huntsville Research and Engineering Center
Huntsville, Alabama

NASA
National Aeronautics
and Space Administration

Scientific and Technical
Information Office

1978

ACKNOWLEDGMENT

The authors appreciate the assistance of Dr. A. C. Jain who was a Senior Resident Research Associate at Marshall Space Flight Center in 1973-74. Dr. Jain stimulated interest in this problem and provided the computer program which he and his colleagues had formulated at the Indian Institute of Technology. Also, Mr. Larry Donehoo of Marshall Space Flight Center provided an interpolation computer subroutine which was used in the viscosity computations.

TABLE OF CONTENTS

LIST OF ILLUSTRATIONS

LIST OF ILLUSTRATIONS (Concluded)

LIST OF TABLES

DEFINITION OF SYMBOLS

Symbol	Definition
$\bar{C}_p$	specific heat at constant pressure
$\bar{C}_v$	specific heat at constant volume
C_H	heat transfer coefficient, $\bar{q}_w / \frac{1}{2} \bar{\rho}_\infty \bar{V}_\infty^3$
D_{ij}	binary diffusion coefficient for species pair i and j
$\bar{e}_i$	specific internal energy of species i
$\vec{\bar{f}}_i$	body force on species i per unit mass of species i
$\bar{h}$	specific enthalpy of mixture
$\bar{h}_i$	specific enthalpy of species i
$\bar{k}$	coefficient of thermal conductivity
k_{fj}	forward reaction rate for jth reaction
k_{rj}	reverse reaction rate for jth reaction
$K_{n\infty}$	freestream Knudsen number, $\bar{\lambda}_\infty / \bar{r}_b$
K^2	hypersonic similarity parameter [see equation (62)]
Le_{ij}	Lewis number of species pair i and j, $\bar{\rho}\, D_{ij}\, \bar{C}_p / \bar{k}$
M_∞	freestream Mach number
M	indicates a catalyst
NS	number of species in gas mixture
n	dimensionless radial distance from the body, $(\bar{r} - \bar{r}_b) / \bar{r}_b$
n_∞	dimensionless radial distance from body to freestream edge (shock layer thickness)

DEFINITION OF SYMBOLS (Continued)

Symbol	Definition
$\bar{P}$	pressure
Pr	Prandtl number, $\bar{C}_p \bar{\mu}/\bar{k}$
$\vec{\bar{q}}$	heat flux vector
$\bar{q}_w$	heat flux to wall
$\bar{r}$	radial distance from body center (see Fig. 1)
$\bar{r}_b$	radius of body
$\bar{R}_i$	gas constant of species i
$\bar{R}$	gas constant of mixture
$\bar{\mathcal{R}}$	universal gas constant
$Re_{0\infty}$	freestream stagnation Reynolds number, $\bar{\rho}_\infty \bar{V}_\infty \bar{r}_b/\bar{\mu}_{0\infty}$
$\bar{S}_{ij}$	collision cross section for particle i with particle j
Sc_{ij}	Schmidt number for species pair i and j, $\bar{\mu}/\bar{\rho}\ \bar{D}_{ij}$
$\bar{T}$	temperature
$\bar{T}_{0\infty}$	freestream stagnation temperature
$\bar{t}$	time
$\bar{u}$	velocity component parallel to body surface (see Fig. 1)
$\bar{v}$	velocity component normal to body surface (see Fig. 1)
$\bar{v}$	specific volume of gas mixture
$\vec{\bar{v}}$	velocity vector

DEFINITION OF SYMBOLS (Continued)

Symbol	Definition
$\bar{V}_\infty$	freestream speed
$\vec{\bar{V}}_i$	diffusion velocity vector of species i
W_i	molecular weight of species i
W	equivalent molecular weight of mixture
$\dot{\bar{w}}_i$	net mass production rate of species i per unit volume
Y_i	mass fraction of species i
γ	ratio of specific heats, C_p/C_v
γ_i	recombination coefficient for species i
η	dimensionless radial distance from body surface [see Fig. 1 and equation (24)]
Θ_{vi}	characteristic temperature for vibration of diatomic species i
θ	circumferential angle (see Fig. 1)
$\bar{\lambda}_i$	mean free path of species i
$\bar{\lambda}_\infty$	freestream mean free path
$\bar{\mu}$	coefficient of absolute viscosity
$\bar{\mu}_{SU}$	Sutherland coefficient of absolute viscosity
$\bar{\mu}_{0\infty}$	coefficient of absolute viscosity at $\bar{T}_{0\infty}$
$\bar{\rho}$	density of mixture
σ	molecule-surface accommodation coefficient

DEFINITION OF SYMBOLS (Concluded)

Symbol	Definition
$\vec{\bar{\tau}}$	viscous stress tensor
$\bar{\Phi}$	viscous dissipation function

Subscripts

i, j	species indices
0 (zero)	stagnation condition
s	edge of Knudsen layer, slip
sh	conditions behind normal shock
w	wall
∞	freestream property

Superscript

$(\bar{\ })$	dimensional quantity

TECHNICAL PAPER

A NUMERICAL SOLUTION OF THE NAVIER-STOKES EQUATIONS FOR CHEMICALLY NONEQUILIBRIUM, MERGED STAGNATION SHOCK LAYERS ON SPHERES AND TWO-DIMENSIONAL CYLINDERS IN AIR

SUMMARY

The complete Navier-Stokes equations are solved along the stagnation streamline in merged stagnation shock layers on spheres and two-dimensional cylinders using an iterative finite-difference numerical procedure known as the accelerated successive replacement method. The fluid medium is chemically reacting air consisting of seven species. Velocity components, thermodynamic properties, species mass fractions, and wall heat transfer rates are computed. This report is intended as an explanation of the method and as a user's manual for the computer program.

I. INTRODUCTION

An aerospace vehicle ascending or descending through the Earth's atmosphere traverses several flow regimes from the continuum boundary layer regime at low altitudes, through the transitional regime at intermediate altitudes, to the free molecular regime at very high altitudes. The character of the flow field changes drastically from the boundary layer regime to the free molecular regime, and no single computational approach is valid throughout this range. The broad transitional regime may be divided into several subregimes as suggested by Hayes and Probstein [1]. Consider the typical spherical nose of an aerospace vehicle. In the boundary layer regime viscous effects are primarily confined to a thin boundary layer, the bow shock can be treated as a discontinuity, and a region of inviscid flow exists between the shock and the boundary layer. However with increasing altitude, the shock wave and boundary layer thicken and eventually merge into a single viscous layer called the shock layer. The flow regime in which this occurs is called the fully merged shock layer regime which is the condition treated in this report.

At the great speed that a vehicle reenters the atmosphere, the temperature near the body becomes extremely high, especially in the stagnation region. Therefore, the air in the shock layer dissociates and ionizes. For an accurate description of the flow field, one must account for these real gas effects. Also an accurate estimate of the ionization level is needed for radio communication purposes. Therefore, a flow field model including finite rate chemistry is required.

This report describes a method for computing flow properties along the stagnation streamlines of a sphere and a circular cylinder transverse to the flow. Heat transfer rates are computed at the body surface. Although this method is limited to the stagnation region, it still provides valuable design information because maximum heating rates usually occur at the nose. The computational method was developed by Jain and Adimurthy [2] for an ideal gas. The method uses the full Navier-Stokes equations to describe the flow in the entire shock layer from the surface to the freestream. The boundary conditions at the wall are provided by slip velocity and temperature jump equations. Using the concept of local similarity, the governing equations are reduced to a system of nonlinear, coupled ordinary differential equations. Numerical solutions are obtained for points on the stagnation streamline using an iterative finite-difference procedure known as the accelerated successive replacement method. The applicability of this approach and the failure of thin-layer theories for the merged shock layer regime is discussed in Reference 2. Nonequilibrium chemical reactions were included in this method by Kumar and Jain [3] using an air model with seven species and six reactions. Hendricks [4] developed surface slip velocity and temperature jump equations for a multi-component gas, including the effects of wall catalysis, to use with this model. Additional modifications have been made in this report, principally by including the two-dimensional cylindrical geometry and using a multi-component gas model to compute viscosity.

II. ANALYSIS

A. Formulation of the Problem

1. Approach. In the present analysis the full Navier-Stokes equations, with nonequilibrium chemistry, are solved through the merged stagnation shock layer from the freestream to the body. The slip conditions at the gas-wall interface include the effect of wall catalysis and a multicomponent, nonequilibrium gas flow.

The thin shock layer assumption is not made in the present analysis. The full Navier-Stokes equations with chemically-reacting, nonequilibrium air are solved through the merged shock and boundary layer. This allows the shock wave to develop within the computational domain. A seven species air model is used. The species considered are N_2, O_2, NO, N, O, NO^+, and e^-. For air dissociation and ionization, the rate expressions recommended by Wray [5] are adopted. Prandtl number, Pr, and Lewis number, Le_{ij}, are taken to be 0.75 and 1.4, respectively, for the cases computed in this report. The viscosity of dissociated and ionized air is obtained from a simple summation formula for a mixture of hard spherical molecules using Hansen's collision cross sections [6].

Solutions are obtained by using the local similarity concept to reduce the governing equations to a set of nonlinear, coupled, ordinary differential equations. This set of equations is integrated using a finite difference method known as the accelerated successive replacement method. It is important to note that the first order local similarity assumption is a good approximation near the stagnation streamline, at least for $Re_{sh} \geq 10$ [7]. Reference 7 gives a thorough discussion of local similarity.

2. Governing Equations. The nonlinear, coupled ordinary differential equations governing the flow of a multicomponent gas near the stagnation streamlines of spheres and two-dimensional cylinders are presented. The coordinate system employed is shown in Figure 1a.

a. Basic Equations. The basic conservation equations and the ideal gas equation of state for a multicomponent, reacting gas mixture are as follows [8]:

Global Continuity (of all species):

$$\frac{\partial \bar{\rho}}{\partial \bar{t}} + \vec{\nabla} \cdot (\bar{\rho} \vec{\bar{v}}) = 0 \quad . \tag{1}$$

Species Continuity:

$$\bar{\rho} \frac{D Y_i}{D\bar{t}} = \dot{\bar{w}}_i - \vec{\nabla} \cdot (\bar{\rho} Y_i \vec{\bar{V}}_i) \qquad i = 1, \ldots, NS \quad , \tag{2}$$

where NS = number of species in mixture (no summation on repeated indices).

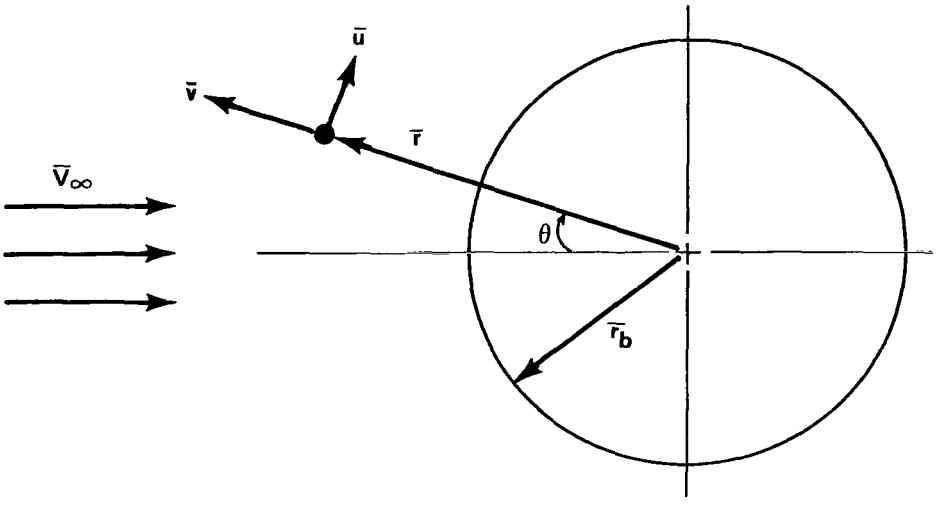

Figure 1a. Dimensional coordinate system.

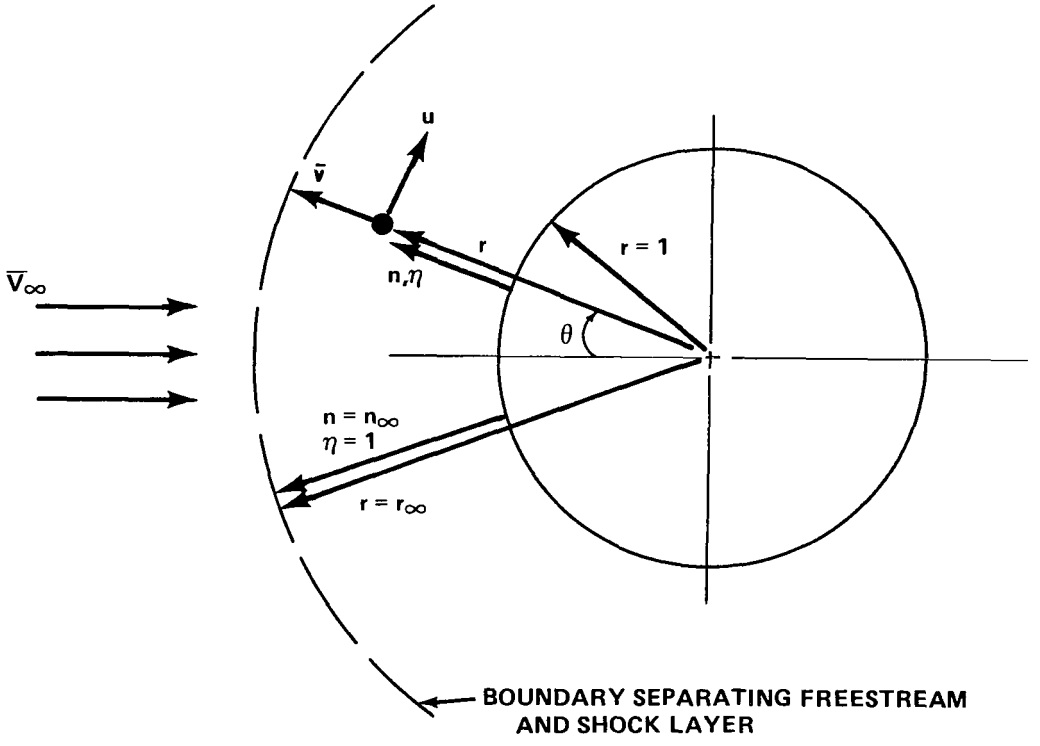

Figure 1b. Dimensionless coordinate system.

Figure 1. Coordinate systems.

Momentum:

$$\bar{\rho} \frac{D \vec{\bar{v}}}{D\bar{t}} = - \vec{\nabla} \bar{P} - \vec{\nabla} \cdot \vec{\vec{\bar{\tau}}} + \bar{\rho} \sum_{i=1}^{NS} Y_i \vec{\bar{f}}_i \quad . \tag{3}$$

The second order tensor, $\vec{\vec{\bar{\tau}}}$, is the viscous stress tensor and $\vec{\bar{f}}_i$ is the body force per unit mass of species i.

Enthalpy:

$$\bar{\rho} \frac{D\bar{h}}{D\bar{t}} = \frac{D\bar{P}}{D\bar{t}} + \bar{\Phi} - \vec{\nabla} \cdot \vec{\bar{q}} \quad . \tag{4}$$

The quantity $\bar{\Phi}$ is the viscous dissipation function and $\vec{\bar{q}}$ is the heat flux vector.

State:

$$\bar{P} = \bar{\rho} \bar{\mathcal{R}} \bar{T} \sum_{i=1}^{NS} \frac{Y_i}{W_i} \quad . \tag{5}$$

b. Nondimensional Equations. The basic equations are put in nondimensional form by introducing dimensionless variables as follows:

$$u = \bar{u}/\bar{V}_\infty \quad ,$$

$$v = \bar{v}/\bar{V}_\infty \quad ,$$

$$\rho = \bar{\rho}/\bar{\rho}_\infty \quad ,$$

$$T = \bar{T}/\bar{T}_{0\infty} \quad ,$$

$$P = \bar{P}/\bar{\rho}_\infty \bar{V}_\infty^2 \quad ,$$

$$h = \bar{h}/\bar{V}_\infty^2 \quad ,$$

$$\mu = \bar{\mu}/\bar{\mu}_{0\infty} \quad ,$$

$$r = \bar{r}/\bar{r}_b \quad ,$$

$$\dot{w}_i = \dot{\bar{w}}_i/(\bar{\rho}_\infty \bar{V}_\infty/\bar{r}_b) \quad ,$$

where $\bar{r}_b$ is the radius of the body, $\bar{T}_{0\infty}$ is the freestream stagnation temperature, and $\bar{\mu}_{0\infty}$ is the coefficient of absolute viscosity evaluated at $\bar{T}_{0\infty}$. The nondimensional similarity parameters

$$Re_{0\infty} = \bar{\rho}_\infty \bar{V}_\infty \bar{r}_b/\bar{\mu}_{0\infty} \quad ,$$

$$Pr = \bar{C}_p \bar{\mu}/\bar{k} \quad ,$$

$$Sc_{ij} = \bar{\mu}/\bar{\rho} \bar{D}_{ij} \quad ,$$

and

$$Le_{ij} = \bar{k}/\bar{\rho} \bar{C}_p \bar{D}_{ij}$$

are also introduced. The basic equations are then simplified by assuming steady flow and Newtonian fluid, neglecting body forces, viscous diffusion stresses, thermal radiation, and thermal diffusion, and using Fick's Law of Diffusion. The equations are presented in cylindrical and spherical coordinates below.

Cylindrical Coordinates:

Global Continuity:

$$\frac{\partial}{\partial r}(\rho r v) + \frac{\partial}{\partial \theta}(\rho u) = 0 \quad . \tag{6}$$

Species Continuity:

$$\rho\left(v\frac{\partial Y_i}{\partial r} + \frac{u}{r}\frac{\partial Y_i}{\partial \theta}\right) = \dot{w}_i + \frac{1}{Re_{0\infty}}\frac{1}{r}\left[\frac{\partial}{\partial r}\left(\frac{\mu r}{Sc}\frac{\partial Y_i}{\partial r}\right) + \frac{\partial}{\partial \theta}\left(\frac{\mu}{Sc\, r}\frac{\partial Y_i}{\partial \theta}\right)\right] . \qquad i = 1, \ldots, NS \tag{7}$$

Transverse Momentum (θ Direction):

$$\rho\left(v\frac{\partial u}{\partial r} + \frac{u}{r}\frac{\partial u}{\partial \theta} + \frac{vu}{r}\right) = -\frac{1}{r}\frac{\partial P}{\partial \theta} + \frac{1}{Re_{0\infty}}\left[\frac{1}{r^2}\frac{\partial}{\partial r}\left\{r^2\mu\left[r\frac{\partial}{\partial r}\left(\frac{u}{r}\right) + \frac{1}{r}\frac{\partial v}{\partial \theta}\right]\right\}\right.$$

$$\left. + \frac{1}{r}\frac{\partial}{\partial \theta}\left(\mu\left\{2\left(\frac{1}{r}\frac{\partial u}{\partial \theta} + \frac{v}{r}\right) - \frac{2}{3}\left[\frac{1}{r}\frac{\partial}{\partial r}(rv) + \frac{1}{r}\frac{\partial u}{\partial \theta}\right]\right\}\right)\right] . \tag{8}$$

Radial Momentum (r Direction):

$$\rho\left(v\frac{\partial v}{\partial r} + \frac{u}{r}\frac{\partial v}{\partial \theta} - \frac{u^2}{r}\right) = -\frac{\partial P}{\partial r} + \frac{1}{Re_{0\infty}}\left[\frac{1}{r}\frac{\partial}{\partial r}\left(r\mu\left\{2\frac{\partial v}{\partial r} - \frac{2}{3}\left[\frac{1}{r}\frac{\partial (rv)}{\partial r} + \frac{1}{r}\frac{\partial u}{\partial \theta}\right]\right\}\right)\right.$$

$$+ \frac{1}{r}\frac{\partial}{\partial \theta}\left\{\mu\left[r\frac{\partial}{\partial r}\left(\frac{u}{r}\right) + \frac{1}{r}\frac{\partial v}{\partial \theta}\right]\right\} - \frac{1}{r}\left(\mu\left\{2\left(\frac{1}{r}\frac{\partial u}{\partial \theta} + \frac{v}{r}\right)\right.\right.$$

$$\left.\left. - \frac{2}{3}\left[\frac{1}{r}\frac{\partial}{\partial r}(rv) + \frac{1}{r}\frac{\partial u}{\partial \theta}\right]\right\}\right)\Bigg] \quad . \tag{9}$$

Enthalpy:

$$\rho\left(v\frac{\partial h}{\partial r}+\frac{u}{r}\frac{\partial h}{\partial \theta}\right) = v\frac{\partial P}{\partial r}+\frac{u}{r}\frac{\partial P}{\partial \theta}+\frac{\mu}{Re_{0\infty}}\left[2\left\{\left(\frac{\partial v}{\partial r}\right)^2+\left(\frac{1}{r}\frac{\partial u}{\partial \theta}+\frac{v}{r}\right)^2\right\}\right.$$

$$\left.+\left(\frac{1}{r}\frac{\partial v}{\partial \theta}+\frac{\partial u}{\partial r}-\frac{u}{r}\right)^2\right]-\frac{2}{3}\frac{\mu}{Re_{0\infty}}\left[\frac{\partial v}{\partial r}+\frac{1}{r}\frac{\partial u}{\partial \theta}+\frac{v}{r}\right]^2$$

$$+\frac{1}{r\,Pr\,Re_{0\infty}}\left\{\frac{\partial}{\partial r}\left(r\mu\frac{\partial h}{\partial r}\right)+\frac{\partial}{\partial \theta}\left(\frac{\mu}{r}\frac{\partial h}{\partial \theta}\right)\right.$$

$$\left.+(Le-1)\frac{\partial}{\partial r}\left[\sum_{i=1}^{NS} r\mu h_i\frac{\partial Y_i}{\partial r}\right]+(Le-1)\frac{\partial}{\partial \theta}\left[\sum_{i=1}^{NS}\frac{\mu h_i}{r}\frac{\partial Y_i}{\partial \theta}\right]\right\} . \tag{10}$$

State:

$$P = \rho\,T\frac{\bar{\mathcal{R}}\bar{T}_{0\infty}}{\bar{V}_\infty^{\,2}}\sum_{i=1}^{NS}\frac{Y_i}{W_i} . \tag{11}$$

Spherical Coordinates:

Global Continuity:

$$\frac{1}{r}\frac{\partial}{\partial r}(\rho r^2 v)+\frac{1}{\sin\theta}\frac{\partial}{\partial \theta}(\rho u\sin\theta) = 0 . \tag{12}$$

Species Continuity:

$$\rho\left(v\frac{\partial Y_i}{\partial r}+\frac{u}{r}\frac{\partial Y_i}{\partial \theta}\right)=\dot{w}_i+\frac{1}{Re_{0\infty}}\frac{1}{r}\left[\frac{1}{r}\frac{\partial}{\partial r}\left(\frac{r^2\mu}{Sc}\frac{\partial Y_i}{\partial r}\right)+\frac{1}{\sin\theta}\frac{\partial}{\partial \theta}\left(\frac{\mu\sin\theta}{Sc\,r}\frac{\partial Y_i}{\partial \theta}\right)\right] \quad . \; i=1,\ldots,NS \quad (13)$$

Transverse Momentum (θ Direction):

$$\rho\left(v\frac{\partial u}{\partial r}+\frac{u}{r}\frac{\partial u}{\partial \theta}+\frac{uv}{r}\right)=-\frac{1}{r}\frac{\partial P}{\partial \theta}+\frac{1}{Re_{0\infty}}\left\{\frac{\partial}{\partial r}\left[\mu r\frac{\partial}{\partial r}\left(\frac{u}{r}\right)+\frac{\mu}{r}\frac{\partial v}{\partial \theta}\right]\right.$$

$$+\frac{1}{r^2}\frac{\partial}{\partial \theta}\left[\frac{4}{3}\mu\left(\frac{\partial u}{\partial \theta}+v\right)-\frac{2}{3}\mu\left(r\frac{\partial v}{\partial r}+v+u\cot\theta\right)\right]$$

$$\left.+\frac{3\mu}{r}\left[r\frac{\partial}{\partial r}\left(\frac{u}{r}\right)+\frac{1}{r}\frac{\partial v}{\partial \theta}\right]+\frac{2\mu\cot\theta}{r^2}\left[\frac{\partial u}{\partial \theta}-u\cot\theta\right]\right\} \quad . \quad (14)$$

Radial Momentum (r Direction):

$$\rho\left(v\frac{\partial v}{\partial r}+\frac{u}{r}\frac{\partial v}{\partial \theta}-\frac{u^2}{r}\right)=-\frac{\partial P}{\partial r}+\frac{1}{Re_{0\infty}}\left\{\frac{\partial}{\partial r}\left[\frac{4}{3}\mu\frac{\partial v}{\partial r}-\frac{2}{3}\frac{\mu}{r}\left(\frac{\partial u}{\partial \theta}+2v+u\cot\theta\right)\right]\right.$$

$$+\frac{1}{r}\frac{\partial}{\partial \theta}\left[\mu r\frac{\partial}{\partial r}\left(\frac{u}{r}\right)+\frac{\mu}{r}\frac{\partial v}{\partial \theta}\right]+\frac{4\mu}{r}\left(\frac{\partial v}{\partial r}-\frac{v}{r}\right)$$

$$\left.-\frac{\mu}{r^2}\left[2\frac{\partial u}{\partial \theta}+2u\cot\theta-r^2\cot\theta\frac{\partial}{\partial r}\left(\frac{u}{r}\right)-\frac{\partial v}{\partial \theta}\cot\theta\right]\right\} \quad . \quad (15)$$

Enthalpy:

$$\rho\left(v\frac{\partial h}{\partial r}+\frac{u}{r}\frac{\partial h}{\partial \theta}\right)=v\frac{\partial P}{\partial r}+\frac{u}{r}\frac{\partial P}{\partial \theta}+\frac{\mu}{Re_{0\infty}}\left[2\left\{\left(\frac{\partial v}{\partial r}\right)^2+\left(\frac{1}{r}\frac{\partial u}{\partial \theta}+\frac{v}{r}\right)^2\right.\right.$$

$$\left.\left.+\left(\frac{v}{r}+\frac{u\cot\theta}{r}\right)^2\right\}+\left\{\frac{1}{r}\frac{\partial v}{\partial \theta}+r\frac{\partial}{\partial r}\left(\frac{u}{r}\right)^2\right\}\right]-\frac{2}{3}\frac{\mu}{Re_{0\infty}}\left[\frac{\partial v}{\partial r}+\frac{1}{r}\frac{\partial u}{\partial \theta}\right.$$

$$\left.+\frac{2v}{r}+\frac{u\cot\theta}{r}\right]^2+\frac{1}{Re_{0\infty}Pr}\left\{\frac{1}{r^2}\frac{\partial}{\partial r}\left(\mu r^2\frac{\partial h}{\partial r}\right)+\frac{1}{r\sin\theta}\frac{\partial}{\partial \theta}\left(\frac{\mu\sin\theta}{r}\frac{\partial h}{\partial \theta}\right)\right.$$

$$+(Le-1)\frac{1}{r^2}\frac{\partial}{\partial r}\sum_{i=1}^{NS}\left(\mu r^2 h_i\frac{\partial Y_i}{\partial r}\right)$$

$$\left.+(Le-1)\frac{1}{r\sin\theta}\frac{\partial}{\partial \theta}\sum_{i=1}^{NS}\left(\frac{\mu h_i\sin\theta}{r}\frac{\partial Y_i}{\partial \theta}\right)\right\} \quad . \tag{16}$$

State:

$$P=\rho T\frac{\bar{\mathcal{R}}\bar{T}_{0\infty}}{\bar{V}_\infty^2}\sum_{i=1}^{NS}\frac{Y_i}{W_i} \quad . \tag{17}$$

In the previous equations, Le_{ij} is assumed to be the same for all species pairs i,j and is, therefore, replaced with Le. Similarly, Sc_{ij} is replaced with Sc.

The local similarity approximation for the zone near the axis of symmetry is given by equations (18) through (24). The validity of this approximation was demonstrated by Kao [7].

$$u(r,\theta) = u_1(r) \sin\theta \tag{18}$$

$$v(r,\theta) = v_1(r) \cos\theta \tag{19}$$

$$h(r,\theta) = h_1(r) \tag{20}$$

$$\rho(r,\theta) = \rho_1(r) \tag{21}$$

$$P(r,\theta) = P_1(r) + P_2(r) \sin^2\theta \tag{22}$$

$$\mu(r,\theta) = \mu_1(r) \tag{23}$$

$$Y_i(r,\theta) = Y_{1i}(r) \quad . \tag{24}$$

Equations (18) through (24) are used to reduce the governing equations to a set of nonlinear, coupled, ordinary differential equations which can be solved rapidly.

A transformation is now made in the normal coordinate by defining

$$\eta \equiv \frac{r - 1}{r_\infty - 1} = \frac{n}{n_\infty} \quad , \tag{25}$$

where r_∞ is the nondimensional distance from the origin to the freestream and n_∞ is the nondimensional distance from the body to the freestream (Fig. 1b). The values of r_∞ and n_∞ are unknown a priori. They are determined as part of the solution. This transformation, equation (25), keeps the body at $\eta = 0$ and the freestream at $\eta = 1$.

By substituting equations (18) through (25) into the governing equations and equating the coefficients of like functions of θ, one obtains the following system of ordinary differential equations:

Cylindrical Coordinates:

$$\frac{\rho_1'}{\rho_1} = -\frac{v_1'}{v_1} - \frac{n_\infty}{1+\eta n_\infty}\left(1+\frac{u_1}{v_i}\right) \quad . \tag{26}$$

$$\frac{u_1''}{n_\infty^2} = \frac{Re_{0\infty}\rho_1}{\mu_1}\left(\frac{v_1 u_1'}{n_\infty} + \frac{u_1^2 + u_1 v_1}{1+\eta n_\infty}\right) + \frac{2 P_2 Re_{0\infty}}{\mu_1(1+\eta n_\infty)}$$

$$+ \frac{u_1 + v_1}{(1+\eta n_\infty)}\left[\frac{\mu_1'}{\mu_1 n_\infty} + \frac{7}{3(1+\eta n_\infty)}\right] - \frac{u_1'}{n_\infty}\left(\frac{2}{1+\eta n_\infty} + \frac{\mu_1'}{\mu_1 n_\infty}\right)$$

$$+ \frac{v_1'}{3n_\infty(1+\eta n_\infty)} \quad . \tag{27}$$

$$\frac{v_1''}{n_\infty^2} = \frac{3}{4}\frac{Re_{0\infty}}{n_\infty \mu_1}(P_1' + \rho_1 v_1 v_1') - \frac{v_1'}{n_\infty}\left(\frac{\mu_1'}{\mu_1 n_\infty} + \frac{1}{1+\eta n_\infty}\right) - \frac{u_1'}{4n_\infty(1+\eta n_\infty)}$$

$$+ \frac{(u_1 + v_1)}{1+\eta n_\infty}\left[\frac{\mu_1'}{2\mu_1 n_\infty} + \frac{7}{4(1+\eta n_\infty)}\right] \quad . \tag{28}$$

$$\frac{P_2'}{n_\infty} = -\frac{P_1'}{n_\infty} + \frac{\rho_1 u_1}{1+\eta n_\infty}(u_1 + v_1) \quad . \tag{29}$$

$$\frac{\rho_1 v_1 h'_1}{n_\infty}(1+\eta n_\infty)^2 = (1+\eta n_\infty)^2\left[\frac{v_1 P'_1}{n_\infty} + \frac{2\mu_1}{Re_{0\infty}}\frac{v'^2_1}{n^2_\infty}\right] + \frac{2\mu_1}{Re_{0\infty}}(u_1+v_1)^2$$

$$-\frac{2}{3}\frac{\mu_1}{Re_{0\infty}}\left[\frac{(1+\eta n_\infty)}{n_\infty}v'_1 + (u_1+v_1)\right]^2$$

$$+\frac{(1+\eta n_\infty)}{Re_{0\infty}\,Pr\,n_\infty}\left\{\mu_1 h'_1 + \frac{(1+\eta n_\infty)}{n_\infty}(h'_1\mu'_1 + \mu_1 h''_1)\right.$$

$$+(Le-1)\left[\left(\mu_1 + \frac{\mu'_1(1+\eta n_\infty)}{n_\infty}\right)\sum_{i=1}^{NS} h_i Y'_{1i}\right.$$

$$\left.\left.+\frac{\mu_1(1+\eta n_\infty)}{n_\infty}\sum_{i=1}^{NS}(h'_i Y'_{1i} + h_i Y''_{1i})\right]\right\} \quad . \tag{30}$$

$$\frac{\rho_1 v_1 Y'_{1i}}{n_\infty} = \dot{w}_i + \frac{1}{(1+\eta n_\infty)\,Re_{0\infty}\,Sc}\left[\frac{\mu_1 Y'_{1i}}{n_\infty} + \frac{\mu'_1 Y'_{1i}(1+\eta n_\infty)}{n^2_\infty}\right.$$

$$\left.+\frac{\mu_1(1+\eta n_\infty)\,Y''_{1i}}{n^2_\infty}\right] \qquad i = 1, \ldots, NS \quad . \tag{31}$$

$$P_1 = \rho_1 T_1\left(\frac{\bar{R}\bar{T}_{0\infty}}{\bar{V}^2_\infty}\right)\sum_{i=1}^{NS}\left(\frac{Y_{1i}}{W_i}\right) \quad . \tag{32}$$

Here, a prime denotes differentiation with respect to η.

Spherical Coordinates:

$$\frac{\rho_1'}{\rho_1} = -\frac{v_1'}{v_1} - \frac{2n_\infty}{1+\eta n_\infty}\left(1+\frac{u_1}{v_1}\right) \tag{33}$$

$$\frac{u_1''}{n_\infty^2} = \frac{Re_{0\infty}\,\rho_1}{\mu_1}\left(\frac{v_1 u_1'}{n_\infty} + \frac{u_1^2 + u_1 v_1}{1+\eta n_\infty}\right) + \frac{2P_2\,Re_{0\infty}}{\mu_1\,(1+\eta n_\infty)}$$

$$+ \frac{u_1 + v_1}{(1+\eta n_\infty)}\left[\frac{\mu_1'}{\mu_1 n_\infty} + \frac{8}{3(1+\eta n_\infty)}\right] - \frac{u_1'}{n_\infty}\left(\frac{2}{1+\eta n_\infty} + \frac{\mu_1'}{\mu_1 n_\infty}\right)$$

$$+ \frac{v_1'}{3n_\infty\,(1+\eta n_\infty)} \quad . \tag{34}$$

$$\frac{v_1''}{n_\infty^2} = \frac{3}{4}\frac{Re_{0\infty}}{n_\infty \mu_1}\,(P_1' + \rho_1 v_1 v_1') - \frac{v_1'}{n_\infty}\left(\frac{\mu_1'}{\mu_1 n_\infty} + \frac{2}{1+\eta n_\infty}\right) - \frac{u_1'}{2n_\infty\,(1+\eta n_\infty)}$$

$$+ \frac{(u_1 + v_1)}{(1+\eta n_\infty)}\left[\frac{\mu_1'}{\mu_1 n_\infty} + \frac{7}{2(1+\eta n_\infty)}\right] \quad . \tag{35}$$

$$\frac{P_2'}{n_\infty} = -\frac{P_1'}{n_\infty} + \frac{\rho_1 u_1}{1+\eta n_\infty}\,(u_1 + v_1) \quad . \tag{36}$$

$$\frac{\rho_1 v_1 h'_1}{n_\infty}(1+\eta n_\infty)^2 = (1+\eta n_\infty)^2\left[\frac{v_1 P'_1}{n_\infty} + \frac{2\mu_1}{Re_{0\infty}}\frac{v'^2_1}{n^2_\infty}\right] + \frac{4\mu_1}{Re_{0\infty}}(u_1+v_1)^2$$

$$- \frac{2}{3}\frac{\mu_1}{Re_{0\infty}}\left[\frac{(1+\eta n_\infty)}{n_\infty} v'_1 + 2(u_1+v_1)\right]^2$$

$$+ \frac{(1+\eta n_\infty)}{Re_{0\infty} Pr\, n_\infty}\left\{2\mu_1 h'_1 + \frac{(1+\eta n_\infty)}{n_\infty}(\mu'_1 h'_1 + \mu'_1 h''_1)\right.$$

$$+ (Le-1)\left[\left(2\mu_1 + \frac{\mu'_1(1+\eta n_\infty)}{n_\infty}\right)\sum_{i=1}^{NS} h_i Y'_{1i}\right.$$

$$\left.\left. + \frac{\mu_1(1+\eta n_\infty)}{n^2_\infty}\sum_{i=1}^{NS}(h'_i Y'_{1i} + h_i Y''_{1i})\right]\right\} \quad . \tag{37}$$

$$\frac{\rho_1 v_1 Y'_{1i}}{n_\infty} = \dot{w}_i + \frac{1}{(1+\eta n_\infty)\, Re_{0\infty}\, Sc}\left[\frac{2\mu_1 Y'_{1i}}{n_\infty} + \frac{\mu_1 Y'_{1i}(1+\eta n_\infty)}{n^2_\infty}\right.$$

$$\left. + \frac{\mu_1(1+\eta n_\infty)\, Y''_{1i}}{n^2_\infty}\right] \qquad i = 1, \ldots, NS \quad . \tag{38}$$

$$P_1 = \rho_1 T_1 \frac{\bar{\mathcal{R}}\bar{T}_{0\infty}}{\bar{V}^2_\infty}\sum_{i=1}^{NS}\left(\frac{Y_{1i}}{W_i}\right) \quad . \tag{39}$$

Equations (26) through (32) and (33) through (39) constitute two sets of nonlinear ordinary differential equations for cylindrical and spherical stagnation regions, respectively. Each of these sets contain $6 + NS$ equations and $8 + 2NS$ unknowns (μ_1, v_1, P_1, P_2, ρ_1, T_1, h_1, μ_1, $\dot{w}_i$, and Y_{1i}). The required additional information and equations are given below for the mass production rates, $\dot{w}_i$, enthalphy, h_1, and viscosity, μ_1, of a dissociated and ionized air mixture. These equations, like the equation of state above, are independent of the coordinate system.

c. Air Chemistry. The freestream air is assumed to consist of N_2 and O_2 molecules only. The air model used for the shock layer consists of seven species and the seven chemical reactions as follows [5]:

$$O_2 + M + 5.1\ eV \underset{k_{r1}}{\overset{k_{f1}}{\rightleftarrows}} O + O + M$$

$$N_2 + M + 9.8\ eV \underset{k_{r2}}{\overset{k_{f2}}{\rightleftarrows}} N + N + M$$

$$NO + M + 6.5\ eV \underset{k_{r3}}{\overset{k_{f3}}{\rightleftarrows}} N + O + M$$

$$NO + O + 1.4\ eV \underset{k_{r4}}{\overset{k_{f4}}{\rightleftarrows}} O_2 + N$$

$$N_2 + O + 3.3\ eV \underset{k_{r5}}{\overset{k_{f5}}{\rightleftarrows}} NO + N$$

$$N_2 + O_2 + 1.9\ eV \underset{k_{r6}}{\overset{k_{f6}}{\rightleftarrows}} NO + NO$$

$$N + O + 2.8\ eV \underset{k_{r7}}{\overset{k_{f7}}{\rightleftharpoons}} NO^{+} + e^{-} \quad .$$

These reactions are written so that the forward reactions are endothermic; the net amounts of energy required to produce the reactions are given on the left side of the equations. The first three reactions are the neutral-particle dissociation-recombination reactions in which the energy of dissociation in the forward reaction is taken primarily from kinetic energy by means of a collision with a "catalytic" molecule M; the chemical energy released in the recombination (reverse reaction) is converted primarily to kinetic energy in a three-body collision involving a catalytic molecule M. The M molecule can be any of the six molecular or atomic species present in the air mixture. The quantities k_{fj} and k_{rj} are the temperature-dependent forward and reverse reaction rates, respectively, for the jth reaction. The experimentally determined reaction rates recommended by Wray [5] are used, together with the concentrations of all constituents, to obtain the mass production rates, $\dot{w}_i$, of each constituent [9]. The reader is referred to Reference 10 for details.

d. Enthalpy. The specific enthalpy of a mixture of gases is given in dimensional form as follows:

$$\bar{h} = \bar{P}\,\bar{v} + \sum_{i=1}^{NS} Y_i\,\bar{e}_i \quad , \tag{40}$$

where

$$\bar{e}_i = \bar{e}_i^0 + \bar{e}_{T_i} + \bar{e}_{R_i} + \bar{e}_{v_i} \tag{41}$$

and

$\bar{e}_i^0$ = specific energy of formation of species i at the reference temperature (zero absolute)

$\bar{e}_{T_i}$ = specific energy of random translation

$\bar{e}_{R_i}$ = specific energy of rotation (for diatomic molecule)

$\bar{e}_{v_i}$ = specific energy of vibration (for diatomic molecules).

We assume that the energy of electronic excited states is negligible, that the rotational state is fully excited, but that the vibrational state is partially excited. Values for these quantities are given by Vincenti and Kruger [9]:

$$\bar{e}_{T_i} = \frac{3}{2} \bar{R}_i \bar{T} \tag{42}$$

$$\bar{e}_{R_i} = \bar{R}_i \bar{T} \tag{43}$$

$$\bar{e}_{v_i} = \frac{\bar{R}_i \Theta_{v_i}}{e^{\Theta_{v_i}/\bar{T}} - 1} \quad , \tag{44}$$

where

Θ_{v_i} = characteristic temperature for vibration of diatomic species i

$\Theta_{v_{O_2}} = 2270$ K

$\Theta_{v_{N_2}} = 3390$ K

$\Theta_{v_{NO}} = 2740$ K

$\Theta_{v_{NO^+}} = 2740$ K .

Equation (40) now becomes

$$\bar{h} = \frac{5}{2}\bar{R}\bar{T}\sum_{i=1}^{NS}\frac{Y_i}{W_i} + \bar{R}\sum_{i\ (\text{for diatomic molecules})}\frac{Y_i}{W_i}\left(\bar{T} + \frac{\bar{\Theta}_{v_i}}{e^{\bar{\Theta}_{v_i}/\bar{T}} - 1}\right) + \sum_{i=1}^{NS}\bar{e}_i^0 \quad . \tag{45}$$

Nondimensionalizing equation (45), we obtain

$$h = \frac{5}{2}\frac{\bar{R}\bar{T}\,\bar{T}_{0\infty}}{\bar{V}_\infty^2}\sum_{i=1}^{NS}\frac{Y_i}{W_i} + \frac{\bar{R}\bar{T}_{0\infty}}{\bar{V}_\infty^2}\sum_{i\ (\text{for diatomic molecules})}\frac{Y_i}{W_i}\left(T + \frac{\Theta_{v_i}}{e^{\Theta_{v_i}/T} - 1}\right)$$

$$+ \frac{1}{\bar{V}_\infty^2}\sum_{i=1}^{NS} Y_i\,\bar{e}_i^0 \quad . \tag{46}$$

e. Viscosity. The Sutherland formula for the viscosity of air gives acceptable results at moderate temperatures, but it fails at the extremely high temperatures encountered in hypersonic flight. The viscosity begins deviating from the Sutherland value due to the onset of dissociation at approximately 3000 K. The viscosity near the wall is also affected by the extremely low pressures encountered at high altitude [11]. This effect is due to velocity slip at the wall (see next section). The Sutherland formula, equation (47), is recommended for temperatures less than 3000 K.

$$\bar{\mu}_{su} = \frac{1.458 \times 10^{-5}\,\bar{T}^{3/2}}{110.4 + \bar{T}} \quad [\text{gm/cm sec}] \quad . \tag{47}$$

This formula is also used in the computer program (Appendix A) to calculate $\bar{\mu}_{0\infty}$ using $\bar{T}_{0\infty}$ computed from the adiabatic relation for temperature,

although it is realized that neither $\bar{\mu}_{su}$ nor $\bar{T}_{0\infty}$ has valid physical meaning at extremely high stagnation enthalpy. This use is justified because $\bar{\mu}_{0\infty}$ is used only for nondimensionalizing $\bar{\mu}$ and for computing $Re_{0\infty}$.

The viscosity of dissociated and ionized air is approximated in Reference 6 using a simple summation formula for a mixture of hard spherical molecules:

$$\frac{\bar{\mu}}{\bar{\mu}_{su}} = \sum_{i=1}^{NS} Y_i \sqrt{\frac{W_R}{W_i}} \frac{\bar{\lambda}_i}{\bar{\lambda}_R} \quad , \tag{48}$$

where

$\bar{\mu}_{su}$ = viscosity at same temperature from Sutherland formula

W_R = equivalent molecular weight of undissociated air

$\bar{\lambda}_i$ = mean free path of species i

$\bar{\lambda}_R$ = mean free path of undissociated air molecules.

The ratio of mean free paths in equation (48) is given by

$$\frac{\bar{\lambda}_R}{\bar{\lambda}_i} = \sum_{j=1}^{NS} \left[Y_j \frac{W_R}{W_j} \frac{\bar{S}_{ij}}{\bar{S}_R} \left(\frac{1 + \frac{W_i}{W_j}}{2} \right)^{1/2} \right] \quad , \tag{49}$$

where

$\bar{S}_{ij}$ = collision cross section for particle i with particle j

$\bar{S}_R$ = collision cross section for undissociated air molecules.

The collision cross sections are tabulated as a function of temperature in Reference 6.

The viscosity given by equation (48) is a function of the composition of the gas mixture and also of the temperature via the dependence of $\bar{S}_R$ and $\bar{S}_{ij}$ on temperature. Since in the present analysis the air is not in chemical equilibrium, the viscosity obtained from the computer program at a given temperature differs greatly from that shown in Reference 6 for equilibrium conditions. As the mass fractions of the components of air approach their undissociated values, the numerical value of the viscosity ratio in equation (48) approaches 1.0, i.e., $\bar{\mu}$ approaches the Sutherland value as expected.

3. Boundary Conditions. To solve the governing equations given in the previous section, freestream and wall boundary conditions are required.

Freestream ($\eta = 1$):

The air at the freestream boundary is in its undisturbed state.

$$u_1 = 1 \ ,$$

$$v_1 = -1 \ ,$$

$$\rho_1 = 1 \ ,$$

$$T_1 = T_\infty \ ,$$

$$P_1 = P_\infty \ ,$$

$$P_2 = 0 \ ,$$

$$Y_{1N_2} = 0.767 \ ,$$

$$Y_{1O_2} = 0.233 \ ,$$

$$Y_{1NO} = Y_{1N} = Y_{1O} = Y_{1NO^+} = Y_{1e^-} = 0 \ .$$

Wall ($\eta = 0$):

In high-altitude, low-Reynolds number flight, the continuum model of the gas breaks down in regions of large gradients of the physical properties near the wall. Hence, the Navier-Stokes description is invalid for the gas layer near the wall (Knudsen layer) with thickness on the order of the mean free path [11]. Also, the familiar continuum zero-velocity and zero-temperature-jump wall boundary conditions are not applicable. Although the Navier-Stokes equations are invalid near the wall, they can still be used, down to quite low Reynolds numbers, to describe the outer flow field if the proper boundary conditions are used at the outer edge of the Knudsen layer. These boundary conditions, known as slip conditions, are the mean velocity, temperature, and species mass fractions. To compute these slip conditions, a kinetic theory approach must be used for the Knudsen layer. The boundary conditions for the Knudsen layer are the mean slip conditions at the outer edge and the kinetic gas-surface conditions at the wall.

The Boltzmann equation is the governing equation for the kinetic theory description of a flow field. However, due to the difficulty in solving the Boltzmann equation for the Knudsen layer, we resorted to an approximate kinetic theory slip model. Reference 4 gives the details of the derivation of the slip conditions for a multicomponent reacting gas. By matching the species, momenta, and energy fluxes at the outer edge of the Knudsen layer to the difference between the incident and reflected fluxes at the wall, the jump in the desired properties across the Knudsen layer is obtained. The fluxes are calculated by taking moments of the velocity distribution function which is approximated by using a Chapman-Enskog expansion for a multicomponent mixture. The species flux is greatly affected by the catalytic nature of the wall. The wall is assumed to be catalytic with respect to recombination of dissociated molecules. Equations are obtained for a partially catalytic wall. The extremes of noncatalytic and fully catalytic walls are easily obtained from the equations for a partially catalytic wall. The resulting nondimensional equations for slip velocity, temperature, and species are as follows:

$$u_s = \frac{\mu_s}{P_w Re_\infty M_\infty}\left[\sqrt{\pi}\left(\frac{2-\sigma}{2\sigma}\right)\sqrt{\frac{2T_s}{\gamma T_\infty}}\left(\frac{\partial u}{\partial r}+\frac{1}{r}\frac{\partial v}{\partial \theta}\right)_s\right.$$

$$+\frac{1}{5(\gamma-1)M_\infty PrT_\infty}\left(\frac{1}{r}\frac{\partial T}{\partial \theta}\right)_s\sum_i\sqrt{\frac{W_i}{W}}$$

$$\left.-\frac{P_w M_\infty Le}{\rho_w Pr}\sum_j\left(\frac{1}{r}\frac{\partial Y_j}{\partial \theta}\right)_s\sum_i\sqrt{\frac{W_i}{W}}\right] . \qquad (50)$$

$$T_s = \left(T_w \sum_i \left\{ \frac{\rho Y_i}{\left[W_i \sum_j \frac{Y_j}{W_j} \right]^{3/2}} \left[1 + \frac{\mu}{3P_i Re_{0\infty}} \left(\frac{1}{r} \frac{\partial u}{\partial \theta} - 2 \frac{\partial v}{\partial r} \right) \right. \right. \right.$$

$$\left. + \frac{\sqrt{\pi}}{Y_i} \left(\frac{2 - \sigma}{\sigma} \right) \frac{M_\infty}{Re_{0\infty}} \frac{Le}{Pr} \left[W_i \sum_j \frac{Y_j}{W_j} \right] \frac{\mu}{\rho} \sqrt{\frac{\gamma W_i T_\infty}{2WT}} \sum_j \frac{\partial Y_j}{\partial r} \right] \Bigg\}_s$$

$$+ \left\{ \frac{2 - \sigma}{\sigma} \sqrt{\pi} \left[\frac{M_\infty}{PrRe_{0\infty}} \frac{\gamma}{\gamma - 1} \frac{\mu}{2} \sqrt{\frac{\gamma T_\infty}{2T}} \frac{\partial T}{\partial r} \right. \right.$$

$$\left. \left. \left. - \frac{5P}{2\rho} \frac{\mu}{Re_{0\infty}} M_\infty^3 \gamma T_\infty \sqrt{\frac{\gamma T_\infty}{2T}} \frac{Le}{Pr} \sum_j \frac{\partial Y_j}{\partial r} \right] \right\}_s \Bigg) \Bigg/$$

$$\left\{ \sum_i \frac{\rho Y_i}{\left[W_i \sum_j \left(\frac{Y_j}{W_j} \right) \right]^{3/2}} \left[1 + \frac{\mu}{2P_i Re_{0\infty}} \left(\frac{1}{r} \frac{\partial u}{\partial \theta} - 2 \frac{\partial v}{\partial r} \right) \right] \right\}_s \quad . \qquad (51)$$

$$Y_i^s = \frac{\frac{2 - \gamma_i}{2\gamma_i} \frac{M_\infty}{Re_{0\infty}} \frac{Le}{Pr} \frac{\mu_s}{\rho_s} \sqrt{\frac{2\pi \gamma W_i T_\infty}{WT_s}} \sum_j \left(\frac{\partial Y_j}{\partial r} \right)_s}{1 + \frac{M_\infty^2}{Re_{0\infty}} \left(\frac{\mu}{3\rho T Y_i} \right)_s \frac{\gamma W_i T_\infty}{W} \left(\frac{1}{r} \frac{\partial u}{\partial \theta} - 2 \frac{\partial v}{\partial r} \right)_s} \quad . \qquad (52)$$

The superscript, s, on Y_i^s denotes the value of Y_i at the outer edge of the Knudsen layer.

The similarity equations (18) through (24) and the coordinate transformation equation (25) are used in equations (50) through (52) to yield the following slip equations:

$$u_{1s} = \frac{\mu_{1s}}{P_{1w} Re_{0\infty} M_\infty} \left[\sqrt{\pi} \left(\frac{2 - \sigma}{2\sigma} \right) \sqrt{\frac{2T_1}{\gamma T_\infty}} \left(\frac{u'_1}{\eta_\infty} \right) \right]_s , \tag{53}$$

$$T_{1s} = \left(T_w \sum_i \left\{ \frac{\rho_1 Y_{1i}}{\left[W_i \sum_j \frac{Y_j}{W_j} \right]^{3/2}} \left[1 + \frac{\mu_1}{3P_{1i} Re_{0\infty}} \left(\frac{u_1}{1 + \eta n_\infty} - \frac{2v'_1}{n_\infty} \right) \right. \right. \right.$$

$$\left. + \frac{\sqrt{\pi}}{Y_{1i}} \left(\frac{2 - \sigma}{\sigma} \right) \frac{M_\infty}{Re_{0\infty}} \frac{Le}{Pr} \left[W_i \sum_j \frac{Y_{1j}}{W_j} \right] \frac{\mu_1}{\rho_1} \sqrt{\frac{\gamma W_i T_\infty}{2WT_1}} \sum_j \frac{Y'_{1j}}{n_\infty} \right] \Bigg\}_s$$

$$+ \frac{2 - \sigma}{\sigma} \sqrt{\pi} \left[\frac{M_\infty}{PrRe_{0\infty}} \frac{\gamma}{\gamma - 1} \frac{\mu_1}{2} \sqrt{\frac{\gamma T_\infty}{2T_1}} \times \frac{T'_1}{n_\infty} \right.$$

$$\left. \left. - \frac{5P_1}{2\rho_1} \frac{\mu_1}{Re_{0\infty}} M_\infty^3 \gamma T_\infty \sqrt{\frac{\gamma T_\infty}{2T_1}} \frac{Le}{Pr} \sum_j \frac{Y'_{1j}}{n_\infty} \right] \right)_s$$

$$\div \left\{ \sum_i \frac{\rho_1 Y_{1i}}{\left[W_i \sum_j \frac{Y_{1j}}{W_j} \right]^{3/2}} \left[1 + \frac{\mu_1}{2P_{1i} Re_{0\infty}} \left(\frac{u_1}{1 + \eta n_\infty} - \frac{2v'_1}{n_\infty} \right) \right] \right\}_s , \tag{54}$$

and

$$Y_{1i}^{s} = \frac{\dfrac{2-\gamma_i}{2\gamma_i}\,\dfrac{M_\infty}{Re_{0\infty}}\,\dfrac{Le}{Pr}\,\dfrac{\mu_{1s}}{\rho_{1s}}\sqrt{\dfrac{2\pi\gamma W_i T_\infty}{W T_{1s}}}\,\sum_j\left(\dfrac{Y'_{1j}}{n_\infty}\right)_s}{1+\dfrac{M_\infty^2}{Re_{0\infty}}\left(\dfrac{\mu_1}{3\rho_1 T_1 Y_{1i}}\right)_s\dfrac{\gamma W_i T_\infty}{W}\left(\dfrac{u_1}{1+\eta n_\infty}-\dfrac{2v'_1}{n_\infty}\right)_s} \quad . \tag{55}$$

The quantity γ_i in equation (55) is the recombination coefficient for the i species; it is a measure of the catalyticity of the wall. The value of γ_i varies from 0 (noncatalytic wall) to 1 (fully catalytic wall).

The computer program used in this report has the fully catalytic wall and noncatalytic wall options, but it does not, in the present form, have a partially catalytic wall option [for a given catalyticity γ_i, equation (55) would give Y_i^s]. In the fully catalytic wall option, the wall is assumed to be catalytic only with respect to recombination of neutral atomic species; it is assumed to be noncatalytic with respect to recombination of the charged particles NO^+ and e^-. The wall boundary conditions on Y_i for these special cases are given as follows:

Noncatalytic Wall:

For a noncatalytic surface ($\gamma_i = 0$), equation (55) reduces to

$$\sum_j (Y'_{1j})_s = 0 \quad . \tag{56}$$

A sufficient condition for equation (56) to be satisfied is that

$$(Y'_{ij})_s = 0 \qquad j = 1, \ldots, NS \quad . \tag{57}$$

Equation (57) is also the most physically plausible means by which equation (56) can be satisfied; therefore, equation (57) is taken as the noncatalytic boundary condition for species mass fractions.

Fully Catalytic Wall:

For the fully catalytic wall, the surface is assumed to be fully catalytic with respect to recombination of neutral atomic species, but it is assumed to be noncatalytic with respect to recombination of the charged particles NO^+ and e^-. Therefore, the effect of the wall is to drive the gas towards its freestream composition, except for the charged particles NO^+ and e^-. The following boundary conditions are then obtained:

$$\left(Y_{N_2}\right)_s = 0.767 \tag{58}$$

$$\left(Y_{O_2}\right)_s = 0.233 \tag{59}$$

$$(Y_{NO})_s = (Y_N)_s = (Y_O)_s = 0 \tag{60}$$

$$(Y'_{NO^+})_s = (Y'_{e^-})_s = 0 \quad . \tag{61}$$

Equations (58), (59), and (61) produce the impossible result that

$$\sum_{i=1}^{NS} Y_i > 1 \quad ;$$

however, because $(Y_{NO^+})_s$ and $(Y_{e^-})_s$ are usually very small, this error is tolerable.

B. Method of Solution

Equations (26) through (32) and (33) through (39) together with equations (46) and (48) constitute two sets of nonlinear, coupled ordinary differential equations with boundary conditions previously given. The first order equations are solved by direct numerical quadrature, and the second order equations are

integrated by a finite difference method known as the successive accelerated replacement method which is an iterative scheme that starts from a guessed solution. The salient feature of this method, proposed by Lieberstein [13], is that the successive corrections applied to the flow profiles in each iteration are controlled by acceleration factors which are used to increase the rate of convergence of the computed quantities. Thus, this method can be successfully applied even if the initial, guessed profiles do not approximate the converged solutions very well. For the present application, this statement holds true in the midrange of the flow regime for which our analysis is applicable. However, divergence problems are encountered at the continuum end of the regime (Appendix A).

C. Computer Program

Details of the computer program are found in Reference 10, while Appendix A is a current users manual.

III. RESULTS

Results from the computer program, with the modifications introduced in this report, are first compared with the "old" program. Then, the program output is compared with some available experimental data. Finally, some general results from the program and input data for running the program are presented.

A. Effect of Computer Program Modifications

The program described as the old program includes all the analysis in this report except the constitutive equations (46) and (48) for enthalpy and viscosity, respectively. The old enthalpy equation assumed a fully excited vibrational state for diatomic molecules. This assumption is always violated near the freestream and near the wall because temperatures in these regions are less than Θ_v. The old viscosity equation (Sutherland) is restricted to nondissociated air or to temperatures less than approximately 3000 K at equilibrium conditions. This temperature is greatly exceeded in the central part of the shock layer at reentry speeds.

B. Comparison of Data Between Old Program and Modified Program

Computed values of shock layer thickness, n_∞; wall heat transfer coefficient at the stagnation point, C_H; and maximum ratio of viscosity to Sutherland viscosity on the stagnation streamline, μ/μ_{su}, are given in Table 1 for a 30.5-cm radius sphere using (1) the "old" program, (2) the program with enthalpy modification only, and (3) the program with enthalpy and viscosity modifications. The conditions for which the runs were made are listed in Table 1. The thermodynamic properties associated with altitude are obtained throughout this report from Reference 14.

TABLE 1. DATA COMPARISON

alt = 86 km

$\bar{r}_b$ = 30.5 cm

$\bar{V}_\infty$ = 793 000 cm/sec

Program Identification	Shock Layer Thickness n_∞	Wall Heat Transfer Coefficient C_H	$\left(\frac{\mu}{\mu_{sv}}\right)_{max}$
1. Old Program	0.1361	0.147	1.0
2. Modified Program (a) New enthalpy computation, equation (46) (b) Sutherland viscosity	0.1409	0.154	1.0
3. Modified Program (a) New enthalpy computation, equation (46) (b) New viscosity, equation (48)	0.1411	0.172	1.37

For these runs, conditions were chosen at which the modifications in viscosity and enthalpy computation would have their greatest effect. These conditions are the ones which yield a high degree of dissociation and ionization, equations (46) and (48), i.e. high speed and high freestream density. Therefore, an altitude was chosen (86 km) where freestream density is near the maximum for which the program will run (see General Results section). The table shows that the enthalpy and viscosity modifications had a significant effect on heat transfer rate and shock layer thickness. The heat transfer rate was increased 17 percent due to the combined effect of both modifications.

C. Comparison with Experimental Data

Very little experimental data exist for the low density, hypersonic, high stagnation enthalpy flow regime for which this computer program was designed. Therefore, we do not have the detailed comparison with experimental data which is desired to validate the present analysis. However, a limited amount of heat transfer and pressure data for spheres are available from an arc-jet facility at moderate stagnation enthalpy [15], and a larger body of stagnation heat transfer data exists for relatively low enthalpy, and hypersonic flow [16].

Figure 2 compares computed stagnation point heat transfer coefficients, C_H, for a sphere with experimental data from References 15 and 16. The data in this figure represent several levels of stagnation enthalpy and, hence, several levels of real gas effects, so good agreement among all the data is not expected. The purpose here is to compare the computed results directly with each set of experimental data and to observe the trend in C_H with changing stagnation enthalpy. A best fit curve through the relatively low enthalpy data of Vidal and Wittliff [16] is shown by the solid line, and the square symbols give the computed values for the same flow conditions. Although the computer program was designed for real gas, chemically reacting flows, it can be run at the low enthalpy conditions of the Vidal and Wittliff data, in which case the computed dissociation levels are very low. The data are plotted as a function of the similarity parameter, K^2, used by Vidal and Wittliff, and defined as follows:

$$K^2 = \frac{Re_\infty}{\gamma_\infty M_\infty^2 C^*} \quad , \tag{62}$$

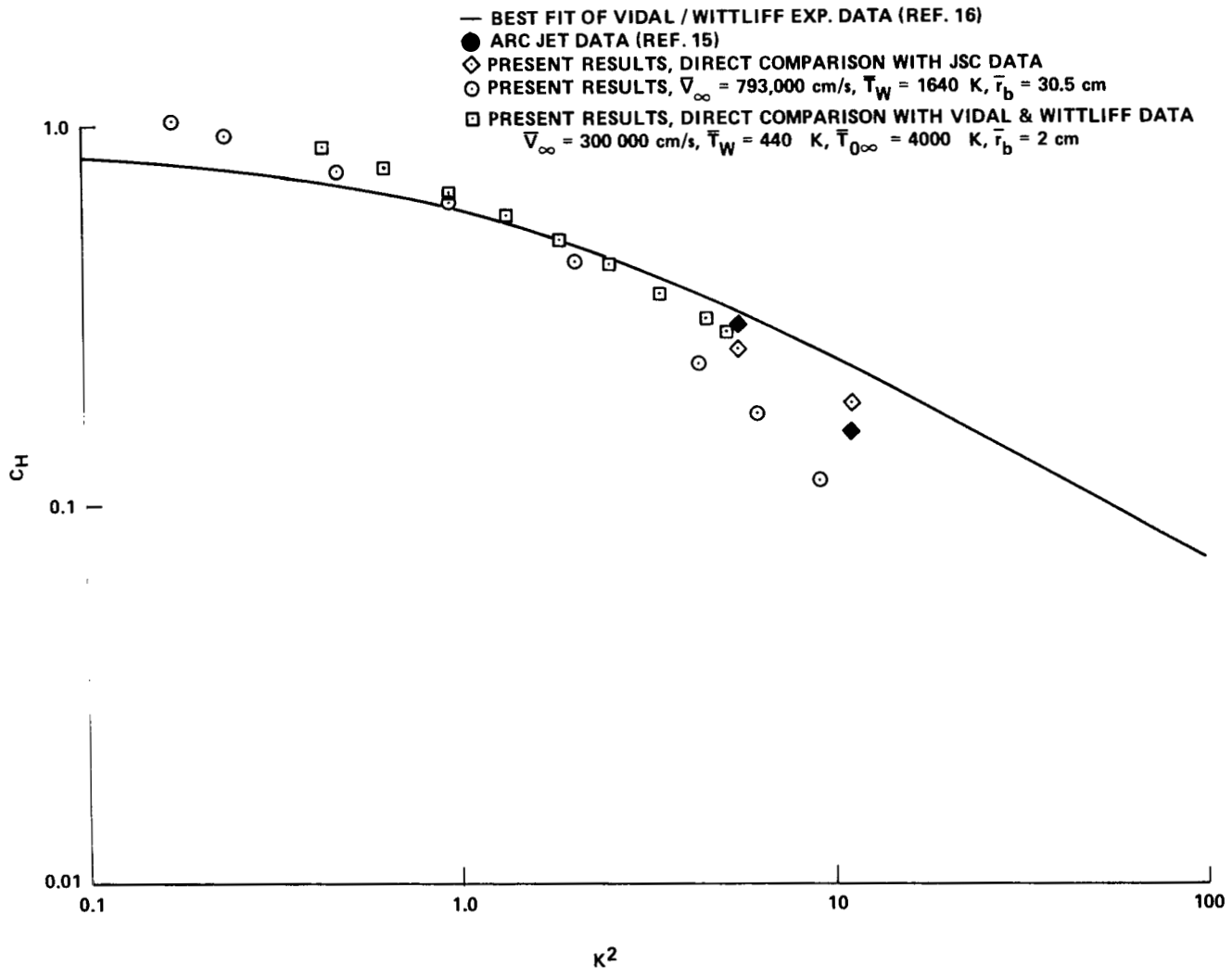

Figure 2. Comparison of present theory with experimental data for stagnation point heating on a sphere.

where

$$C^* = \frac{\bar{\mu}^*}{\bar{\mu}_\infty} \frac{\bar{T}_\infty}{\bar{T}^*} \tag{63}$$

and

$$\bar{T}^* = \frac{1}{2} (\bar{T}_{0\infty} + \bar{T}_w) \quad , \tag{64}$$

where

$\bar{\mu}^*$ = viscosity computed by Sutherland's formula using $\bar{T}^*$

$\bar{\mu}_\infty$ = viscosity computed by Sutherland's formula using $\bar{T}_\infty$.

The computed data do not agree with the mean of the Vidal and Wittliff data as well as we would like, but the computed data points fall within the scatter of the experimental points [16]. The computed values tend to overestimate C_H at rarefied conditions and underestimate it for denser flow. It is important to note that at the higher enthalpy cases, the wall catalysis can affect the value of C_H by a factor of 3 or more [4]. Hence, any comparison of experimental and calculated heating must be for similar wall catalysis.

The arc-jet data of Scott [15] are shown by the filled diamond symbols, and computed data for the same conditions are shown by the empty diamond symbols. The flow conditions for these tests are given in Table 2.

The freestream boundary conditions in the computer program were modified to match the dissociated arc-jet freestream. Also, the spheres in the arc-jet tests were coated with teflon to produce a noncatalytic wall and, therefore, the noncatalytic wall option in the computer program was used for comparison with these data points. The noncatalytic wall option was also used for the remainder of the computer data in this figure and the entire report unless otherwise noted.

The comparison of the computed data with Scott's experimental data is considered acceptable.

TABLE 2. ARC-JET FLOW FIELD PROPERTIES

	Case 1	Case 2
Mach number, M_∞	10	8
Reynolds number, Re_∞	380	553
Freestream speed, $\bar{V}_\infty$ (cm/sec)	423 000	412 000
Freestream temperature, $\bar{T}_\infty$ (K)	270	414
Freestream density, $\bar{\rho}_\infty$ (gm/cm^3)	3.28×10^{-8}	6.41×10^{-8}
Wall temperature, $\bar{T}_w$ (K)	450	450
Radius of sphere, $\bar{r}_b$ (cm)	5.08	5.08
Species mass fractions in freestream:		
N_2	0.4138	0.6124
O_2	0.6519×10^{-5}	0.1084×10^{-4}
N	0.3514	0.1522
O	0.2348	0.2347
NO	0.5380×10^{-5}	0.3761×10^{-4}
NO^+	0.2221×10^{-5}	0.6849×10^{-5}
e^-	0.3850×10^{-10}	0.1187×10^{-9}

Some high-enthalpy computed data, for which the dissociation and ionization levels are very high, are shown in Figure 2 by the circular symbols. These data points fall considerably below the lower enthalpy data at the continuum end of the flow regime (at large values of K^2) where there is a consistent trend of decreasing C_H with increasing enthalpy for a given K^2. The parameter K^2 does not account for real gas effects and, therefore, should not be expected to correlate data with widely different enthalpy levels.

Acceptable comparisons have also been obtained with other theoretical predictions by Kumar and Jain [3] who used an analysis identical to the present one except for slip, enthalpy, and viscosity computations.

D. General Results

Figures 3 and 4 illustrate typical convergence behavior of the solutions with increasing number of iterations. Figure 3 shows the successive computed nondimensional temperature profiles, including the initial guess, along the stagnation streamline of a sphere with noncatalytic wall. The temperature profiles did not quite converge by the final iteration (2000), so it was necessary to make a rerun using the output of run No. 1 as input data for run No. 2. The figure illustrates that extremely accurate initial guesses are not generally required to achieve convergence; however, the more accurate the initial guess, the faster the solutions will converge. At very large Reynolds numbers, where gradients in flow properties are large, more accurate initial guesses are required to avoid divergence. Figure 4 shows the convergence behavior of wall heat transfer coefficient, C_H, for the same run. The converged value of C_H, obtained in run No. 2, is shown at the right margin.

Figure 5a gives the computed velocity components, and the pressure, temperature, and density profiles along the stagnation streamline of a sphere with noncatalytic wall at relatively high freestream Reynolds number (1315). Figure 5b gives the mass fraction profiles for the same run. This run is approaching the maximum Reynolds number for which the program will converge easily without extremely accurate input data or modifications to the program such as spacing the computation increments closer together. The meaning of the quantities in Figure 5a are given in equations (18) through (24); e.g. P_1 is the pressure on the stagnation streamline, and P_2 gives the correction in pressure for small angles away from the stagnation streamline. A thick "shock wave" is indicated by the steep gradients in the region $1.06 < r < 1.12$.

The same quantities presented in Figure 5 are plotted in Figure 6 for a smaller Reynolds number (185). Figure 6a reveals that all evidence of a shock wave has disappeared at this low Reynolds number. Comparison of Figures 5b and 6b shows that the degree of dissociation and ionization decreases drastically in lower density flow.

Figure 7 gives the flow profiles along the stagnation streamline of a sphere with fully catalytic wall at a medium Reynolds number (458). The Sutherland viscosity formula was used because this run was made before the

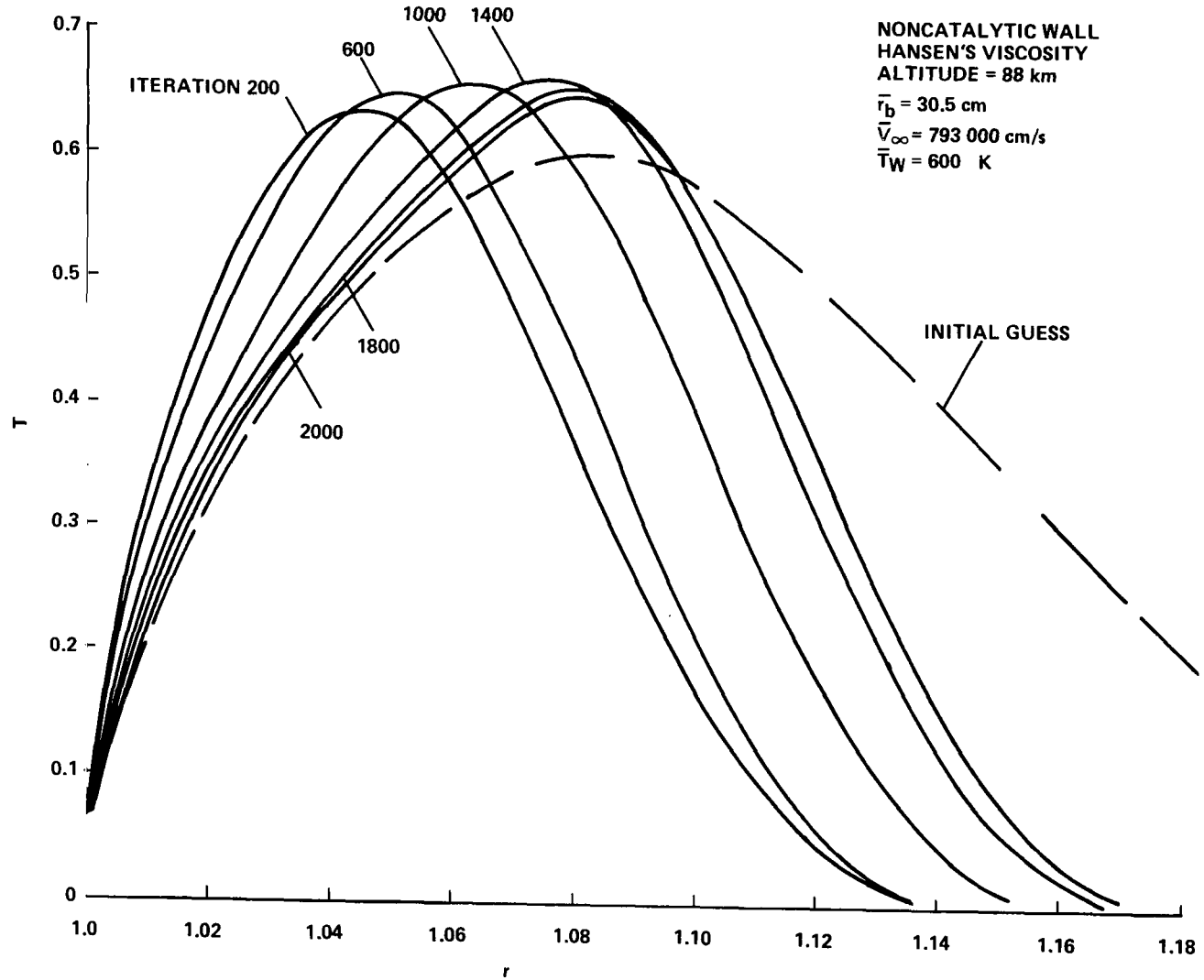

Figure 3. Convergence of temperature profiles for sphere with increasing number of iterations.

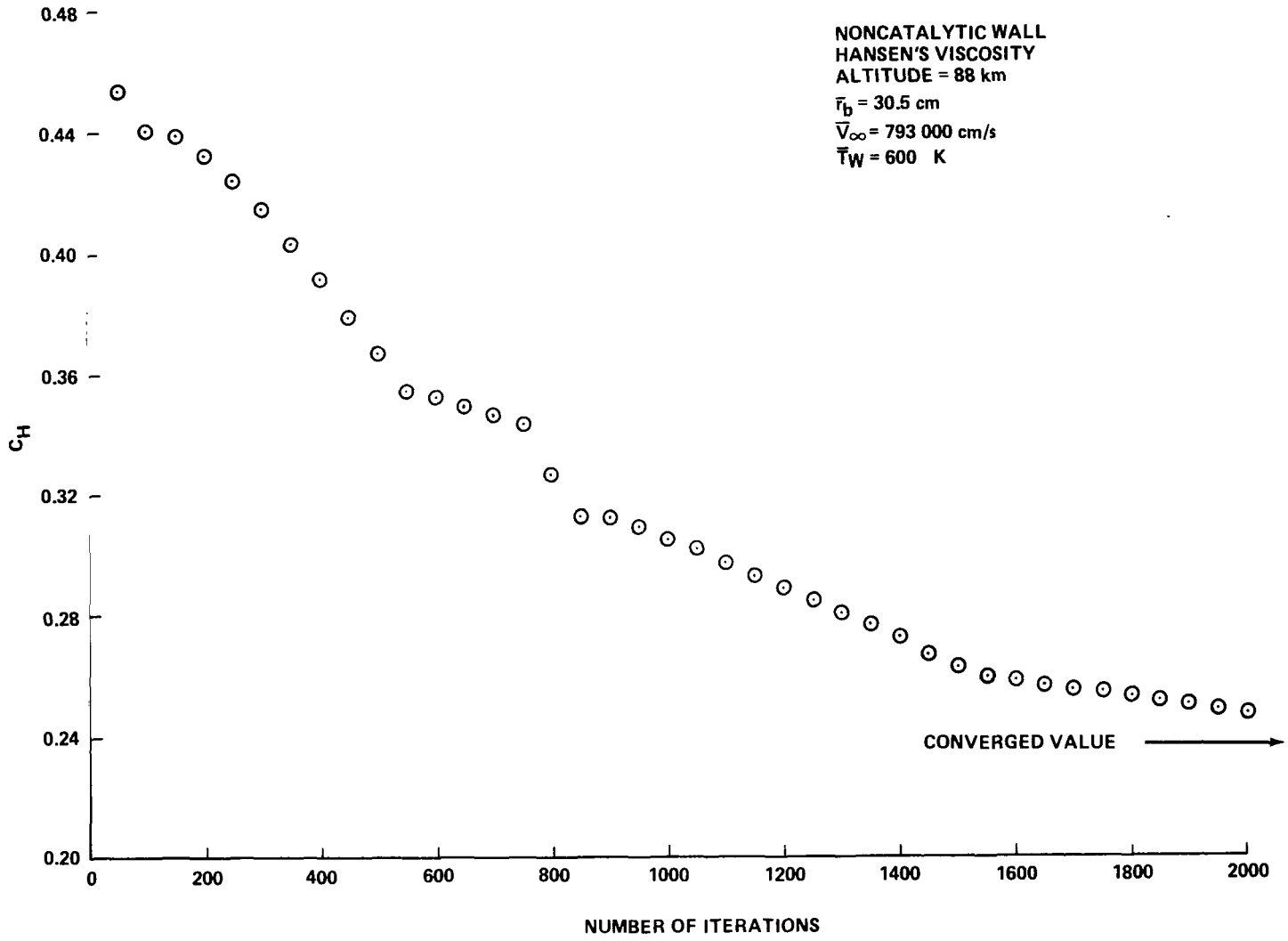

Figure 4. Typical convergence of stagnation point heat transfer coefficient for sphere with increasing number of iterations.

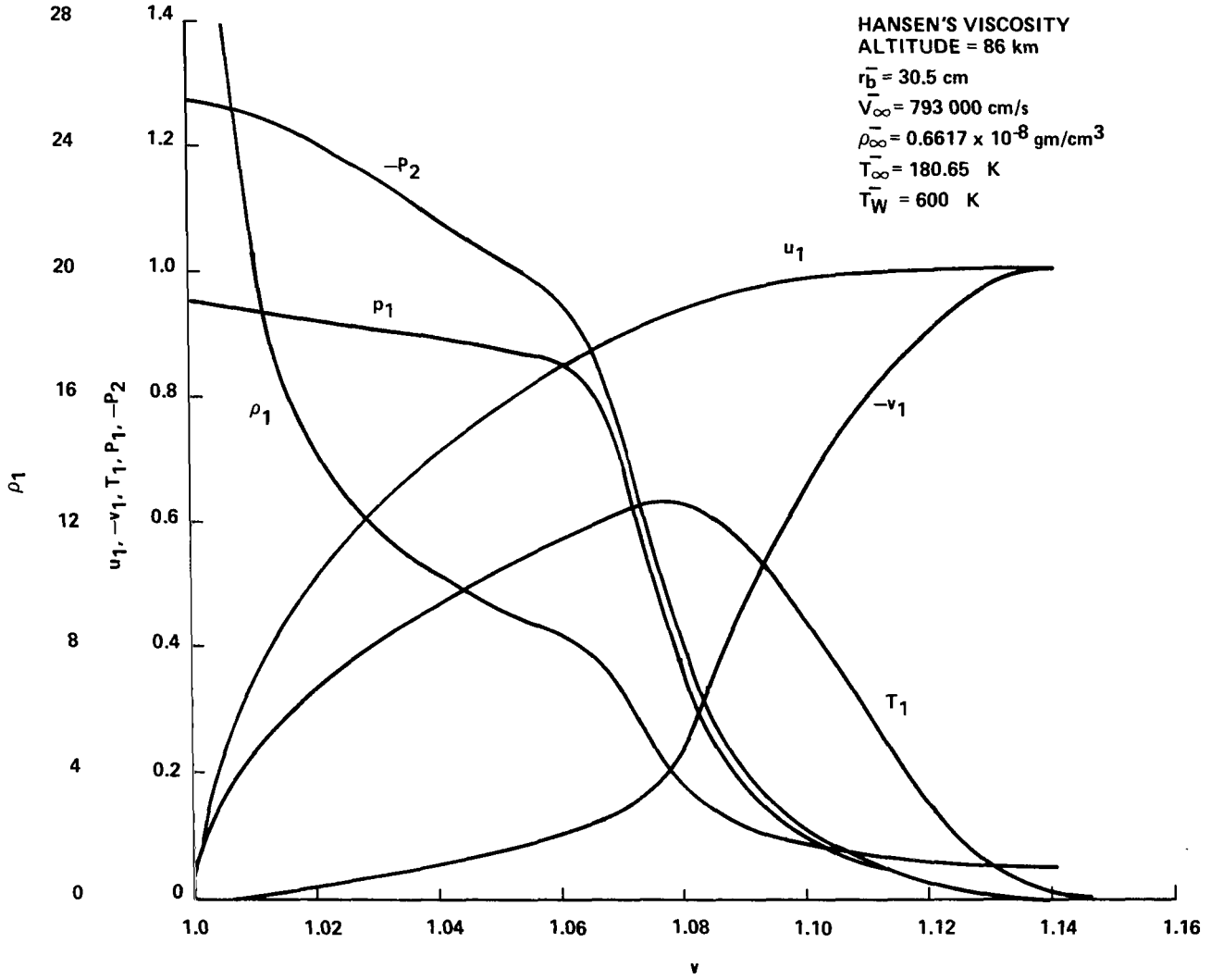

a. Velocity and thermodynamic property profiles.

Figure 5. Flow profiles for sphere with noncatalytic wall at large Reynolds number (Re_∞ = 1315).

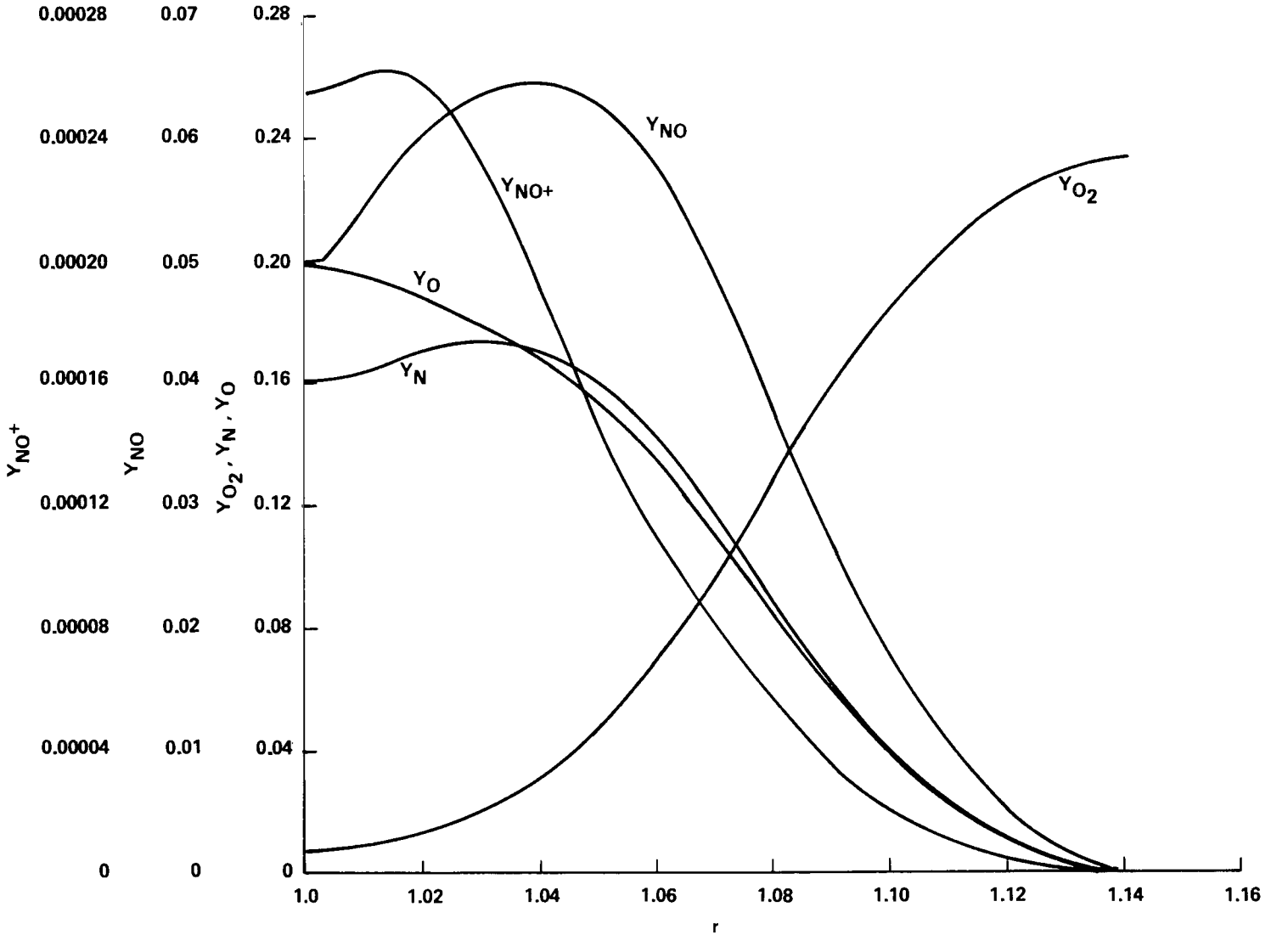

b. Mass fraction profiles.

Figure 5. (Concluded)

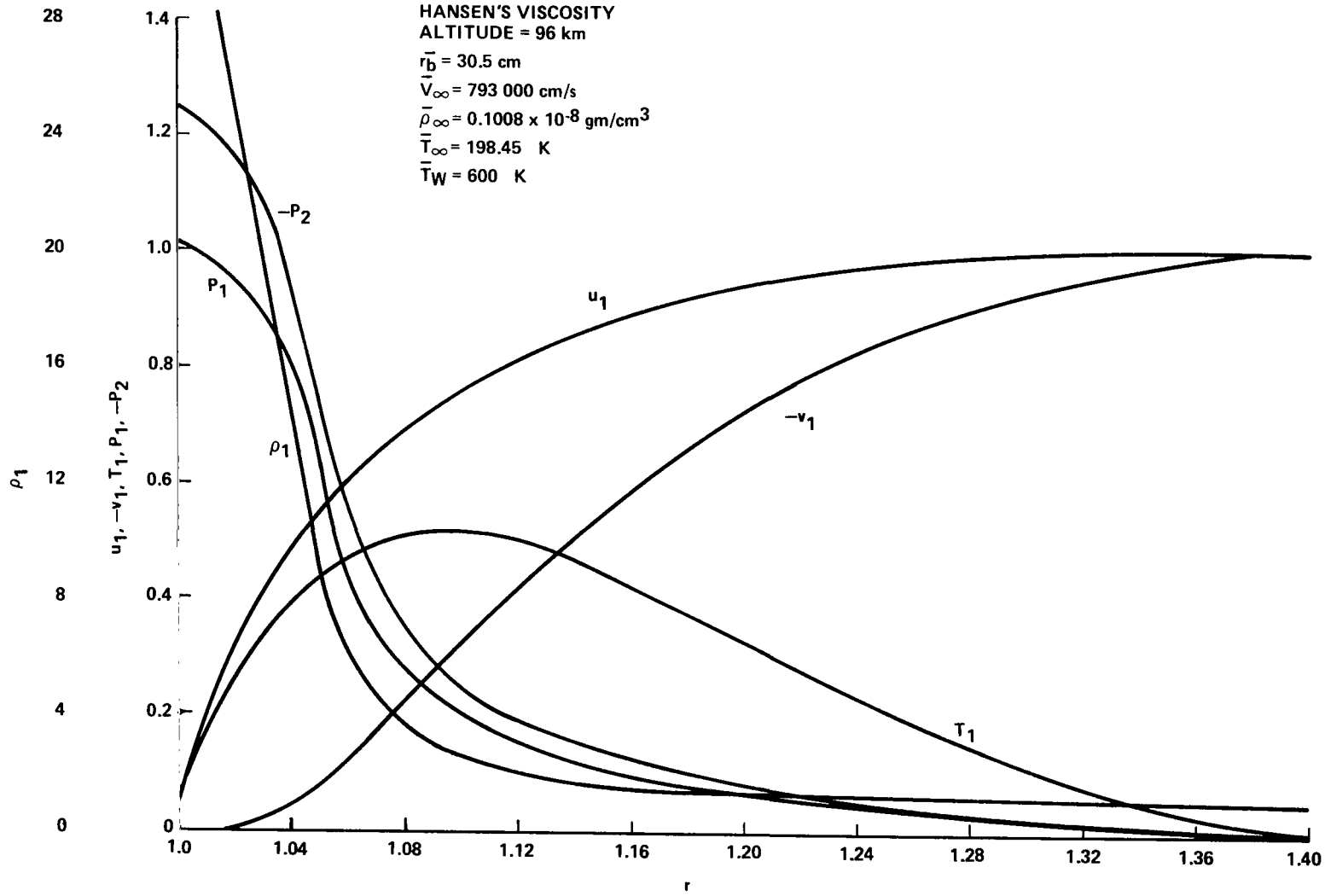

a. Velocity and thermodynamic property profiles.

Figure 6. Flow profiles for sphere with noncatalytic wall at small Reynolds number ($Re_\infty = 185$).

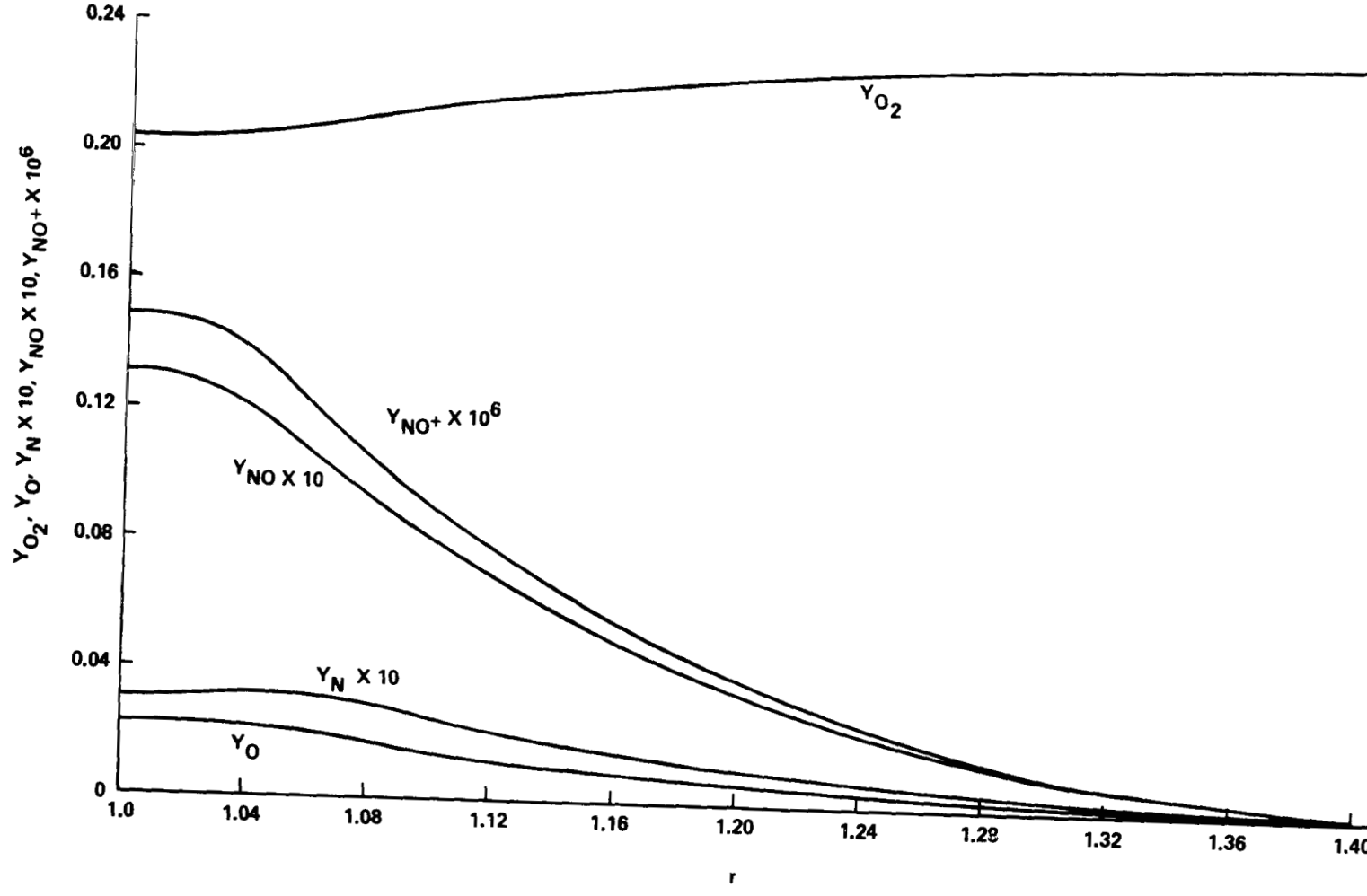

b. Mass fraction profiles.

Figure 6. (Concluded)

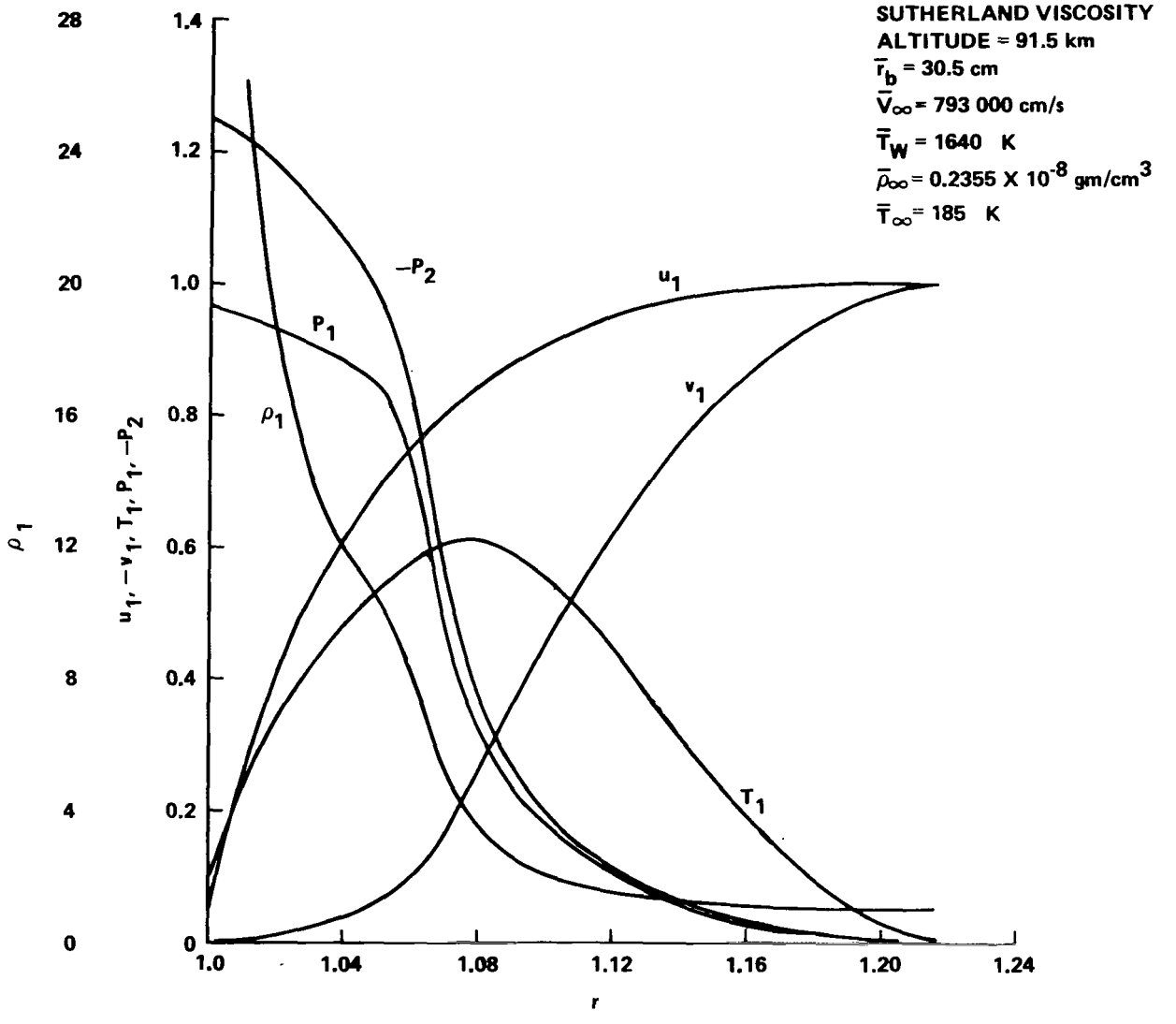

a. Velocity and thermodynamic property profiles.

Figure 7. Flow profiles for sphere with fully catalytic wall ($Re_\infty = 458$).

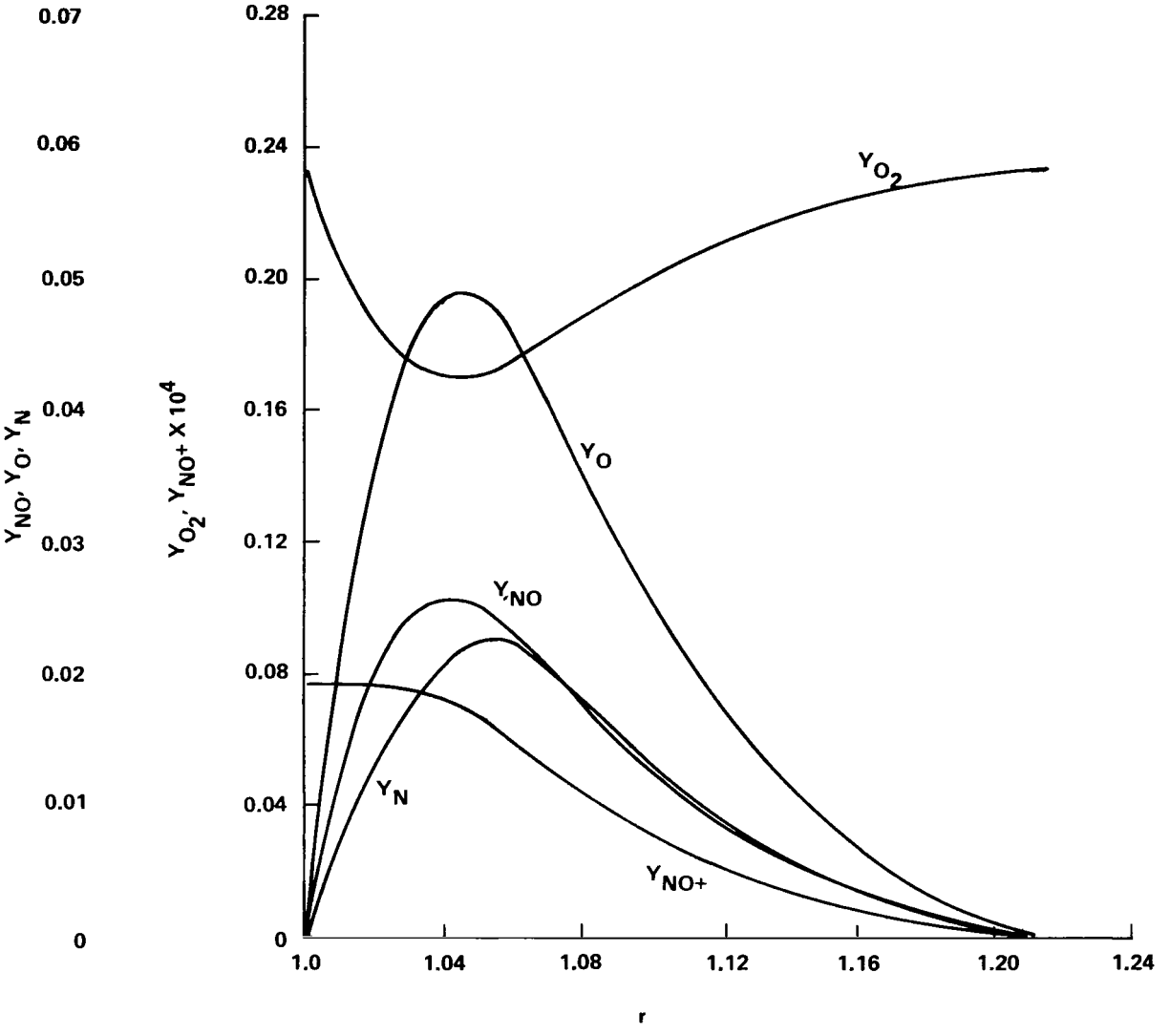

b. Mass fraction profiles.

Figure 7. (Concluded)

viscosity modification to the program. The density profile gives a hint of a shock wave similar to that shown in Figure 5a. Comparison of Figures 5b, 6b, and 7b illustrate the difference in species mass fraction profiles between a noncatalytic wall and a fully catalytic wall. The species mass fractions approach their freestream values at the catalytic wall except for the ions NO^+ and e^-. The wall is assumed noncatalytic with respect to ion recombination in this program.

Figures 5 through 7 provide useful starting data for running the program at conditions near the ones in these figures.

Figure 8 compares temperature, density, and velocity profiles for a sphere and cylinder at the same flow conditions as in Figure 5. The profiles are remarkably similar. Therefore, the profiles for a sphere, Figures 5, 6, and 7, are adequate to use as starting data for the cylindrical option of the program.

The change in the stagnation line temperature profile with freestream density, or Re_∞, is illustrated in Figure 9. The peak value in nondimensional temperature decreases and the shock layer thickness increases with increasing altitude or decreasing density.

The freestream density and speed greatly affect the degree of dissociation of the air molecules and, hence, the viscosity of the gas mixture. Figure 10 gives the peak values from the viscosity and mass fraction profiles for N, O, and NO as a function of altitude for a fixed large value of freestream speed. As before, the freestream thermodynamic properties associated with altitude are obtained from Reference 14. Although the stagnation enthalpy is large, the figure shows that dissociation becomes negligible and viscosity approaches the Sutherland value at altitudes greater than approximately 100 km. This is due to the decreased reaction rates at the lower temperatures which occur in the shock layer at higher altitudes (Fig. 9). Figure 11 illustrates that dissociation and the viscosity ratio increase with increasing freestream speed at the fixed altitude of 96 km.

A parametric study was made to determine the effect of altitude (or density), freestream speed, and wall temperature on the stagnation point heat transfer coefficient, C_H. Figure 12 gives C_H for a sphere and cylinder as a function of altitude with fixed freestream speed and wall temperature. Hansen's viscosity, equation (48), was used for the sphere, but Sutherland's viscosity was used for the cylinder because those runs were made before the program was modified to compute Hansen's viscosity. The figure shows a steady increase

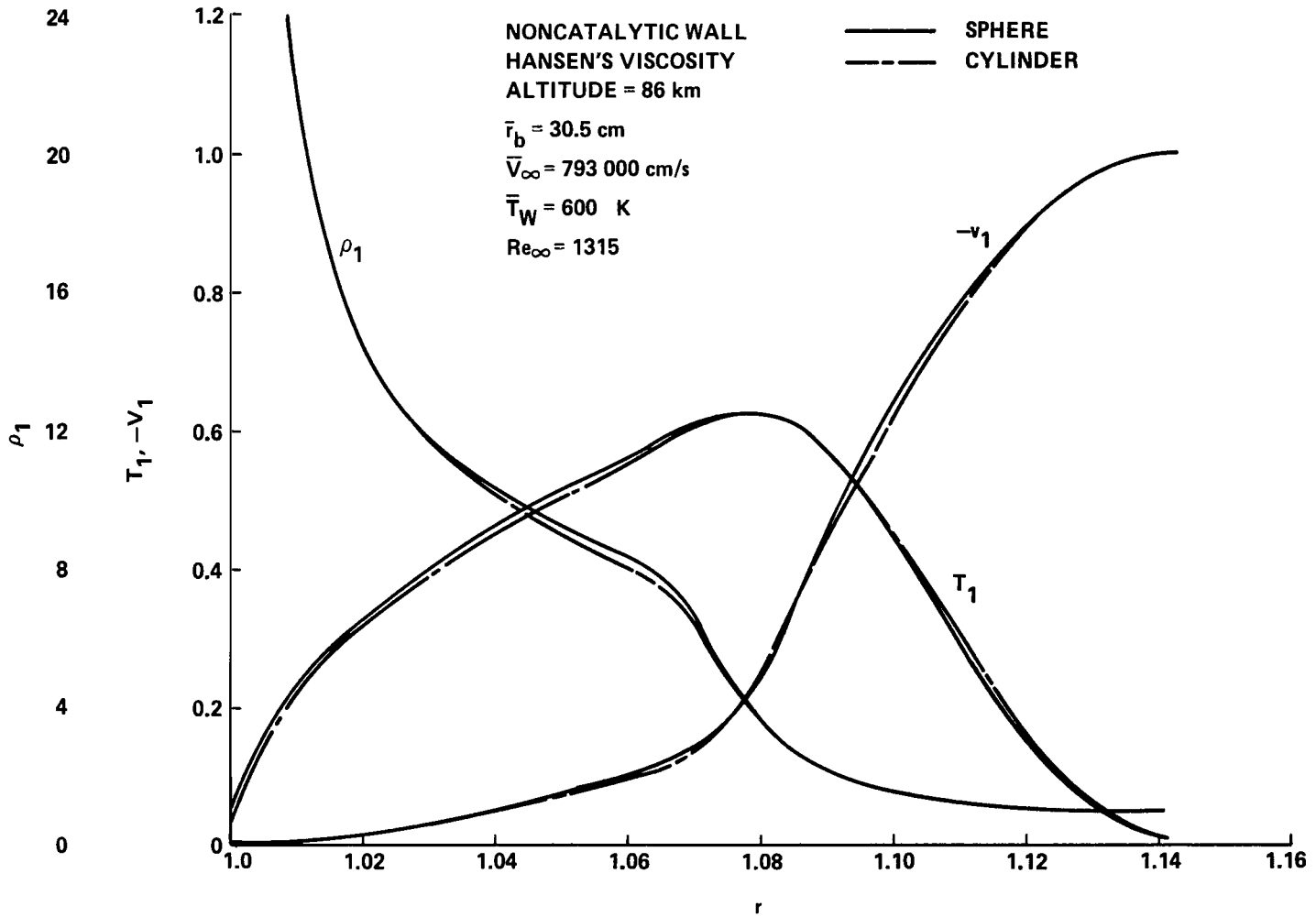

Figure 8. Comparison of flow profiles for sphere and cylinder.

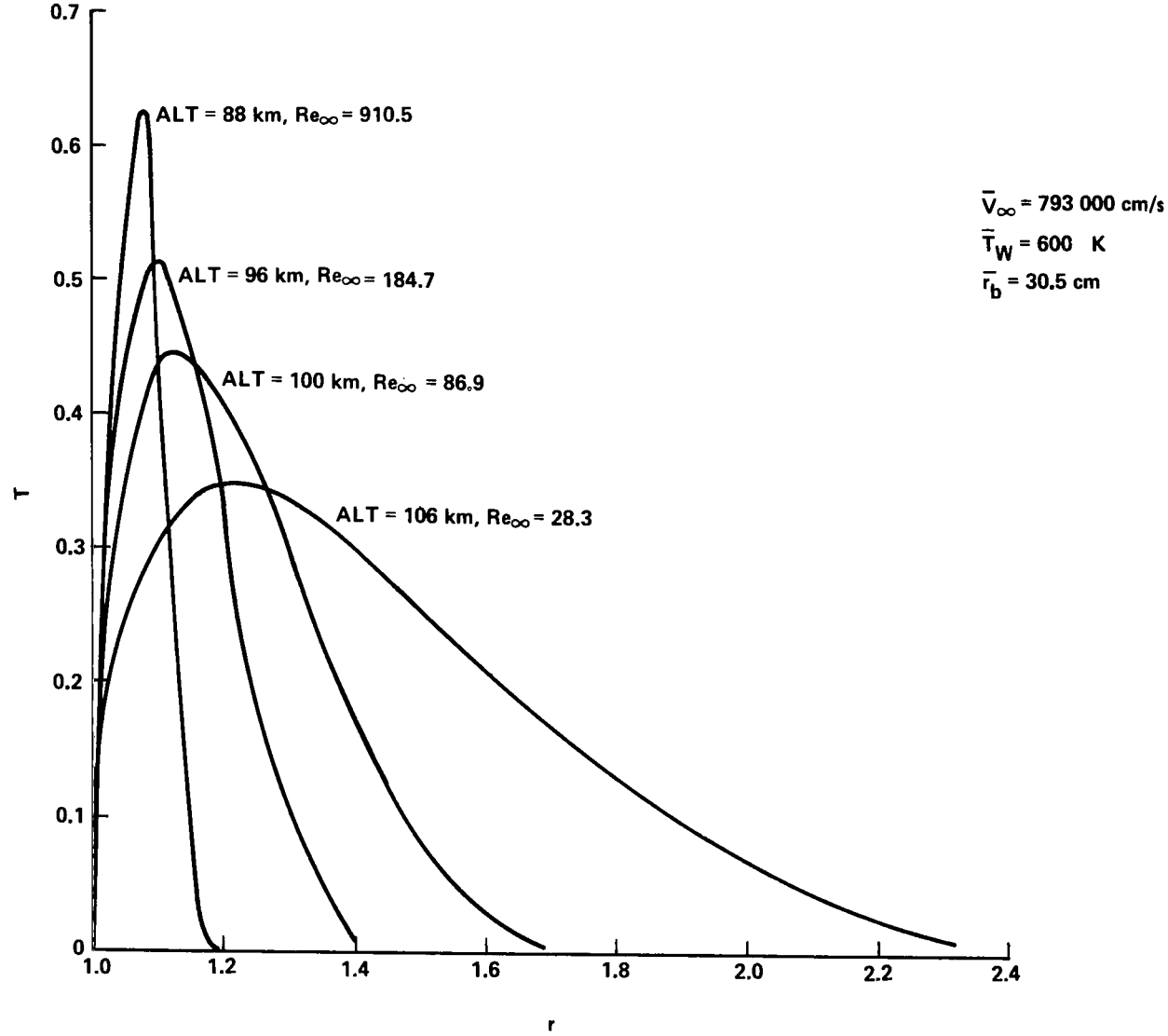

Figure 9. Temperature profiles at various Reynolds numbers for sphere.

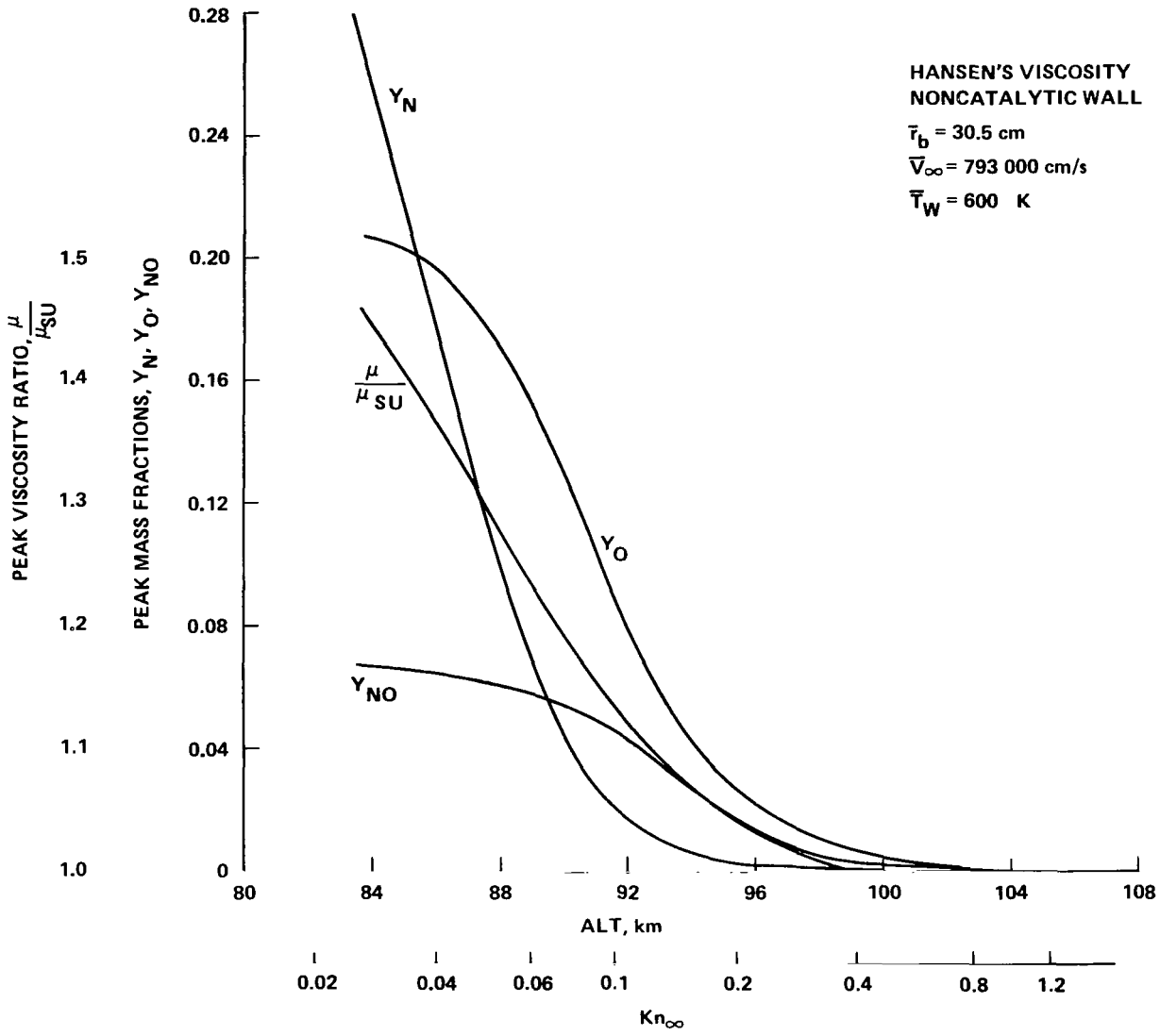

Figure 10. Effect of variation in altitude on dissociation and viscosity in shock layer of sphere.

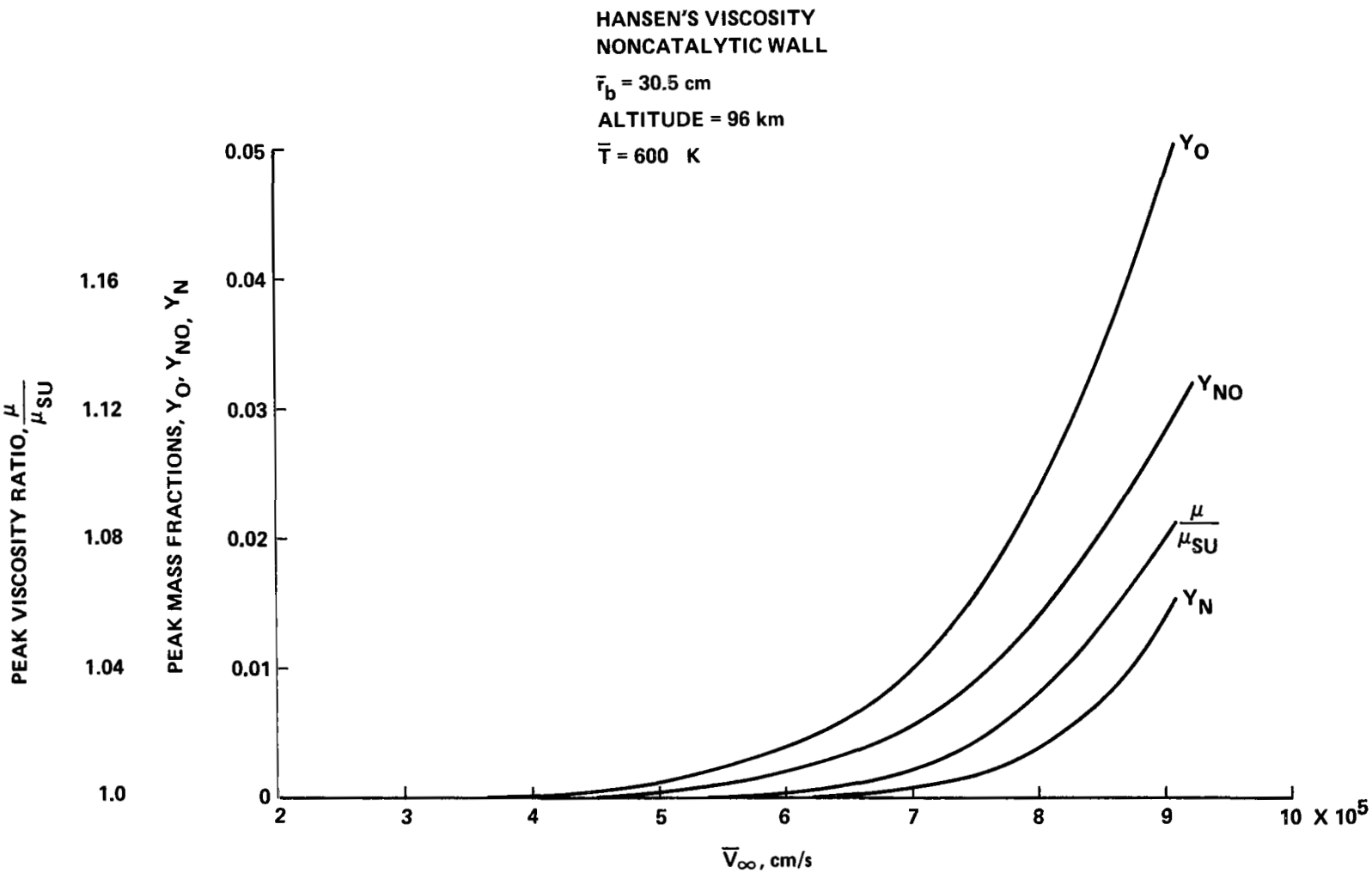

Figure 11. Effect of freestream speed on dissociation and viscosity in shock layer of sphere.

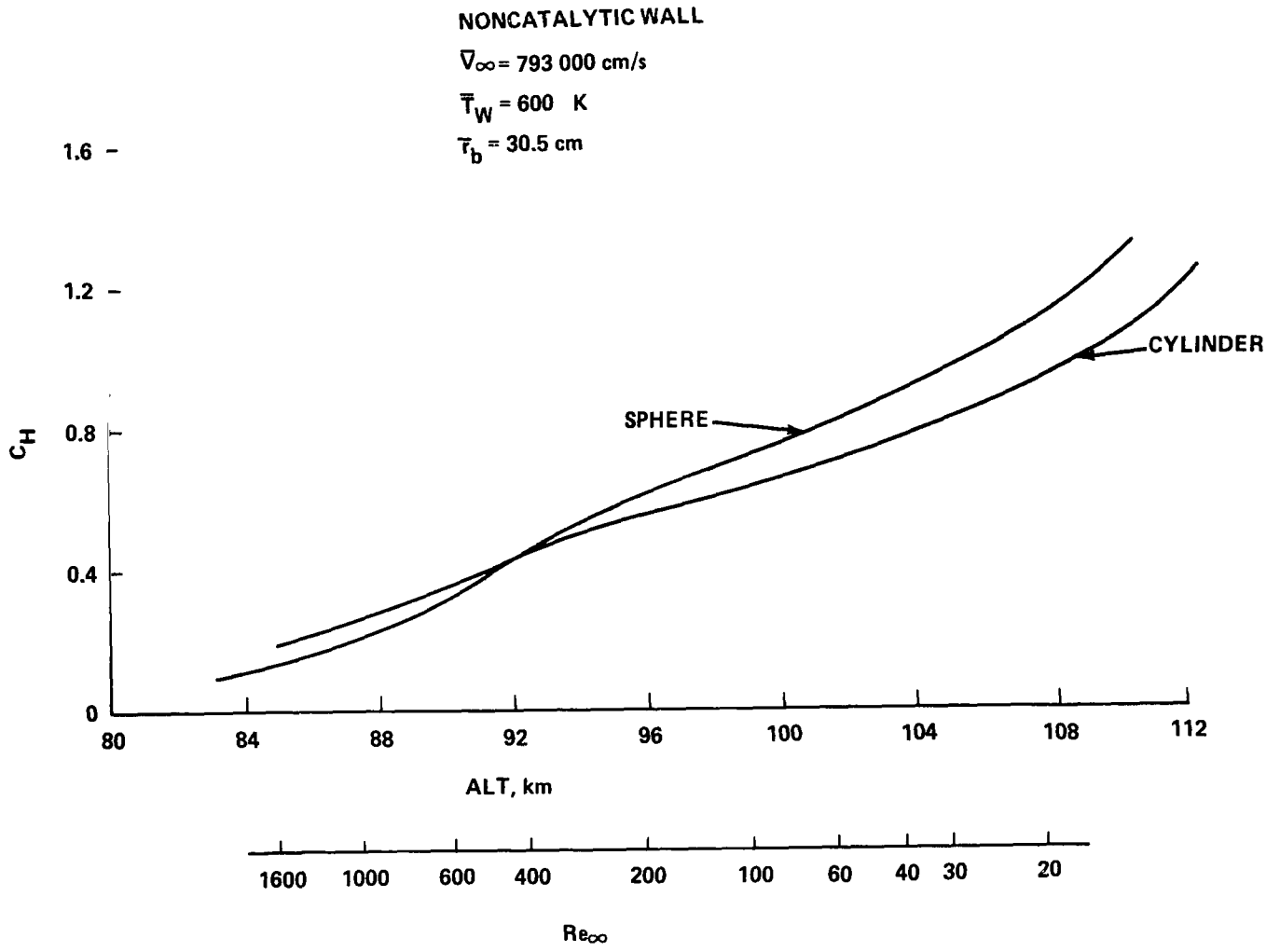

Figure 12. Stagnation point heat transfer coefficients for spheres and cylinders as a function of altitude.

in C_H with increasing altitude. The theoretical free molecular value ($C_H = 1.0$) is exceeded for the sphere at approximately 106 km and for the cylinder at approximately 109 km. The curves continue to climb with increasing slope at higher altitudes. This unrealistic behavior for a fixed wall temperature might be attributed to a breakdown in the continuum approach (Navier-Stokes equations with slip boundary conditions) at extremely high altitudes and low densities. In particular, the assumption of a thin Knudsen layer, which is implicit in the present analysis, becomes invalid at very low densities. One must also consider the practicality of a specified T_w in rarefied flow. This breakdown is gradual, and one cannot pinpoint a sharp boundary beyond which the program gives invalid results. However, the results should be treated with increasing skepticism, for this body size and flow conditions, at altitudes greater than approximately 104 km, or $Re_\infty < 40$.

An interesting feature of Figure 12 is the crossover of the curves for the sphere and cylinder. This crossover should not be attributed to the differences in viscosity computation because the effects of Hansen's viscosity (used for the sphere but not for the cylinder) is to increase C_H at low altitudes but not to affect C_H at high altitudes where dissociation is negligible. Therefore, if Hansen's viscosity were also used for the cylinder, the crossover of the two curves should be expected at a higher altitude. The explanation for this crossover is a result of the stronger merged shock layer effect on the sphere.

The variation of C_H with freestream speed for a sphere at fixed altitude (96 km) and wall temperature (600 K) is shown in Figure 13. The effect of increasing freestream speed, or stagnation enthalpy, is to decrease C_H.

Figure 14 gives the variation in C_H with wall temperature for a sphere at fixed altitude (96 km) and speed (793 000 cm/sec). An increase in wall temperature produces an increase in C_H.

The data in Figures 12 through 14 are replotted in Figure 15 as a function of K^2; the similarity parameter is given by equation (62). This parameter includes all the independent variables in Figures 12, 13, and 14, but the effect of freestream density is obviously dominant in determining the value of K^2 and C_H. The data were also plotted as a function of other similarity parameters (not shown), but K^2 correlated the data as well as, or better than, any of the other parameters. This is not the case if wall catalysis is varied. Therefore, K^2 was selected as the similarity parameter to use in presenting the remainder of the data.

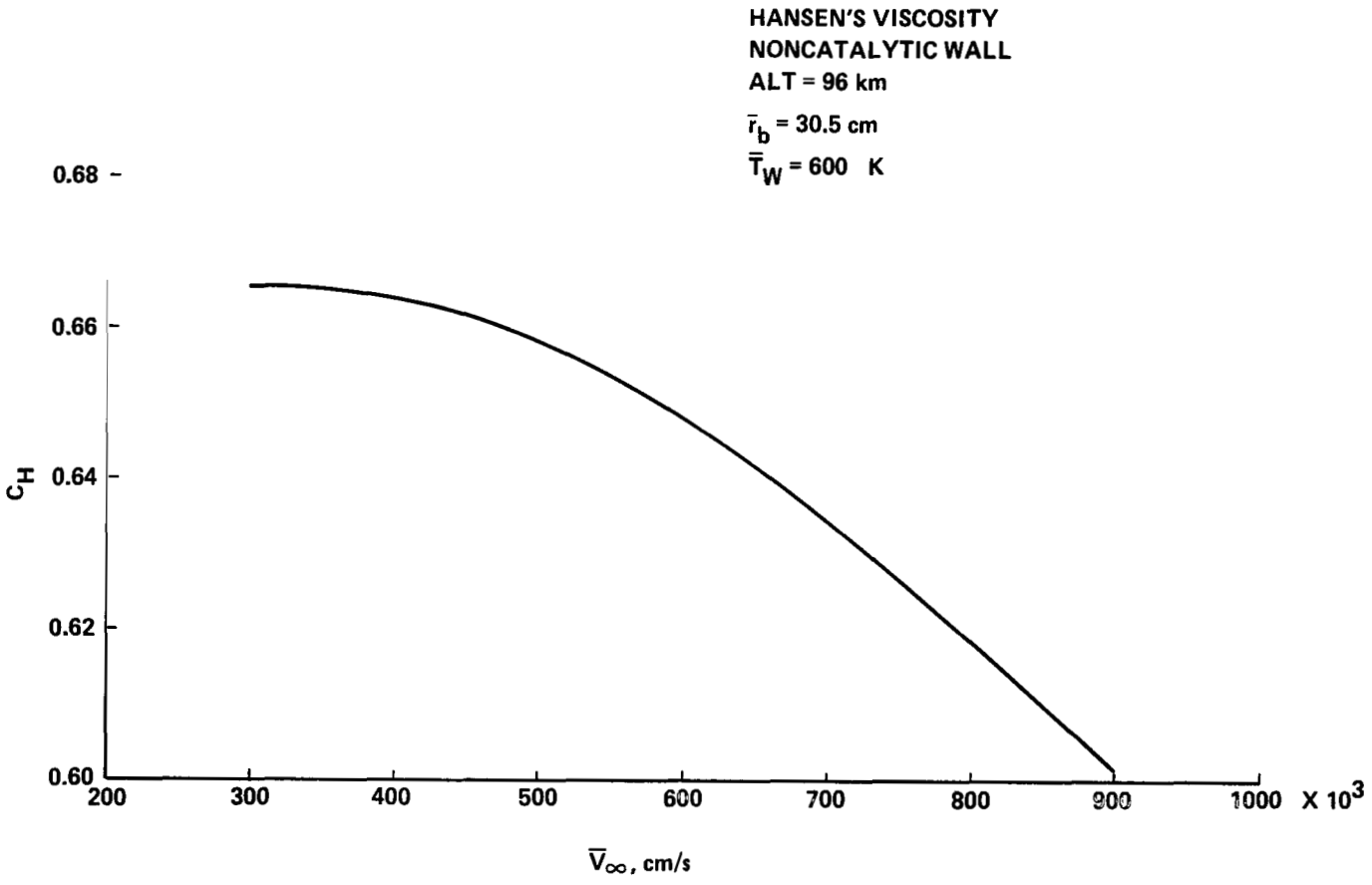

Figure 13. Stagnation point heat transfer coefficient for sphere as function of freestream speed.

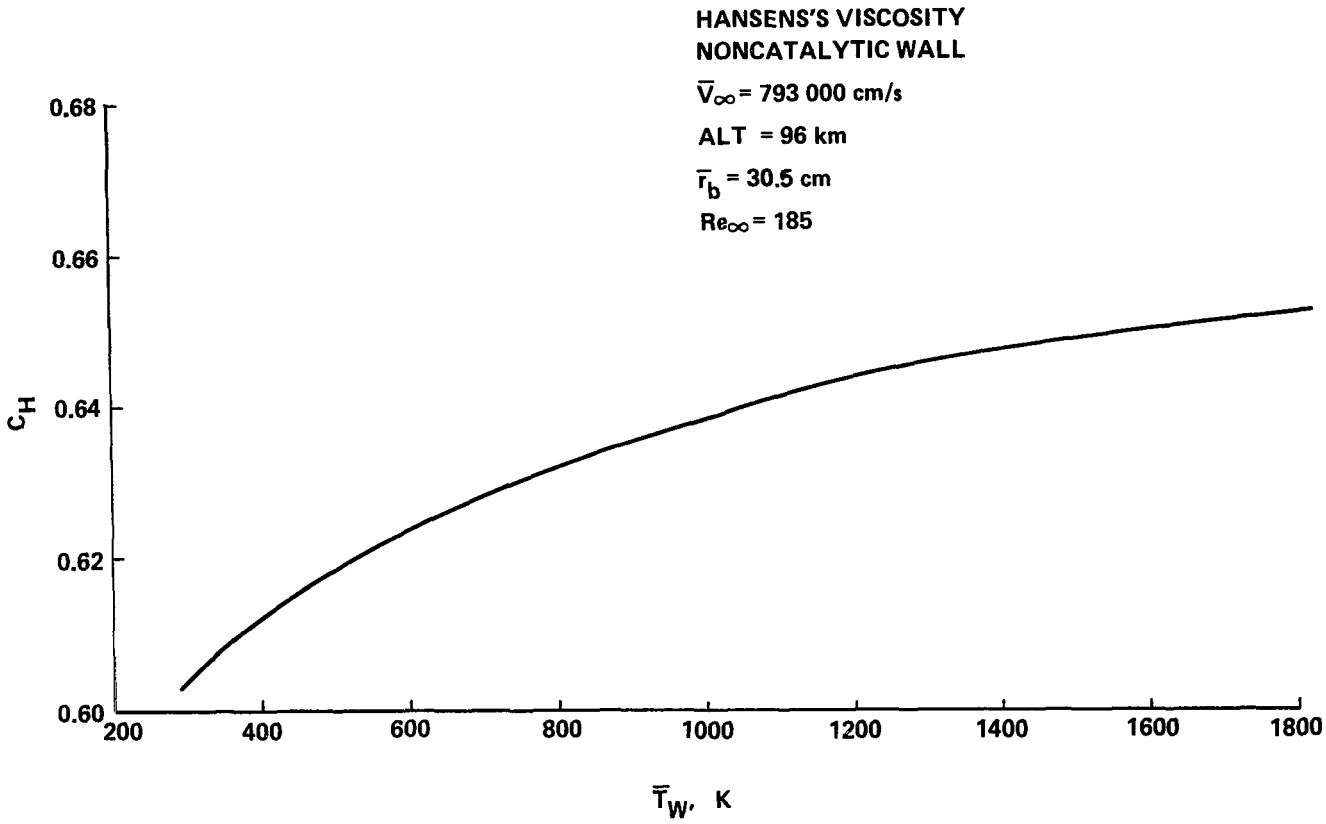

Figure 14. Stagnation point heat transfer coefficient for sphere as function of wall temperature.

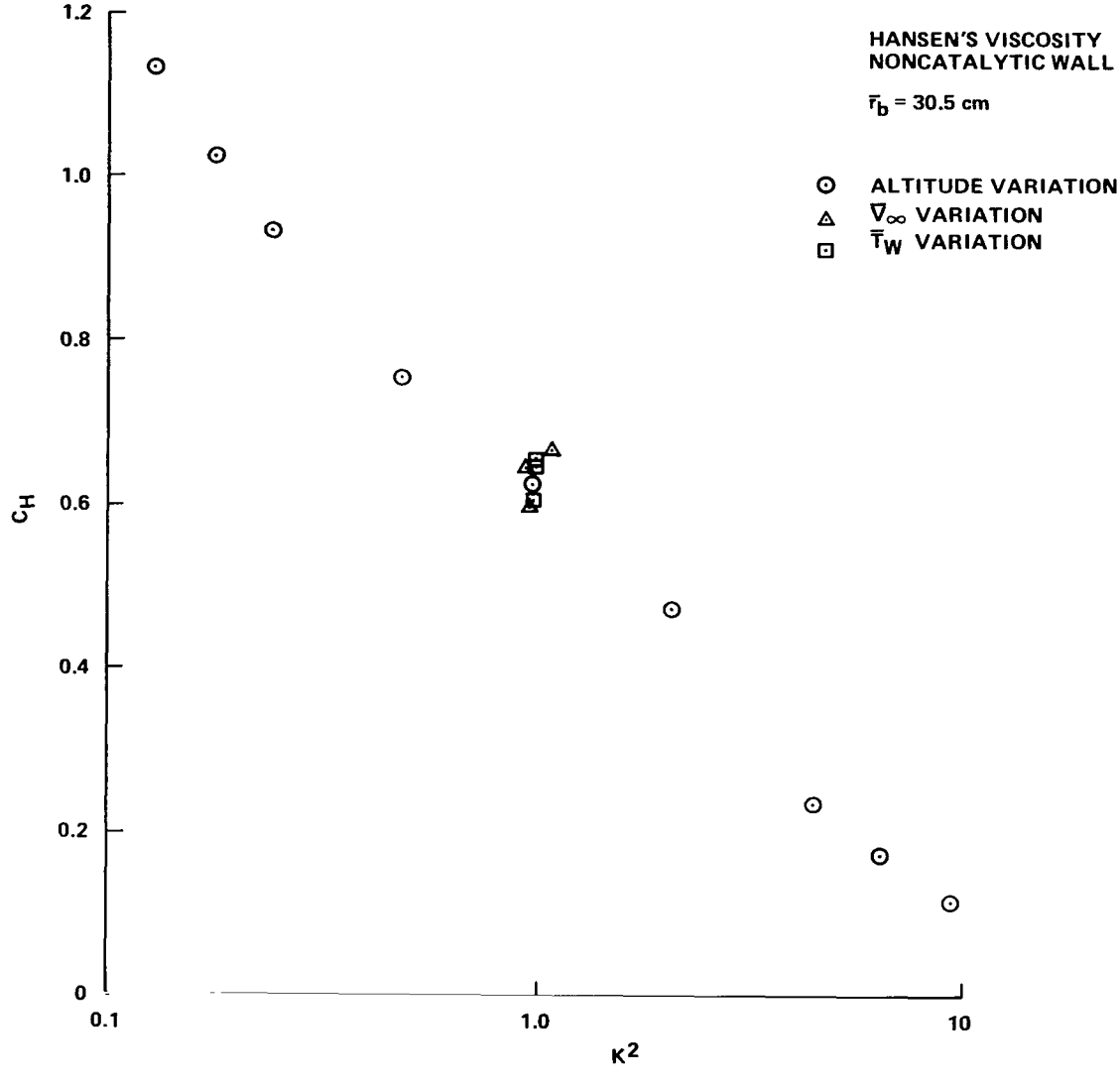

Figure 15. Stagnation point heat transfer coefficient for sphere as function of K^2.

Figure 16 gives the nondimensional shock layer thickness, n_∞, for spheres and cylinders as a function of K^2. The shock layer is thin at the continuum end (large K^2) of the flow regime and becomes very thick at highly rarefied conditions (small K^2).

Figure 17 presents the computed slip speed for a sphere and cylinder as a function of K^2. The slip speed is computed at the outer edge of the Knudsen layer, but it is applied at the wall in the outer flow solution, i.e., a thin Knudsen layer is assumed. This is a source of error at high altitudes where the Knudsen layer thickness becomes significant. The slip speed is greatly affected by variation in freestream speed and wall temperature. However, these effects are not correlated well by the parameter K^2 as shown for the sphere by the partially filled symbols. To estimate the slip speed for given conditions, one can extrapolate from the solid curves using the partially filled symbols as a guide in correcting for freestream speed and wall temperature. Once again it appears that the proper T_W must be used for rarefied flow calculations. The decrease in slip speed with increasing altitude (decreasing K^2) at high altitude (small K^2) seems unrealistic and has been criticized. However, decreasing slip speed decreases the C_H computed by this program. Since the computed C_H is too large at high altitudes for a fixed T_W (Figs. 12 and 15), the decrease in slip speed at high altitudes tends to compensate for the overprediction of C_H and is, from a practical standpoint, a favorable phenomenon.

The temperature at the edge of the Knudsen layer is given as a function of K^2 in Figure 18. This temperature also depends strongly on freestream speed and wall temperature.

The information in Figures 15 through 18 is useful as input data in running the computer program (Appendix A).

An example of the practical use of this computer program is given in Figure 19. Stagnation point heating rates for the spherical nose of the Space Shuttle External Tank are given as a function of trajectory time. The solid curve is the heating rate predicted by the MSFC Thermal Environment Branch (ED33) and is based on theoretical continuum methods at low altitudes and experimental data at high altitudes. The filled diamond symbols were computed using the present program. The trajectory time interval from approximately 275 to 475 sec corresponds to an altitude interval which is too high for this program, i.e., the predicted values of C_H were unrealistically large. For a

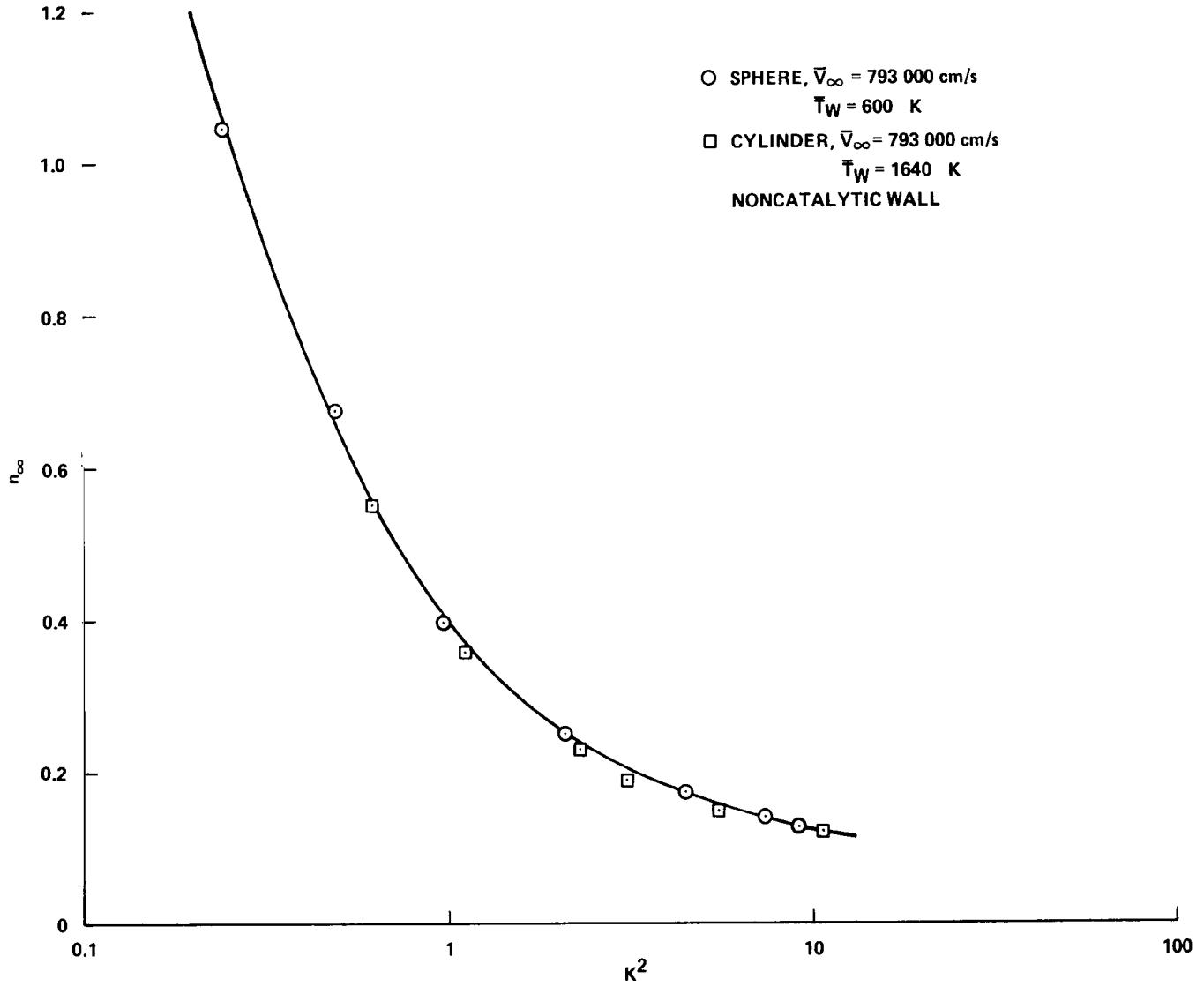

Figure 16. Shock layer thickness for sphere and cylinder.

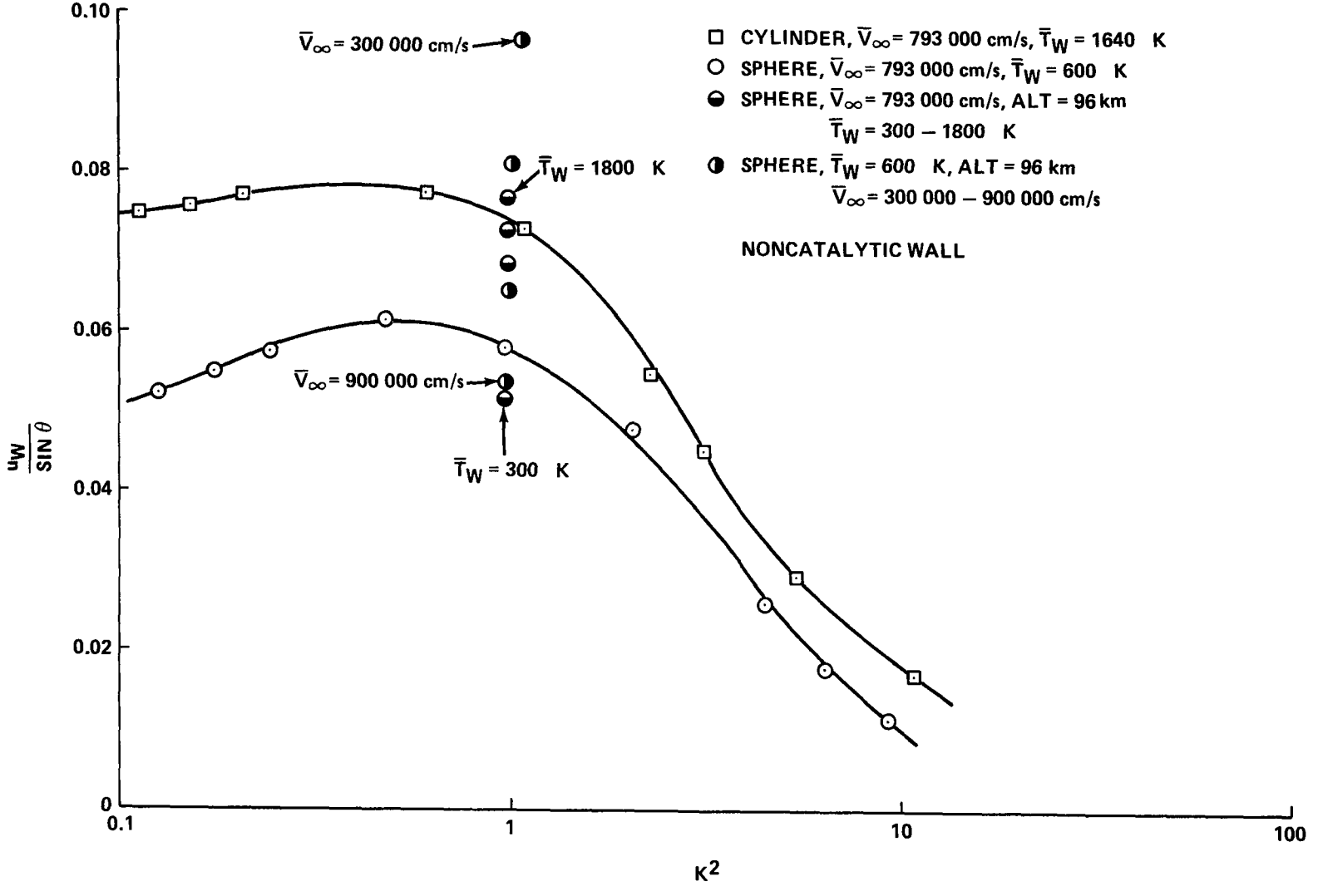

Figure 17. Slip speed at body surface for sphere and cylinder.

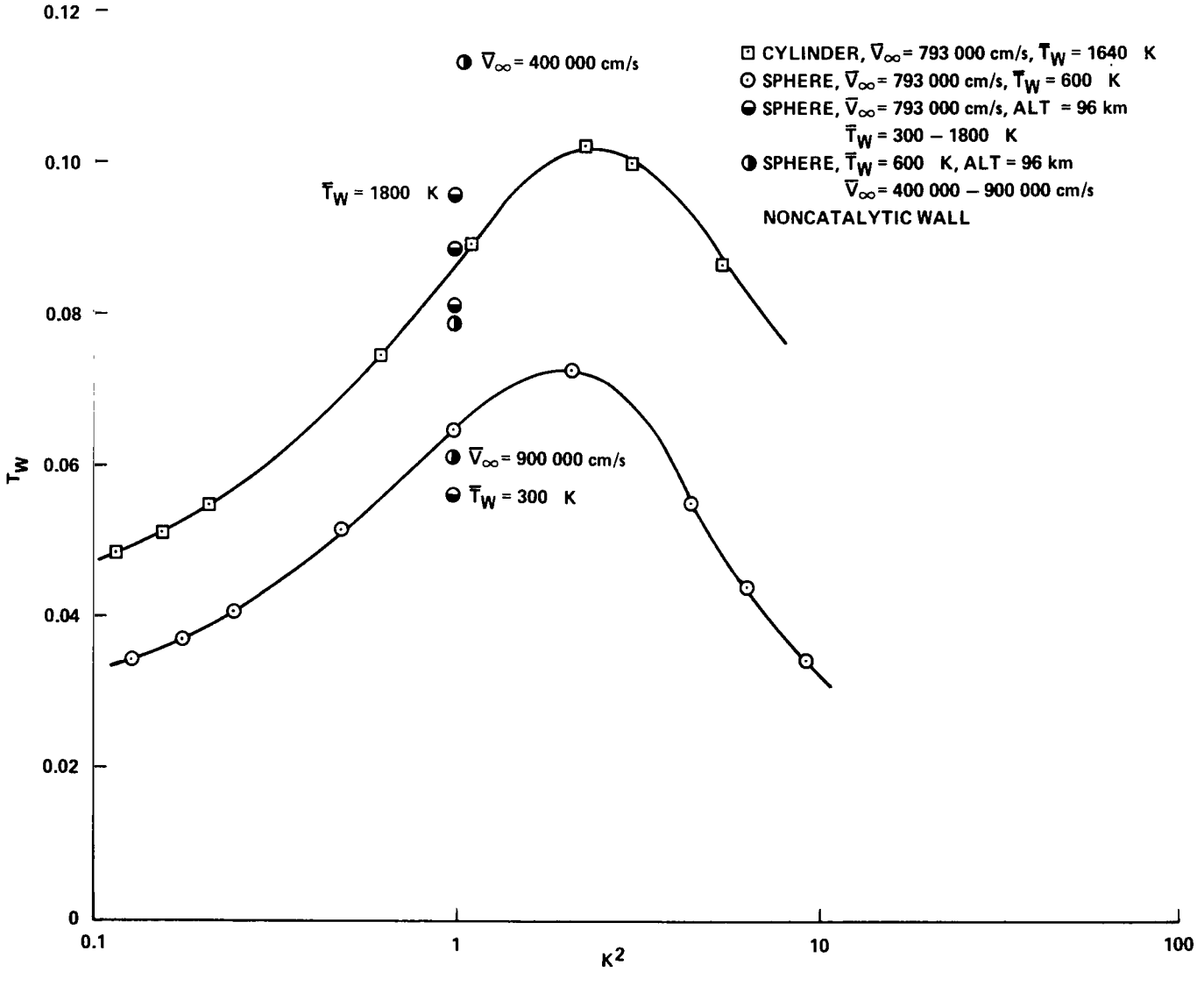

Figure 18. Temperature of air at wall for sphere and cylinder.

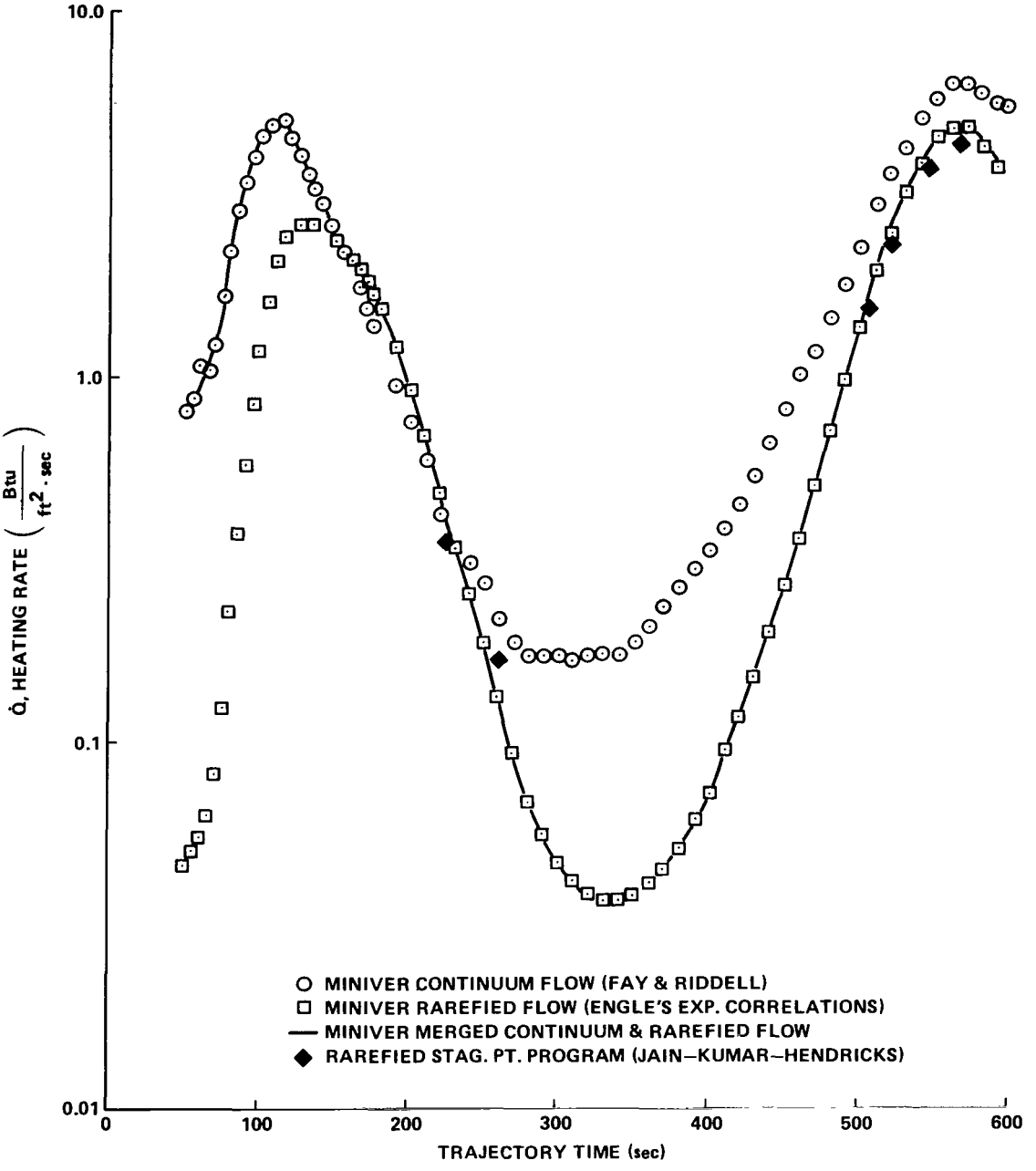

Figure 19. Space Shuttle external tank stagnation point heating rate.

body of this size ($\bar{r}_b = 30.5$ cm), the altitude interval for which this program is applicable is approximately 86 to 105 km. For this altitude interval, the predicted values from this program agree quite well with the predictions from experimental data for a known T_w.

APPENDIX A. COMPUTER PROGRAM

APPENDIX A. COMPUTER PROGRAM

General Information

The computer program is written in Fortran IV language, and it is run on the Univac 1108 computer at MSFC. As currently written, the program is limited to a maximum of 2000 iterations. If convergence is not achieved in 2000 iterations, the program is rerun using the output from the first run as starting data for the second run.

The program has three options:

(1) Body: sphere or two-dimensional circular cylinder

(2) Wall catalyticity: noncatalytic wall or fully catalytic wall

(3) Viscosity: Sutherland or Hansen's high temperature model.

The choices made in options (1) and (2) make very little difference in the computer time used. However, the Hansen viscosity option takes significantly more computer time than the Sutherland option; e.g., if the full 2000 iterations are used, the Sutherland option takes approximately 8 min and the Hansen option takes about 10 min.

Program Input

The quantities needed for input to the program are defined and their functions described as follows:

Computer Program Variable	Symbol Used in Report	Dimensions	Description	Suggested Source or Range of Values
EFFR1	n_∞	Dimensionless	Initial guess for nondimensional shock layer thickness	Figure 16
TOL		Dimensionless	Computation is stopped when C_H converges within a prescribed tolerance. If $\left\|C_{H_N} - C_{H_{N-1}}\right\| < \text{TOL}$, stop program and print results	0.00001 - 0.0001
EPSI		Dimensionless	Maximum change allowed in all computed dimensional quantities from one iteration to the next	0.001 - 0.005

Computer Program Variable	Symbol Used in Report	Dimensions	Description	Suggested Source or Range of Values
ALT		km	Altitude corresponding to the freestream thermodynamic properties (used for identification only)	
RADB	$\bar{r}_b$	cm	Radius of body	
UFS	$\bar{V}_\infty$	cm/s	Freestream speed	
TFS	$\bar{T}_\infty$	K	Freestream temperature	
TWK	$\bar{T}_W$	K	Temperature of body surface	
ROFS	$\bar{\rho}_\infty$	gm/cm^3	Freestream density	
U(1)	$u_{1w} = u_W/\sin\theta$	Dimensionless	Initial guess for (slip speed)/$\sin\theta$	Figure 17
T(1)	T_{1w}	Dimensionless	Initial guess for nondimensional temperature of gas at outer edge of Knudsen layer	Figure 18
U(I)	u_1	Dimensionless	Initial guess for u_1 (see equation 18) at location I (I = 2, 3, ..., 50)	Figures 5-7
V(I)	v_1	Dimensionless	Initial guess for v_1 (see equation 19) at location I (I = 2, 3, ..., 50)	Figures 5-7
T(1)	T_1	Dimensionless	Initial guess for T_1 (see equation 20) at location I (I = 2, 3, ..., 50)	Figures 5-7
RO(I)	ρ_1	Dimensionless	Initial guess for ρ_1 (see equation 21) at location I (I = 2, 3, ..., 50)	Figures 5-7
P2(I)	P_2	Dimensionless	Initial guess for P_2 (see equation 22) at location I (I = 2, 3, ..., 50)	Figures 5-7
CO2(I)	Y_{O_2}	Dimensionless	Initial guess for mass fraction of O_2 at location I (I = 2, 3, ..., 50)	Figures 5-7

Computer Program Variable	Symbol Used in Report	Dimensions	Description	Suggested Source or Range of Values
CNOI(I)	Y_{NO^+}	Dimensionless	Initial guess for mass fraction of NO^+ at location I (I = 2, 3, ..., 50)	Figures 5-7
CNO(I)	Y_{NO}	Dimensionless	Initial guess for mass fraction of NO at location I (I = 2, 3, ..., 50)	Figures 5-7
CN(I)	Y_N	Dimensionless	Initial guess for mass fraction of N at location I (I = 2, 3, ..., 50)	Figures 5-7
CO(I)	Y_O	Dimensionless	Initial guess for mass fraction of O at location I (I = 2, 3, ..., 50)	Figures 5-7

The quantities U(I) through CO(I) must be input for each of the 49 equally-spaced points in the shock layer along the stagnation streamline starting with I = 2 near the wall and ending with I = 50 near the freestream (see Fig. A-1). The wall (I = 1) and freestream (I = 51) boundary conditions are given by the quantities UFS through T(1).

The format for the input data is as follows:

Card	Format	Variable Name(s)	Location and Description
1	12A6	AB1, ..., AB/2	Columns 1-72 contain a comment for project identification
2	3F10.0	XBOD	Columns 1-10 contain the body option (sphere = 1.0, cylinder = 2.0)
		XCAT	Columns 11-20 contain the wall catalyticity option (noncatalytic wall = 1.0, fully catalytic wall)
		XVIS	Columns 21-30 contain the viscosity option (Sutherland viscosity = 1.0, Hansen viscosity = 2.0)
3	2F10.0	CASE	Columns 1-10 contain the run number. This identification is useful to distinguish between runs whenever a rerun is necessary

Card	Format	Variable Name(s)	Location and Description
		EFFR1	Columns 11-20
4	2F10.0	TOL	Columns 1-10
		EPSI	Columns 11-20
5	5F10.0	ALT	Columns 1-10
		RADB	Columns 11-20
		UFS	Columns 21-30
		TFS	Columns 31-40
		TWK	Columns 41-50
6	E13.8	ROFS	Columns 1-13
7	2F10.0	U(1)	Columns 1-10
		T(1)	Columns 11-20
8-56	5E16.9	U(I)	Columns 1-16
		V(I)	Columns 17-32
		T(I)	Columns 33-48
		RO(I)	Columns 49-64
		P2(I)	Columns 65-80
57-105	5E16.9	CO2(I)	Columns 1-16
		CNOI(i)	Columns 17-32
		CNO(I)	Columns 33-48
		CN(I)	Columns 49-64
		CO(I)	Columns 65-80

PROGRAM OUTPUT

The program printout is described in this section. Figure 5 of the text was obtained from this printout. Explanation of the printout follows.

Title Page

Options used — The options which were selected for body, wall catalyticity, and viscosity are printed out here.

Input data — The input data are printed out for record.

Computed freestream data — Some freestream quantities which are used for nondimensionalizing and for computation of various similarity parameters are printed here. The equations used are as follows:

$$\text{VSOUND} = \sqrt{\gamma \bar{R} \bar{T}_\infty} \quad [\text{cm/sec}] \quad , \tag{A-1}$$

where

$$\gamma = 1.4$$

$$\bar{R} = 2.8708 \times 10^6 \ \text{cm}^2/\text{sec}^2\text{K} \quad .$$

$$M_\infty = \text{AMACH} = \frac{\text{UFS}}{\text{VSOUND}} \tag{A-2}$$

$$\bar{T}_{0\infty} = \text{STAGFS} = \bar{T}_\infty \left(1 + \frac{\gamma - 1}{2} M_\infty^2\right) \quad [°\text{K}] \tag{A-3}$$

$$\bar{\mu}_\infty = \text{RTFS} = \frac{1.458 \times 10^{-5} \bar{T}_\infty}{\bar{T}_\infty + 110.4} \quad [\text{gm/cm}\cdot\text{sec}] \tag{A-4}$$

$$\bar{\mu}_{0\infty} = \text{RTSTAG} = \frac{1.458 \times 10^{-5} \bar{T}_{0\infty}}{\bar{T}_{0\infty} + 110.4} \quad [\text{gm/cm}\cdot\text{sec}] . \tag{A-5}$$

It is recognized that the stagnation temperature, equation (A-3), has little physical meaning at the high stagnation enthalpies for which this computer program is intended. This is because equation (A-3) is based on the assumption of constant specific heat for temperatures up to $\bar{T}_{0\infty}$; the assumption of constant specific heat is violated at moderate temperatures. However, $\bar{T}_{0\infty}$ is used only for nondimensionalizing and for computing $\bar{\mu}_{0\infty}$. It does not influence the computation of the flow field in any way. Likewise, $\bar{\mu}_{0\infty}$ is a fictitious viscosity because $\bar{T}_{0\infty}$ is fictitious and also because the Sutherland formula is not applicable at high temperatures.

Similarity Parameters — Some similarity parameters are printed out here. Several of these have been used, with some success, in correlating hypersonic or low density data. The similarity parameters are defined as follows:

$$Re_{\infty} = REYF = \frac{\bar{\rho}_{\infty} \bar{V}_{\infty} \bar{r}_b}{\bar{\mu}_{\infty}} , \tag{A-6}$$

$$Re_{0\infty} = REYN = \frac{\bar{\rho}_{\infty} \bar{V}_{\infty} \bar{r}_b}{\bar{\mu}_{0\infty}} , \tag{A-7}$$

$$Re_{w} = REWALL = \frac{\bar{\rho}_{\infty} \bar{V}_{\infty} \bar{r}_b}{\bar{\mu}_{w}} , \tag{A-8}$$

where $\bar{\mu}_w$ is computed by the Sutherland formula using $\bar{T}_w$.

$$K_{n_{\infty}} = XKNFS = \frac{\bar{\lambda}_{\infty}}{\bar{r}_b} , \tag{A-9}$$

$$\bar{V} = \text{VBAR} = M_\infty \sqrt{\frac{C_\infty}{Re_\infty}} \quad , \tag{A-10}$$

where

$$C_\infty = \frac{\bar{\mu}_w}{\bar{\mu}_\infty} \frac{\bar{T}_\infty}{\bar{T}_w} \quad .$$

$$K^2 = \text{XKSQ} = \frac{Re_\infty}{\gamma_\infty M_\infty^2 C_*} \quad , \tag{A-11}$$

where

$$C_* = \frac{\bar{\mu}_*}{\bar{\mu}_\infty} \frac{\bar{T}_\infty}{\bar{T}_*}$$

and

$$T_* = \frac{1}{2} (\bar{T}_{0\infty} + \bar{T}_w)$$

$\bar{\mu}_*$ = Sutherland viscosity computed at $\bar{T}_*$.

The similarity parameter ϕ is given as the final item in the printout. It is placed in this location because it uses the computed enthalpy at the wall. This parameter was suggested by Potter (Rarefied Gas Dynamics, Supplement 5, Vol. I, 1969).

$$\phi = \text{PHI} = Re_w \left(\frac{2\bar{h}_w}{\bar{V}_\infty^2} \right)^{0.6} \quad . \tag{A-12}$$

Data Pages

A set of computed data is printed out after every 200 iterations. Each set of data consists of three pages.

1. First Page. The computed shock layer thickness (EFFR) and wall heat transfer coefficient (C_H) are printed at the top of the page after every 50 iterations. The control factors which are used to update the computed quantities to obtain input variables for the next iteration are also printed here.

The columns on this page give nondimensional values of (1) radial position from the center of the body to the equally-spaced points at which the independent variables are computed, (2) the velocity component u_1 [see equation (18)], (3) the velocity component v_1 [see equation (19)], (4) specific enthalpy, (5) temperature, (6) viscosity ratio, local ratio of Hansen viscosity to Sutherland viscosity, (7) pressure P_1 [see equation (22)], (8) pressure correction P_2 [see equation (22)], and (9) density.

Note that VFS is the same as UFS elsewhere in the program. It is the freestream speed $\bar{V}_\infty$.

2. Second Page. This page gives the reaction rates for each of the seven species.

3. Third Page. This page gives the mass fractions of the chemical species which compose the air. Note that mass fraction was denoted by "Y" in the text rather than by "C." The electron number density is also given.

When C_H converges within the prescribed tolerance, or when the iterations reach 2000, the iterations are stopped and the final data set is printed out. At this point a set of 98 cards is punched to record the velocity and thermodynamic data given on page 1 and the mass fraction data on page 3 of the data printout. This set of cards can then be used as starting data for a new run.

To determine whether or not the program has converged sufficiently and whether the results are reasonable, the following checks are suggested.

(1) Check EFFR for convergence

(2) Check C_H for convergence

(3) Check the slip conditions for convergence, i.e. compare U1 and T at RAD/RADB = 1.0 for the last few sets of data

(4) Scan the velocity component and thermodynamic property columns to determine if the profiles are smooth and the values are reasonable

(5) Scan the mass fraction columns to check for reasonable behavior. Particularly check the N_2 column near the wall to determine if these mass fractions exceed the freestream value.

SOME DIFFICULTIES ENCOUNTERED IN RUNNING PROGRAM

The program generally runs without much difficulty if the starting data are within reasonable bounds; however, problems do occur, and some of the most common problems are discussed as follows.

1. Failure of EFFR to Converge. The shock layer thickness, EFFR, usually is the first quantity to converge; however, it sometimes diverges. The most common cause of this is using starting data from a run with a much different stagnation enthalpy, or $\bar{T}_{0\infty}$, from the case being run. This causes a discontinuity in the nondimensional temperature profile between the points I = 50 and I = 51 because the point I = 50 comes from the starting data from a previous run and point I = 51 is the freestream boundary condition. The decision on whether to decrease, increase, or not change EFFR is made on the basis of the temperature gradient near the freestream (see Appendix B). Therefore, if a sizable discontinuity in temperature exists at this location, EFFR will diverge.

One solution to this problem is to modify the last few input cards to make a smooth transition in the temperature profile to the freestream temperature. Probably a better solution would be to change the nondimensionalizing temperature from $\bar{T}_{0\infty}$ to $\bar{T}_{\infty}$. This would guarantee a smooth transition, in the starting data, to the freestream temperature. To prevent divergence of EFFR, the program has been modified to restrict EFFR within the range

$$\frac{1}{2}\,\text{EFFR1} \leq \text{EFFR} \leq \frac{3}{2}\,\text{EFFR1} \quad .$$

If EFFR1 is not guessed closely enough, this restriction will necessitate a rerun using a different EFFR1.

2. Unrealistic Chemical Composition. If the species mass fractions in the starting data are greatly different from the true values for the case being run, unrealistic computed mass fractions can result. This can lead to unrealistic computed values for all other quantities. For example, this might occur for a rather low speed, high density case in which dissociation should be negligible (Fig. 11). However, since starting data from a low speed, high density run were not available, data were used from a high speed, high density run in which the degree of dissociation was high. The program could not handle the grossly incorrect starting data, and the computed results became more and more unrealistic from one iteration to the next. The unrealistic data included mass fractions for N_2 much larger than the freestream value, negative C_H (heat transferred from the body to the gas) and a monotonically increasing EFFR beyond reasonable bounds (Fig. 16). Note that C_H was called "STANC" in the older printout.

SOME SUGGESTIONS FOR RUNNING PROGRAM

To minimize the previously discussed problems and to facilitate operation of the program, the following suggestions on input data are made.

1. EFFR1, U(1), T(1), and TOL. Figures 16, 17, and 18 can be used for obtaining initial guesses for EFFR1, U(1), and T(1), respectively. The value for TOL probably should be set smaller than the desired tolerance on C_H to assure that the other quantities converge also. A value of 0.00001 for TOL was used in most of the runs made for this report.

2. Velocity, Thermodynamic Property, and Mass Fraction Profiles. For best results, the starting data profiles for the quantities U(I) through CO(I) should be obtained from a run which matches the required freestream conditions of the new run as closely as possible. Close matching is especially important at low altitude, high density conditions for which gradients in the flow properties are large. The question arises as to what constitutes a

sufficiently close "match" and which matching, or similarity, parameter should be used. If every freestream and body condition is matched fairly closely, it is unnecessary to use a similarity parameter. From experience, it is found that, for a given body, changes in freestream density, $\bar{\rho}_\infty$, and speed, $\bar{V}_\infty$, in that order, have the greatest effect on the outcome of the run. Therefore, for bodies of the same size, one should try to match $\bar{\rho}_\infty$ and $\bar{V}_\infty$. A good rule of thumb is that $\bar{\rho}_\infty$ for the new run should not differ from $\bar{\rho}_\infty$ for the starting data run by more than the equivalent of 3 km altitude in the standard atmosphere. Near the low altitude extreme of the program's capability, this difference should not be more than approximately 1 km. A difference in $\bar{V}_\infty$ of approximately 2000 m/sec can usually be tolerated. For bodies of greatly different size, one should probably use a similarity parameter, such as K^2, to match starting data to the new run.

Figures 5, 6, and 7 can be used for starting data. If the desired freestream properties for the new run are farther removed from those of Figures 5, 6, and 7 than the previously suggested increments, it is advisable to reach the desired conditions in two or more runs. If severe difficulties like those previously discussed are encountered, it is probably best to go back to a "good," or converged, set of starting data and use smaller increments in freestream properties rather than to use the output of the "bad" run as starting data for a rerun. If the program is used frequently, a library of starting data card sets can be built up to cover the range of possible freestream conditions for which the program is applicable.

3. Hansen-Sutherland Viscosity Option. If the computed ratio of Hansen's viscosity to Sutherland's viscosity is approximately 1.0 for a given set of freestream conditions, one can use the Sutherland viscosity option for nearby freestream conditions to reduce computer time.

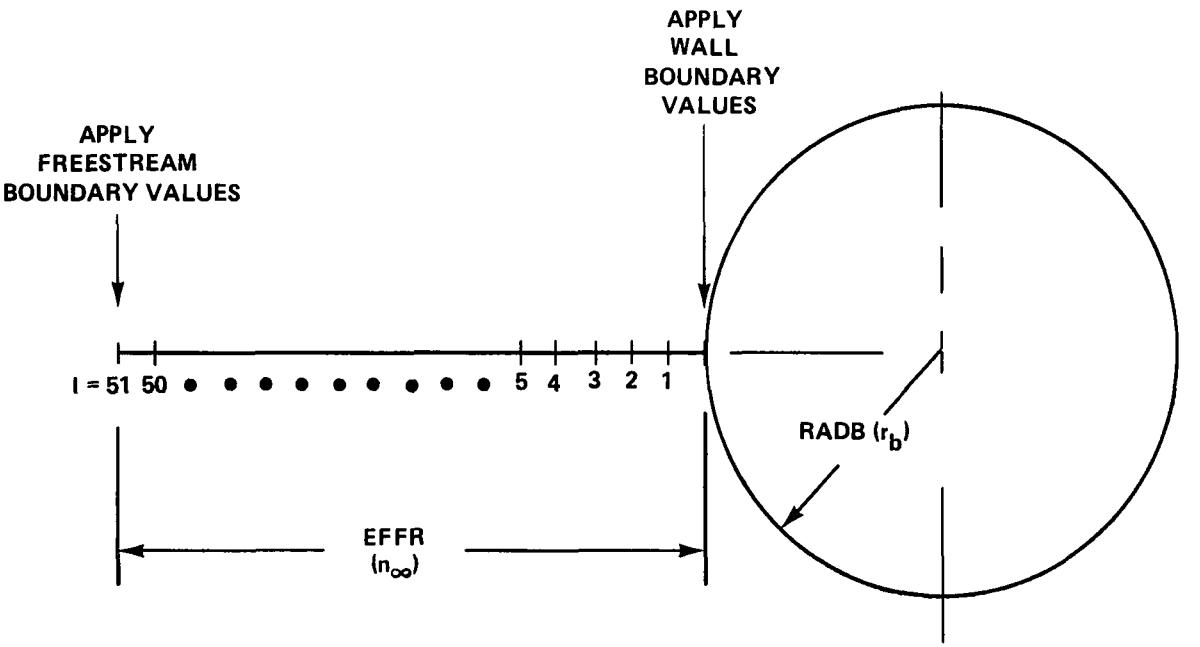

Figure A-1. Location of computation points.

APPENDIX B. LISTING OF PROGRAM

```
00100     1*     C     SUCCESSIVE ACCELERATED REPLACEMENT METHOD                                  000000
00100     2*     C     NONEQUILIBRIUM FLOW IN THE MERGED SHOCK LAYER OF A BLUNT BODY              000000
00100     3*     C     NEAR THE STAGNATION REGION USING FULL N.S. EQUATIONS                       000000
00100     4*     C     SLIP CONDITIONS AT THE WALL                                                000000
00100     5*     C     CATALYTIC OR NONCATALYTIC WALL                                             000000
00100     6*     C     ************************************************************               000000
00100     7*     C                                                                                000000
00101     8*           DIMENSION U(100),V(100),T(100),H(100),P(100),P2(100),RT(100),              000000
00101     9*          1D(100),RAD(100),X(100),C02(100),CNZ(100),CNO(100),CN(100),CO(100),         000000
00101    10*          1CNOI(100),CEL(100),RO(100)                                                000000
00103    11*           DIMENSION W02(100),WN2(100),WNO(100),WN(100),WO(100),WNOI(100),           000001
00103    12*          1WEL(100),PEL(100)                                                         000001
00104    13*           DIMENSION HN2(100),H02(100),HO(100),HN(100),HNO(100),HNOI(100)            000001
00105    14*           DIMENSION HEL(100)                                                        000001
00106    15*           DIMENSION C1(10),C2(10),C3(10),PP1(10),W(10),EL(10)                       000001
00106    16*     C                                                                               000001
00106    17*     C     INPUT HANSEN'S VISCOSITY DATA                                             000001
00107    18*           DIMENSION XMUSU(100),TABS(100),XMURAT(100),XMU(100)                       000001
00110    19*           DIMENSION TEMP(37),TAB1(37),TAB2(37),TAB3(37),TAB4(37)                    000001
00111    20*           DATA TEMP /2000.0,2500.0,3000.0,3500.0,4000.0,4500.0,5000.0,              000001
00111    21*          1 5500.0,6000.0,6500.0,7000.0,7500.0,8000.0,8500.0,9000.0,9500.0,          000001
00111    22*          2 10000.0,10500.0,11000.0,11500.0,12000.0,12500.0,13000.0,13500.0,         000001
00111    23*          3 14000.0,14500.0,15000.0,15500.0,16000.0,16500.0,17000.0,17500.0,         000001
00111    24*          4 18000.0,18500.0,19000.0,19500.0,20000.0/                                 000001
00113    25*           DATA TAB1 /0.886,0.846,0.830,0.815,0.803,0.792,0.782,0.773,0.764,         000001
00113    26*          1 0.757,0.750,0.743,0.737,0.731,0.725,0.720,0.715,0.710,0.706,             000001
00113    27*          2 0.701,0.697,0.693,0.689,0.685,0.681,0.677,0.672,0.668,0.664,             000001
00113    28*          3 0.660,0.656,0.651,0.647,0.643,0.639,0.635,0.630/                         000001
00115    29*           DATA TAB2 /0.742,0.705,0.676,0.650,0.628,0.608,0.591,0.575,0.561,         000001
00115    30*          1 0.548,0.536,0.524,0.514,0.504,0.495,0.486,0.478,0.470,0.463,             000001
00115    31*          2 0.456,0.448,0.443,0.437,0.431,0.426,0.420,0.415,0.407,0.401,             000001
00115    32*          3 0.395,0.389,0.384,0.376,0.371,0.365,0.359,0.352/                         000001
00117    33*           DATA TAB3 /0.468,0.457,0.445,0.434,0.423,0.412,0.401,0.397,0.380,         000001
00117    34*          1 0.366,0.353,0.342,0.331,0.321,0.313,0.304,0.297,0.290,0.283,             000001
00117    35*          2 0.281,0.270,0.266,0.261,0.256,0.252,0.247,0.243,0.236,0.230,             000001
00117    36*          3 0.224,0.218,0.213,0.206,0.201,0.196,0.190,0.185/                         000001
00121    37*           DATA TAB4 /123.30,122.20,120.80,118.10,114.80,109.70,120.00,              000001
00121    38*          1 89.90,75.60,64.50,55.70,48.60,42.80,37.90,33.80,30.40,27.40,             000001
00121    39*          2 24.90,22.70,20.80,19.09,17.60,16.27,15.10,14.04,13.09,12.24,             000001
00121    40*          3 11.25,10.38,10.48,10.01,9.50,9.01,8.75,8.01,7.51,7.68/                   000001
00121    41*     C                                                                               000001
00121    42*     C     ************************************                                      000001
00121    43*     C                                                                               000001
00123    44*           READ(5,702)AB1,AB2,AB3,AB4,AB5,AB6,AB7,AB8,AB9,AB10,AB11,AB12             000001
00141    45*       702 FORMAT(12A6)                                                              000022
00142    46*           READ(5,700)   XBOD,XCAT,XVIS                                              000022
00147    47*           READ(5,700)CASE,EFFR1                                                     000032
00153    48*           READ(5,700)TOL,EPSI                                                       000041
00157    49*           READ(5,700)ALT,RADB,UFS,TFS,TWK                                           000050
00166    50*       700 FORMAT(6F10.0)                                                            000062
00167    51*           READ(5,701)IROFS                                                          000062
00172    52*       701 FORMAT(I3.8)                                                              000070
00173    53*           EFFR=EFFR1                                                                000070
00174    54*           ICASE=CASE                                                                000072
00174    55*     C                                                                               000072
```

```
MAIN                                                                    DATE 120877

00174    56*     C     ****************************************                000072
00174    57*     C                                                             000072
00174    58*     C     BOUNDARY CONDITIONS AT THE BODY                         000072
00175    59*           READ(5,700)U(1),T(1)                                    000101
00201    60*           V(1)=0.                                                 000110
00201    61*     C     ****************************************                000110
00201    62*     C                                                             000110
00201    63*     C     EL REPRESENTS LEWIS NUMBER AND A IS AVAGADRO NUMBER      000110
00202    64*           DO 1 K=1,7                                              000114
00205    65*         1 EL(K)=1.4                                               000114
00207    66*           EL1=1.4                                                 000116
00210    67*           EL2=1.4                                                 000117
00211    68*           PR=0.75                                                 000120
00212    69*           GAMMA=1.4                                               000122
00213    70*           SC1=PR/EL1                                              000123
00214    71*           SC2=PR/EL2                                              000125
00214    72*     C                                                             000125
00214    73*     C     ****************************************                000125
00214    74*     C                                                             000125
00214    75*     C     PRINT PROGRAM TITLE AND INPUT DATA                      000125
00215    76*           PRINT 10                                                000130
00217    77*        10 FORMAT(1H1,///25X,'HYPERSONIC, MERGED SHOCK LAYER, STAGNATION LINE   000134
00217    78*          1 FLOW FIELD FOR SPHERE OR CIRCULAR CYLINDER')           000134
00220    79*           PRINT 11                                                000134
00222    80*        11 FORMAT(/50X,'JAIN-KUMAR-HENDRICKS PROGRAM')             000140
00223    81*           PRINT 12                                                000140
00225    82*        12 FORMAT(45X,'(OBTAINED FROM BILL HENDRICKS, JULY 1975)')  000144
00226    83*           PRINT 13                                                000144
00230    84*        13 FORMAT(////40X,'FEATURES: SIMILARITY SOLUTION OF NAVIER-STOKES EQU   000150
00230    85*          1ATIONS')                                                000150
00231    86*           PRINT 14                                                000150
00233    87*        14 FORMAT(50X,'NONEQUILIBRIUM CHEMISTRY'                   000154
00233    88*          1  /50X,'SLIP BOUNDARY CONDITIONS')                      000154
00234    89*           PRINT 19                                                000154
00236    90*        19 FORMAT(//31X,'AVAILABLE OPTIONS:')                      000160
00237    91*           PRINT 21                                                000160
00241    92*        21 FORMAT(50X,35H1. BODY: (A) SPHERE OR (B) CYLINDER)      000164
00242    93*           PRINT 22                                                000164
00244    94*        22 FORMAT(50X,  '2. WALL CATALYTICITY: (A) NONCATALYTIC WALL OR (B) F   000170
00244    95*          1ULLY CATALYTIC WALL')                                   000170
00245    96*           PRINT 23                                                000170
00247    97*        23 FORMAT(50X, '3. VISCOSITY: (A) SUTHERLAND OR (B) HANSEN''S HIGH TE   000174
00247    98*          1MP. MODEL(NACA TR R-50)')                               000174
00250    99*           PRINT 24                                                000174
00252   100*        24 FORMAT(//35X,'MODIFICATIONS:')                          000200
00253   101*           PRINT 25                                                000200
00255   102*        25 FORMAT(50X,'1. 9/2/76 (KEN JOHNSTON) ENTHALPY COMPUTATION MODIFIED   000204
00255   103*          1 TO ALLOW FOR PARTIALLY'/55X,'EXCITED VIBRATIONAL STATE (VINCENTI    000204
00255   104*          2AND KRUGER, P.135) STATEMENTS 30,130.' /53X, 'PREVIOUS ASSUMPTION    000204
00255   105*          3: FULLY EXCITED VIBRATIONAL STATE')                     000204
00256   106*           PRINT 26                                                000204
00260   107*        26 FORMAT(/50X,'2. 9/27/76 (KEN JOHNSTON) OPTION ADDED TO COMPUTE VISC  000210
00260   108*          1OSITY BY HANSEN''S HIGH TEMP.'/55X,'MODEL. (SUTHERLAND''S FORMULA    000210
00260   109*          2BECOMES INACCURATE AT HIGH TEMP.)')                     000210
00261   110*           PRINT 350                                               000210
00263   111*       350 FORMAT(/50X,'3. 9/29/76 (KEN JOHNSTON) CATALYTIC AND NONCATALYTIC P   000214
```

```
00263   112*        1ROGRAMS COMBINED.*/55X,*(OPTION AVAILABLE TO CHOOSE DESIRED WALL C          000214
00263   113*       2ATALYTIC CONDITION)*)                                                       000214
00264   114*         PRINT 351                                                                  000214
00266   115*       351 FORMAT(/50X,*4. 9/9/76 (KEN JOHNSTON) SPHERE AND CYLINDER PROGRAMS       000220
00266   116*          1 COMBINED.*/55X,*(OPTION AVAILABLE TO CHOOSE DESIRED BODY)*)            000220
00267   117*          PRINT 18,AB1,AB2,AB3,AB4,AB5,AB6,AB7,AB8,AB9,AB10,AB11,AB12             000220
00305   118*        18 FORMAT(///8X, *PROJECT: *,12A6)                                         000240
00306   119*           PRINT 27                                                                000240
00310   120*        27 FORMAT(/13X,*OPTIONS USED:*)                                            000244
00311   121*           IF(XBOD-0.9 .GT. 0.2) GO TO 29                                          000244
00313   122*           PRINT 28                                                                000251
00315   123*        28 FORMAT(27X,*SPHERE*)                                                    000255
00316   124*           GO TO 41                                                                000255
00317   125*        29 PRINT 40                                                                000257
00321   126*        40 FORMAT(27X,*CIRCULAR CYLINDER*)                                         000263
00322   127*        41 IF(XCAT-0.9 .GT. 0.2) GO TO 43                                          000263
00324   128*           PRINT 42                                                                000267
00326   129*        42 FORMAT(27X,*NONCATALYTIC WALL*)                                         000273
00327   130*           GO TO 45                                                                000273
00330   131*        43 PRINT 44                                                                000275
00332   132*        44 FORMAT(27X,*FULLY CATALYTIC WALL*)                                      000301
00333   133*        45 IF(XVIS-0.9 .GT. 0.9) GO TO 47                                          000301
00335   134*           PRINT 46                                                                000305
00337   135*        46 FORMAT(27X,*SUTHERLAND VISCOSITY FORMULA*)                              000311
00340   136*           GO TO 49                                                                000311
00341   137*        47 PRINT 48                                                                000313
00343   139*        48 FORMAT(27X,*HANSEN**S HIGH TEMP VISCOSITY FORMULA*) '                   000317
00344   139*        49 PRINT 15,ICASE,EFFR1,U(1),T(1),TOL,EPSI                                 000317
00354   140*        15 FORMAT(//18X,*RUN NO.:*,I4,                                             000330
00354   141*           1  ///15X,*INPUT DATA:*                                                000330
00354   142*           1  //18X,*EFFECTIVE RADIUS (EFFR) = *,F7.4,*  (STANDOFF DISTANCE/BO    000330
00354   143*           1DY RADIUS)*                                                           000330
00354   144*           2 /36X,*U1(1) = *,F8.5,* (U1BAR(1)/FREESTREAM SPEED)*                  000330
00354   145*           3 /36X,*T1(1) = *,F8.5,* (T1BAR(1)/FREESTREAM STAG. TEMP.)*            000330
00354   146*           4 /4X,*HEAT TRANSFER COEFF. TOLERANCE (TOL) = *F8.6,                   000330
00354   147*           5 /37X,*EPSI = *,F8.6,7)                                               000330
00355   149*           PRINT 16,ALT,RADB,UFS,TFS                                              000330
00363   149*        16 FORMAT(27X,17HALTITUDE (ALT) = ,F9.4,  4H  KM/23X,21HBODY RADIUS (R    000340
00363   150*           1ADB) = ,F9.4,  4H  CM/19X,25HFREESTREAM SPEED (UFS) = ,F11.3,  8H  C  000340
00363   151*           2M/SEC/13X,31HFREESTREAM TEMPERATURE (TFS) = ,F9.4,12H  DEG KELVIN)    000340
00364   152*           PRINT 17,ROFS,TWK                                                      000340
00370   153*        17 FORMAT(16X,*FREESTREAM DENSITY (ROFS) = *,E10.5,*  GM/CM**3*           000346
00370   154*           1 /19X,*WALL TEMPERATURE (TWK) = *,F9.4,*  DEG KELVIN*)              000346
00370   155*     C                                                                           000346
00370   156*     C     **********************************                                    000346
00370   157*     C                                                                           000346
00370   158*     C     COMPUTE AND PRINT FREESTREAM CONDITIONS AND SIMILARITY PARAMETERS      000346
00371   159*           VSOUND=100.0* (1.4*287.08*TFS)**0.5                                    000346
00372   160*           RTFS=(1.458E-05*TFS**1.5)/(TFS+110.4)                                  000357
00373   161*           AMACH=UFS/VSOUND                                                       000371
00374   162*           STAGFS=TFS*(1.0+((GAMMA-1.0)/2.0)*AMACH**2)                            000374
00375   163*           RTSTAG=(1.458E-05*STAGFS**1.5)/(STAGFS+110.4)                          000406
00376   164*           RTWALL=(1.458E-05*TWK**1.5)/(TWK+110.4)                                000416
00377   165*           REYF=UFS*ROFS*RADB/RTFS                                                000430
00400   166*           REYN=REYF*RTFS/RTSTAG                                                  000435
00401   167*           REWALL=REYF*RTFS/RTWALL                                                000441
```

```
00402   163*          XLAMDA=(1.2562*RTFS)/(ROFS*(2.8702E+06*TFS)**0.5)                    000444
00403   169*          XKNFS=XLAMDA/RADB                                                    000460
00404   170*          CFG= RTWALL*TFS/(RTFS*TWK)                                           000462
00405   171*          VBAR= AMACH*(CFS/REYF)**0.5                                          000470
00406   172*          TSTAR=0.5*(STAGFS+TWK)                                               000500
00407   173*          RTSTAR=(1.458E-05*TSTAR**1.5)/(TSTAR+110.4)                          000504
00410   174*          CSTAR=RTSTAR*TFS/(RTFS*TSTAR)                                        000515
00411   175*          XKSQ= REYF/(GAMMA*AMACH**2*CSTAR)                                    000522
00412   176*          PRINT 400                                                            000530
00414   177*      400 FORMAT(//'COMPUTED FREESTREAM DATA:'/)                               000534
00415   178*          PRINT 401,VSOUND,AMACH,STAGFS                                        000534
00422   179*      401 FORMAT(7X,'FREESTREAM SPEED OF SOUND (VSOUND) = ',F10.3,' CM/SEC'    000543
00422   180*         1  /11X,'FREESTREAM MACH NUMBER (AMACH) = ',F6.3,/12X,'FREESTREAM S   000543
00422   181*         2TAC TEMP (STAGFS) = ',F9.3,'  DEG KELVIN')                           000543
00423   182*          PRINT 402,RTFS,RTSTAC                                                000543
00427   183*      402 FORMAT(14X,'FREESTREAM VISCOSITY (RTFS) = ',E10.5,'  GM/CM-SEC'      000551
00427   184*         1 /7X,'FREESTREAM STAC VISCOSITY (RTSTAG) = ',E10.5,'  GM/CM-SEC')   000551
00430   185*          PRINT 403                                                            000551
00432   186*      403 FORMAT(/4X,'SIMILARITY PARAMETERS:'/)                                000555
00433   187*          PRINT 404,REYF,REYN,REWALL,XKNFS,VBAR,XKSQ                           000555
00443   188*      404 FORMAT(8X,'FREESTREAM REYNOLDS NUMBER (REYF) = ',F9.2,               000567
00443   189*         1    /6X,'STAGNATION REYNOLDS NUMBER (REYN) = ',F9.2,                000567
00443   190*         2   /12X,'WALL REYNOLDS NUMBER (REWALL) = ',F9.2,                    000567
00443   191*         3   /8X,'FREESTREAM KNUDSEN NUMBER (XKNFS) = ',F9.4,               000567
00443   192*         4   /37X,'VBAR = ',F9.4,                                          000567
00443   193*         5   /25X,'K SQUARED (XKSQ) = ',F9.4,//)                            000567
00443   194*     C                                                                     000567
00443   195*     C    NOTE THE SUBSTITUTION REYN=REYF FOR REMAINDER OF PROGRAM         000567
00444   196*          REYN=REYF                                                        000567
00445   197*          PRINT 180                                                        000571
00445   198*     C                                                                     000571
00445   199*     C    ************************************************              000571
00445   200*     C                                                                     000571
00447   201*          UNIR=1.987                                                       000575
00450   202*          AVG=.0222*10.**23                                                000577
00451   203*          WTN2=28.0                                                        000601
00452   204*          WTO2=32.0                                                        000603
00453   205*          WTN=14.0                                                         000605
00454   206*          WTO=16.0                                                         000607
00455   207*          WTNO=30.0                                                        000611
00456   208*          WTNOI=30.0                                                       000613
00457   209*          WTEL=1./1820.                                                    000614
00460   210*          NDIV=50                                                          000616
00461   211*          DIVN=NDIV                                                        000620
00462   212*          DELTA=1./DIVN                                                    000623
00463   213*          NDIV1=NDIV+1                                                     000626
00464   214*          HALT=25.0                                                        000633
00464   215*     C                                                                     000633
00464   216*     C    ************************************************************  000633
00464   217*     C                                                                     000633
00465   218*          READ 300,(U(I),V(I),T(I),RO(I),P2(I),I=2,NDIV)                   000635
00477   219*          READ 300,(CO2(I),CNOI(I),CNO(I),CN(I),CO(I),I=2,NDIV)            000653
00477   220*     C                                                                     000653
00477   221*     C    ************************************************              000653
00477   222*     C                                                                     000653
00477   223*     C    BOUNDARY CONDITIONS AT FREESTREAM                                000653
```

```
00511   224*          U(NDIV1)=1.                                                    000670
00512   225*          V(NDIV1)=-1.                                                   000672
00513   226*          T(NDIV1)=TFS/STAGFS                                            000673
00514   227*          RO(NDIV1)=1.                                                   000676
00515   228*          RT(NDIV1)=1.0                                                  000677
00516   229*          P2(NDIV1)=0.                                                   000700
00517   230*          CN2(NDIV1)=0.767                                               000701
00520   231*          CO2(NDIV1)=0.233                                               000703
00521   232*          CNO(NDIV1)=0.                                                  000705
00522   233*          CO(NDIV1)=0.                                                   000706
00523   234*          CN(NDIV1)=0.                                                   000707
00524   235*          CNOI(NDIV1)=0.                                                 000710
00525   236*          CEL(NDIV1)=0.                                                  000711
00525   237*     C                                                                   000711
00525   238*     C    ***************************************************            000711
00525   239*     C                                                                   000711
00525   240*     C    CATALYTIC BOUNDARY CONDITIONS                                  000711
00525   241*     C                                                                   000711
00525   242*     C    ***************************************************            000711
00526   243*          IF(XCAT-0.9 .LT. 0.2)GO TO 450                                 000712
00530   244*          CN2(1)=0.767                                                   000717
00531   245*          CO2(1)=0.233                                                   000720
00532   246*          CNO(1)=0.                                                      000721
00533   247*          CN(1)=0.0                                                      000722
00534   248*          CO(1)=0.0                                                      000723
00535   249*          CNOI(1)=CNOI(2)                                                000724
00536   250*          CEL(1)=CNOI(2)*WTEL/WTNOI                                      000726
00537   251*          PEL(1)=A*RO(1)*ROFS*CNOI(1)/WTNOI                              000732
00540   252*          GO TO 451                                                      000740
00540   253*     C    ***************************************************            000740
00540   254*     C                                                                   000740
00540   255*     C    NONCATALYTIC WALL BOUNDARY CONDITIONS (FOR FIRST ITERATION)    000740
00540   256*     C                                                                   000740
00540   257*     C    ***************************************************            000740
00541   253*       450 CN2(2)=1.0-CO2(2)-CNO(2)-CN(2)-CO(2)-CNOI(2)*(1.0*WTEL/WTNOI)  000742
00542   259*          CN2(1)=CN2(2)                                                  000754
00543   260*          CO2(1)=CO2(2)                                                  000755
00544   261*          CNO(1)=CNO(2)                                                  000757
00545   262*          CN(1)=CN(2)                                                    000761
00546   263*          CO(1)=CO(2)                                                    000763
00547   264*          CNOI(1)=CNOI(2)                                                000765
00550   265*          CEL(1)=CNOI(2)*WTEL/WTNOI                                      000767
00551   266*          PEL(1)=0.                                                      000773
00551   267*     C                                                                   000773
00551   268*     C    ***************************************************            000773
00551   269*     C                                                                   000773
00551   270*     C    INITIAL GUESS FOR CNOI,CEL AND H                               000773
00552   271*       451 HIN2=0.0                                                     000775
00553   272*          HIO2=0.                                                        000775
00554   273*          HINO=3050.*10.**7                                              000776
00555   274*          HIN=33620.*10.**7                                              001000
00556   275*          HIO=15430.*10.**7                                              001002
00557   276*          HINOI=9000.*10.**7                                             001004
00560   277*          HICL=0.                                                        001006
00561   278*          W1=8.3143*10.**7*STAGFS/UFS**2                                 001007
00562   279*          DO 30 I=1,NDIV1                                                001200
```

```
00565    280*          CN2(I)=1.-CO2(I)-CNO(I)-CN(I)-CO(I)-CNOI(I)*(1.+WTEL/WTNOI)                001216
00566    281*          CEL(I)=CNOI(I)*WTEL/WTNOI                                                  001226
00567    282*          W31=T(I)*STAGFS                                                            001232
00570    283*          VN2=3390./W31                                                              001235
00571    284*          VO2=2270./W31                                                              001240
00572    285*          VNO=2740./W31                                                              001243
00573    286*          VNOI=2740./W31                                                             001246
00574    287*          IF(VN2 .GT. 80.0)GO TO 455                                                 001247
00576    288*          VIB=(CN2(I)/28.)*VN2/(EXP(VN2)-1.)+(CO2(I)/32.)*VO2/(EXP(VO2)-1.)         001252
00576    289*         1+(CNO(I)/30.)*VNO/(EXP(VNO)-1.)+(CNOI(I)/30.)*VNOI/(EXP(VNOI)-1.)         001252
00577    290*          GO TO 456                                                                  001317
00600    291*      455 VIB=0.0                                                                    001321
00601    292*      456 CONTINUE                                                                   001322
00602    293*          H(I)=3.5*(CN2(I)/28.+CO2(I)/32.+CNO(I)/30.+CNOI(I)/30.)+VIB                001322
00602    294*         1+2.5*(CN(I)/14.+CO(I)/16.+CNOI(I)/30.)                                     001322
00603    295*   30     H(I)=W1*T(I)*H(I)+(CNO(I)*HINO+CN(I)*HIN+CO(I)*HIO+CNOI(I)*HINOI)          001347
00603    296*         1/W1**2                                                                     001347
00603    297*   C                                                                                001347
00603    298*   C     ***********************************************************                001347
00603    299*   C                                                                                001347
00605    300*          DO 500 K=1,2000                                                            001374
00610    301*          Q=EFFR*DELTA                                                               001377
00610    302*   C      TO FIND P AND MUE AT ALL POINTS                                           001377
00611    303*          DO 50 I=1,NDIV1                                                            001406
00614    304*          TABS(I)=T(I)*STAGFS                                                        001406
00615    305*          IF(I .EQ. 1) GO TO 31                                                      001411
00617    306*          P(I)=RO(I)*T(I)*W1*(CN2(I)/WTN2+CO2(I)/WTO2+CNO(I)/WTNO+CN(I)/WTN          001414
00617    307*         1+CO(I)/WTO+2.*CNOI(I)/WTNOI)                                               001414
00620    308*      31 XMUSU(I) = 1.458E-05*TABS(I)**1.5/(TABS(I) + 110.4)                         001444
00621    309*          IF(XVIS-0.9 .LT. 0.2)GO TO 33                                              001457
00623    310*          IF(TABS(I) .GE. 2000.0) GO TO 32                                           001461
00625    311*      33 XMURAT(I)=1.0                                                               001466
00626    312*          GO TO 37                                                                   001467
00627    313*      32 TABS=TABS(I)                                                                001471
00630    314*          CALL INTERP(1,4,1,37,TEMP,TABS)                                            001472
00631    315*          CALL INTERP(2,4,1,37,TAB1,SN2N)                                            001502
00632    316*          CALL INTERP(2,4,1,37,TAB2,SNN)                                             001512
00633    317*          CALL INTERP(2,4,1,37,TAB3,SNE)                                             001522
00634    318*          CALL INTERP(2,4,1,37,TAB4,SEE)                                             001532
00635    319*          XLMN2=1.03329*CN2(I)+.87542*CO2(I)+2.5310*CN(I)*SN2N                       001542
00635    320*         1 +2.12036*CO(I)*SN2N+.94819*CNO(I)+.94819*CNOI(I)                          001542
00636    321*          XLMO2=1.0696*CN2(I)+.90413*CO2(I)+2.6488*CN(I)*SN2N                        001566
00636    322*         1 +2.2146*CO(I)*SN2N+.9803*CNO(I)+.9803*CNOI(I)                             001566
00637    323*          XLMN=.8949*CN2(I)*SN2N+.7665*CO2(I)*SN2N+2.0666*CN(I)*SNN                  001612
00637    324*         1 +1.7508*CO(I)*SNN+.8259*CNO(I)*SN2N+.8259*CNOI(I)*SN2N                    001612
00640    325*          XLMO=.9159*CN2(I)*SN2N+.783D*CO2(I)*SN2N+2.1391*CN(I)*SNN                  001642
00640    326*         1 +1.8083*CO(I)*SNN+.8444*CNO(I)*SN2N+.8444*CNOI(I)*SN2N                    001642
00641    327*          XLMNO=1.0516*CN2(I)+.8899*CO2(I)+2.5906*CN(I)*SN2N                         001672
00641    328*         1 +2.1680*CO(I)*SN2N+.9644*CNO(I)+.9644*CNOI(I)                             001672
00642    329*          XLMNOI=1.0516*CN2(I)+.8759*CO2(I)+3.2475*CN(I)*SN2N                        001716
00642    330*         1 +2.1680*CO(I)*SN2N+.9644*CNO(I)+.9644*CNOI(I)                             001716
00643    331*          XLMEL=.7307*CN2(I)*SNN+.6393*CO2(I)*SNN+1.4613*CN(I)*SNE                   001731
00643    332*         1 +.2786*CO(I)*SNE+.6819*CNO(I)*SNN+.6819*CNOI(I)*SEE                       001731
00643    333*         2 +52656.24*CEL(I)*SEE                                                      001731
00644    334*          XMURAT(I)=1.0165*CN2(I)/XLMN2+.9509*CO2(I)/XLMO2                           001765
00644    335*         1 +1.4376*CN(I)/XLMN+1.8083*CO(I)/XLMO+.9820*CNO(I)/XLMNO                   001765
```

```
00644   335*          2    +0.3820*CNOI(I)/XLMNOI + 229.469*CEL(I)/XLMEL                    001765
00645   337*        37 XMU(I) = XMURAT(I)*XMUSU(I)                                          002022
00646   338*        50 RT(I) = XMU(I)/RTFS                                                  002024
00646   339*     C     TO FIND PRESSURE ON THE SURFACE USING MOMENTUM EQUATION             002024
00650   340*           U1C=(4.*U(2)-U(3)-3.*U(1))/DELTA/2.                                 002030
00651   341*           V1C=(4.*V(2)-V(3)-3.*V(1))/DELTA/2.                                 002041
00652   342*           RT1C=(4.*RT(2)-RT(3)-3.*RT(1))/DELTA/2.                             002051
00653   343*           V2C=-V(4)+4.*V(3)-5.*V(2)+2.*V(1)                                   002062
00654   344*           DEL4V=V(5)-4.*V(4)+6.*V(3)-4.*V(2)+V(1)                             002074
00655   345*           V2C=V2C+11./12.*DEL4V                                               002105
00656   346*           V2C=V2C/DELTA**2                                                    002110
00656   347*     C     SPHERE/CYLINDER OPTION FOLLOWS                                      002110
00657   348*           IF(XSOD-0.9 .GT. 0.2) GO TO 51                                      002112
00657   349*     C     SPHERE                                                              002112
00661   350*           P1C=V2C*RT(1)/EFFR+V1C*(2.*RT(1)+RT1C/EFFR)+U1C*RT(1)/2.-U(1)*(     002114
00661   351*          1RT1C+3.5*RT(1)*EFFR)                                                002114
00662   352*           GO TO 52                                                            002137
00662   353*     C     CYLINDER                                                            002137
00663   354*        51 P1C=V2C*RT(1)/EFFR+V1C*(RT(1)+RT1C/EFFR)+U1C*RT(1)/4.0-U(1)*        002141
00663   355*          1 (RT1C/2.0+7.0/4.0*RT(1)*EFFR)                                      002141
00664   356*        52 P1C=P1C*4.0/3.0/REYN                                                002166
00665   357*           P(1)=P(2)-DELTA*P1C                                                 002172
00666   358*           R0(1)=P(1)/W1/T(1)/(CN2(1)/WTN2+CO2(1)/WTO2+CNO(1)/WTNO+CN(1)/WTN   002175
00666   359*          1+CO(1)/WTO+2.*CNOI(1)/WTNOI)                                        002175
00667   360*           DO 60 N=2,NDIV                                                      002252
00672   361*           EN=N                                                                002267
00673   362*     60    X(N)=1.+(EN-1.)*Q                                                   002272
00673   363*     C                                                                         002272
00673   364*     C     SLIP CONDITIONS                                                     002272
00673   365*     C                                                                         002272
00675   366*           AC=1.0                                                              002301
00676   367*           W(1)=WTN2                                                           002303
00677   368*           W(2)=WTO2                                                           002305
00700   369*           W(3)=WTN                                                            002307
00701   370*           W(4)=WTO                                                            002311
00702   371*           W(5)=WTNO                                                           002313
00703   372*           W(6)=WTNOI                                                          002315
00704   373*           W(7)=WTEL                                                           002317
00705   374*           C1(1)=CN2(1)                                                        002321
00706   375*           C1(2)=CO2(1)                                                        002323
00707   376*           C1(3)=CN(1)                                                         002325
00710   377*           C1(4)=CO(1)                                                         002327
00711   378*           C1(5)=CNO(1)                                                        002331
00712   379*           C1(6)=CNOI(1)                                                       002333
00713   380*           C1(7)=CEL(1)                                                        002335
00714   381*           C2(1)=CN2(2)                                                        002337
00715   382*           C2(2)=CO2(2)                                                        002341
00716   383*           C2(3)=CN(2)                                                         002343
00717   384*           C2(4)=CO(2)                                                         002345
00720   385*           C2(5)=CNO(2)                                                        002347
00721   386*           C2(6)=CNOI(2)                                                       002351
00722   387*           C2(7)=CEL(2)                                                        002353
00723   388*           C3(1)=CN2(3)                                                        002355
00724   389*           C3(2)=CO2(3)                                                        002357
00725   390*           C3(3)=CN(3)                                                         002361
00726   391*           C3(4)=CO(3)                                                         002363
```

```
00727   392*          C3(5)=CNO(3)                                                    002365
00730   393*          C3(6)=CNOI(3)                                                   002367
00731   394*          C3(7)=CEL(3)                                                    002371
00732   395*          TW=TWK/STAGFS                                                   002373
00733   396*          SUM1=0.0                                                        002375
00734   397*          DO 61 J=1,7                                                     002406
00737   398*       61 SUM1=SUM1+C1(J)/W(J)                                            002406
00741   399*          DO 62 J=1,7                                                     002415
00744   400*       62 PP1(J)=(C1(J)/W(J))*P(1)/SUM1                                   002415
00746   401*          SUM2=0.0                                                        002422
00747   402*          DO 63 J=1,7                                                     002426
00752   403*       63 SUM2=SUM2+(C2(J)-C1(J))/Q                                       002426
00754   404*          SUM3=1.                                                         002433
00755   405*          SUM4=0.0                                                        002435
00756   406*          DO 65 J=1,7                                                     002441
00761   407*       65 SUM4=SUM4+(TW*RO(1)*C1(J)/(W(J)*SUM1)**1.5)*(1.+RT(1)/3./PP1(J)/   002442
00761   408*         1REYN*(U(1)-4.*V(2)/Q+V(3)/Q)+((3.1416*GAMMA*W(J)*SUM1*TFS/2./T(1)/   002442
00761   409*         2STAGFS)**0.5)/C1(J)*(2.-AC)/AC*AMACH/REYN*EL(J)/PR*(W(J)*SUM1)*      002442
00761   410*         3RT(1)/RO(1)*SUM2)                                              002442
00763   411*          SUM5=0.0                                                        002514
00764   412*          DO 66 J=1,7                                                     002520
00767   413*       66 SUM5=SUM5+C1(J)*RO(1)/((W(J)*SUM1)**1.5)*(1.+RT(1)/2./PP1(J)/REYN   002520
00767   414*         1*(U(1)-4.*V(2)/Q+V(3)/3))                                      002520
00771   415*          USLIP=RT(1)/P(1)/REYN/AMACH*((6.2832*STAGFS*T(1)/GAMMA/TFS)**0.5)*    002544
00771   416*         1(2.-AC)/AC/2.*(4.*U(2)-3.*U(1)-U(3))/2./Q                      002544
00772   417*          TSLIP=(2.-AC)/AC*(3.1416**0.5)                                  002600
00773   418*          TSLIP=TSLIP*(AMACH*RT(1)*GAMMA/PR/REYN/2./(GAMMA-1.)*((GAMMA*TFS/     002604
00773   419*         12./T(1)/STAGFS)**.5)*(T(2)-T(1))/Q-2.5*P(1)*RT(1)*             002604
00773   420*         *AMACH**3.                                                      002604
00773   421*         2*((GAMMA*TFS/STAGFS)**1.5)/RO(1)/REYN/((2.*T(1))**0.5)*EL1/PR*    002604
00773   422*         3SUM2)*SUM3                                                     002604
00774   423*          TSLIP=(TSLIP*SUM4)/SUM5                                         002661
00775   424*          USCONT=(USLIP-U(1))/U(1)                                        002664
00776   425*          USCONS=USCONT                                                   002670
00777   426*          USCONT=ABS(USCONT)                                              002671
01000   427*          IF(USCONT.GT.EPSI) U(1)=U(1)+USCONS/USCONT*EPSI*U(1)            002673
01002   428*          IF(USCONT.LE.EPSI) U(1)=USLIP                                   002705
01004   429*          TSCONT=(TSLIP-T(1))/T(1)                                        002713
01005   430*          TSCONS=TSCONT                                                   002717
01006   431*          TSCONT=ABS(TSCONT)                                              002720
01007   432*          IF(TSCONT.GT.EPSI) T(1)=T(1)+TSCONS/TSCONT*EPSI*T(1)            002722
01011   433*          IF(TSCONT.LE.EPSI) T(1)=TSLIP                                   002734
01013   434*          RT(1)=(1.458E-05*(T(1)*STAGFS)**1.5)/((T(1)*STAGFS+110.4)*RTFS)   002742
01013   435*    C     CORRECTION TO V PROFILE                                         002742
01014   436*          DO 70 N=2,NDIV                                                  002762
01017   437*          V2=V(N+1)-2.*V(N)+V(N-1)                                        002764
01020   438*          P1=P(N+1)-P(N-1)                                                002771
01021   439*          V1=V(N+1)-V(N-1)                                                002774
01022   440*          RT1=RT(N+1)-RT(N-1)                                             002777
01023   441*          U1=U(N+1)-U(N-1)                                                003002
01023   442*    C     SPHERE/CYLINDER OPTION FOLLOWS                                  003002
01024   443*          IF(XBOD-0.9 .GT. 0.2) GO TO 67                                  003005
01024   444*    C     SPHERE                                                          003005
01026   445*          CAPV=-RT(N)*V2/Q**2+0.375*REYN/Q*(P1+RO(N)*V(N)*V1)-V1/Q        003007
01026   446*         1*(RT(N)/X(N)+RT1/4./Q)-RT(N)*U1/4./Q/X(N)                       003007
01027   447*          CAPV=CAPV+(U(N)+V(N))/X(N)*(3.5*RT(N)/X(N)+RT1/2./Q)            003035
```

```
01030   448*          DERV=2.*RT(N)/Q**2+0.375*REYN/Q*RO(N)*V1+3.5*RT(N)/X(N)**2                  003052
01030   449*         1+RT1/2./Q/X(N)                                                              003052
01031   450*          GO TO 68                                                                    003072
01031   451*    C     CYLINDER                                                                    003072
01032   452*       67 CAPV=-RT(N)*V2/Q**2+0.375*REYN/Q*(P1+RO(N)*V(N)*V1)-V1/Q/2.0                003074
01032   453*         1 +(RT(N)/X(N)+RT1/2.0/Q)-RT(N)*U1/8.0/Q/X(N)                               003074
01033   454*          CAPV=CAPV+(U(N)+V(N))/X(N)*(7.0*RT(N)/X(N)+RT1/Q)/4.0                       003126
01034   455*          DERV=2.0*RT(N)/Q**2+0.375*REYN/Q*RO(N)*V1+(7.0*RT(N)/X(N)**2                003145
01034   455*         1 +RT1/Q/X(N))/4.0                                                           003145
01034   457*    C     TO FIND CCCV                                                                003145
01035   458*       68 SIGV=ABS(EPSI*DERV*V(N)/CAPV)                                               003167
01036   459*          IF(SIGV.LT.1.)CCCV=SIGV                                                     003174
01040   460*          IF(SIGV.GE.1.)CCCV=1.                                                       003202
01042   461*       70 V(N)=V(N)-CCCV*CAPV/DERV                                                    003210
01044   462*          V(2)=(V(3)-4.*DELTA*U(1)*EFFR)/4.                                           003216
01044   463*    C     TO FIND CORRECTION TO U PROFILE                                             003216
01045   464*          DO 80 N=2,NDIV                                                              003224
01050   465*          U2=U(N+1)-2.*U(N)+U(N-1)                                                    003245
01051   466*          U1=U(N+1)-U(N-1)                                                            003252
01052   467*          RT1=RT(N+1)-RT(N-1)                                                         003255
01053   468*          V1=V(N+1)-V(N-1)                                                            003260
01054   469*          CAPU=-RT(N)*U2/Q**2+REYN*RO(N)*V(N)*U1/2./Q                                 003263
01054   470*    C     SPHERE/CYLINDER OPTION FOLLOWS                                              003263
01055   471*          IF(XBOD-0.9 .GT. 0.2) GO TO 71                                              003274
01055   472*    C     SPHERE                                                                      003274
01057   473*          CAPU=CAPU+(U(N)+V(N))/X(N)*(8.*RT(N)/3./X(N)+RT1/2./Q+REYN*RO(N)            003276
01057   474*         1*U(N))                                                                      003276
01060   475*          DERU=2.*RT(N)/Q**2+8.*RT(N)/3./X(N)**2+RT1/2./Q/X(N)+REYN*RO(N)             003314
01060   476*         1*(2.*U(N)+V(N))/X(N)                                                        003314
01061   477*          GO TO 73                                                                    003335
01061   478*    C     CYLINDER                                                                    003335
01062   479*       71 CAPU=CAPU+(U(N)+V(N))/X(N)*(7.*RT(N)/3./X(N)+RT1/2./Q+REYN*RO(N)          003337
01062   480*         1   *U(N))                                                                   003337
01063   481*          DERU=2.*RT(N)/Q**2+7.0*RT(N)/3./X(N)**2+RT1/2./Q/X(N)+REYN*RO(N)           003362
01063   482*         1    *(2.0*U(N)+V(N))/X(N)                                                  003362
01064   483*       73 CAPU=CAPU+RT(N)*V1/6.0/Q/X(N)-U1/Q*(RT(N)/X(N)+RT1/4.0/Q)                 003404
01064   484*         1    +2.0*P2(N)*REYN/X(N)                                                   003404
01064   485*    C     TO FIND CCCU                                                                003404
01065   486*          SIGU=ABS(EPSI*DERU*U(N)/CAPU)                                               003431
01066   487*          IF(SIGU.LT.1.)CCCU=SIGU                                                     003437
01070   488*          IF(SIGU.GE.1.)CCCU=1.                                                       003445
01072   489*       80 U(N)=U(N)-CCCU*CAPU/DERU                                                    003453
01072   490*    C     SPECIES PRODUCTION RATE                                                     003453
01074   491*          DO 90 N=1,NDIV1                                                             003461
01077   492*          W5=T(N)*STAGFS                                                              003474
01100   493*          W6=UNIR*W5                                                                  003476
01101   494*          W7=118000./W6                                                               003500
01102   495*          W8=W7**1.5                                                                  003503
01103   496*          W9=224900./W6                                                               003510
01104   497*          W10=150000./W6                                                              003513
01105   498*          W11=W10**2                                                                  003516
01106   499*          W12=39100./W6                                                               003520
01107   500*          W13=7080./W6                                                                003523
01110   501*          W14=75500./W6                                                               003526
01111   502*          W15=128500./W6                                                              003531
01112   503*          W16=85520./W6                                                               003534
```

```
C1113   504*          W17=6329C./W6                                                  003537
C1114   505*          W18=W5**0.5                                                    003542
C1115   506*          W19=W5**2.5                                                    003547
C1116   507*          W2C=5CC./W6                                                    003554
C1117   503*          W21C=-1C./W6                                                   003557
C1120   509*          IF(W7.GT.8C.)GO TO 81                                          003562
C1122   510*          FK1=2.5*1C.**11*W18*W3/EXP(W7)                                 003566
C1123   511*          GO TO 82                                                       003576
C1124   512*    81    FK1=C.                                                         003600
C1125   513*    82    RK1=2.CB*1C.**8*W5*W8                                          003601
C1126   514*          IF(W9.GT.8C.)GO TO 83                                          003604
C1130   515*          FK2=1.7*1C.**12*W18*W9/EXP(W9)                                 003610
C1131   516*          GO TO 84                                                       003620
C1132   517*    83    FK2=C.                                                         003622
C1133   518*    84    RK2=9.444*1C.**1C*W18*W9                                       003627
C1134   519*          IF(W1C.GT.8C.)GO TO 85                                         003626
C1136   520*          FK3=7.*1C.**1C*W18*W11/EXP(W10)                                003632
C1137   521*          CO TO 86                                                       003642
C1140   522*    85    FK3=C.                                                         003644
C1141   523*    86    RK3=1.75*1C.**1C*W18*W11                                       003645
C1142   524*          IF(W12.GT.8C.)GO TO 87                                         003650
C1144   525*          FK4=3.2*1C.**9*W5/EXP(W12)                                     003654
C1145   526*          GO TO 88                                                       003663
C1146   527*    87    FK4=C.                                                         003665
C1147   528*          IF(W13.GT.8C) GO TO 881                                        003665
C1151   529*    88    RK4=13.33*1C.**9*W5/EXP(W13)                                   003672
C1152   530*          GO TO 882                                                      003700
C1153   531*   881 RK4=C.C                                                          003702
C1154   532*   882 IF(W14.GT.8C.)GO TO 91                                          003703
C1156   533*          FK5=7.*1C.**13/EXP(W14)                                        003706
C1157   534*          GO TO 92                                                       003714
C1160   535*    91    FK5=C.                                                         003716
C1161   536*          IF(W2C.GT.8C.) GO TO 921                                       003716
C1163   537*    92    RK5=1.55*1C.**13/EXP(W2C)                                      003723
C1164   538*          GO TO 922                                                      003730
C1165   539*   921 RK5=C.C                                                          003732
C1166   540*   922 IF(W15.GT.8C.)GO TO 93                                          003733
C1170   541*          FK6=9.1*1C.**24/W19/EXP(W15)                                   003736
C1171   542*          GO TO 94                                                       003745
C1172   543*    93    FK6=C.                                                         003747
C1173   544*    94    IF(W16.GT.8C.)GO TO 95                                         003750
C1175   545*          RK6=4.79*1C.**23/W19/EXP(W16)                                  003753
C1176   546*          GO TO 96                                                       003762
C1177   547*    95    RK6=C.                                                         003764
C1200   548*    96    IF(W17.GT.8C.)GO TO 97                                         003765
C1202   549*          FK7=6.4*1C.**9*W18/EXP(W17)                                    003770
C1203   550*          GO TO 98                                                       003777
C1204   551*    97    FK7=C.                                                         004001
C1205   552*    98    RK7=1.79*1C.**19/W5/EXP(W21C).                                 004002
C1206   553*          W2=RO(N)*ROFS                                                  004010
C1207   554*          W3=W2**2                                                       004013
C1210   555*          R1=W3*(CN(N)/WTN+CNO(N)/WTNO+2.*CN2(N)/WTN2+9.*C02(N)/WT02+     004015
C1210   556*         125.*CO(N)/WTO)                                                 004015
C1211   557*          R1=R1*(FK1*C02(N)/WT02-W2*RK1*C0(N)**2/WTO**2)                 004041
C1212   558*          R2=W3*(CO(N)/WTO+C02(N)/WT02+CNO(N)/WTNO+2.47*CN2(N)/WTN2+2.15* 004055
C1212   559*         110.**5*CN(N)/W5/WTN)                                           004055
```

```
01213   560*          R2=R2*(FK2*CN2(N)/WTN2-W2*RK2*CN(N)**2/WTN**2)                    004077
01214   561*          R3=W3*(CO2(N)/WTO2+CN2(N)/WTN2+2D.*(CNO(N)/WTNO+CO(N)/WTO+        004113
01214   562*         1CN(N)/WTN))                                                       004113
01215   563*          R3=R3*(FK3*CNO(N)/WTNO-W2*RK3*CN(N)*CO(N)/WTN/WTO)                004127
01216   564*          R4=W3*(FK4*CNO(N)*CO(N)/WTNO/WTO-RK4*CO2(N)*CN(N)/WTO2/WTN)       004143
01217   565*          R5=W3*(FK5*CN2(N)*CO(N)/WTN2/WTO-RK5*CNO(N)*CN(N)/WTNO/WTN)       004160
01220   566*          R6=W3*(FK6*CN2(N)*CO2(N)/WTO2/WTN2-RK6*(CNO(N)/WTNO)**2)          004175
01221   567*          R7=W3*(FK7*CN(N)*CO(N)/WTN/WTO-RK7*(CNOI(N)/WTNOI)**2)            004211
01222   568*          W4=ROFS*UFS/RADB                                                  004225
01223   569*          WO2(N)=WTO2*(-R1+R4-R6)/W4                                        004227
01224   570*          WN2(N)=-WTN2*(R2+R5+R6)/W4                                        004234
01225   571*          WNO(N)=WTNO*(-R3-R4+R5+2.*R6)/W4                                  004241
01226   572*          WN(N)=WTN*(2.*R2+R3+R4+R5-R7)/W4                                  004251
01227   573*          WO(N)=WTO*(2.*R1+R3-R4-R5-R7)/W4                                  004262
01230   574*          WNOI(N)=WTNOI*R7/W4                                               004273
01231   575*          WEL(N)=WTEL*R7/W4                                                 004277
01232   576*    30    CONTINUE                                                          004310
01232   577*    C     CORRECTION TO CONCENTRATION PROFILES                              004310
01234   578*          DO 100 N=2,NDIV                                                   004310
01237   579*          RT1=RT(N+1)-RT(N-1)                                               004315
01240   580*          W21=-RO(N)*V(N)/2./Q                                              004320
01241   581*          W22=(2.*RT(N)/X(N)+RT1/2./Q)/2./Q/REYN/SC1                        004325
01242   582*          W23=RT(N)/Q**2/REYN/SC1                                           004337
01243   583*          DERC=-2.*RT(N)/REYN/SC1/Q**2                                      004344
01243   584*    C     OXYGEN MOLECULE                                                   004344
01244   585*          CO21=CO2(N+1)-CO2(N-1)                                            004351
01245   586*          CO23=CO2(N+1)-2.*CO2(N)+CO2(N-1)                                  004354
01246   587*          CAPO2=WO2(N)+(W21+W22)*CO21+W23*CO23                              004361
01247   588*          SIGO2=ABS(EPSI*DERC*CO2(N)/CAPO2)                                 004367
01250   589*          IF(SIGO2.LT.1.)CCCO2=SIGO2                                        004377
01252   590*          IF(SIGO2.GE.1.)CCCO2=1.                                           004405
01254   591*          CO2(N)=CO2(N)-CCCO2*CAPO2/DERC                                    004413
01254   592*    C     NO ION                                                            004413
01255   593*          W221=(2.*RT(N)/X(N)+RT1/2./Q)/2./Q/REYN/SC2                       004420
01256   594*          W231=RT(N)/Q**2/REYN/SC2                                          004430
01257   595*          DERC1=-2.*RT(N)/REYN/SC2/Q**2                                     004435
01260   596*          CNOI1=CNOI(N+1)-CNOI(N-1)                                         004442
01261   597*          CNOI3=CNOI(N+1)-2.*CNOI(N)+CNOI(N-1)                              004445
01262   598*          CAPNOI=WNOI(N)+(W21+W221)*CNOI1+W231*CNOI3                        004452
01263   599*          SIGNOI=ABS(EPSI*DERC1*CNOI(N)/CAPNOI)                             004460
01264   600*          IF(SIGNOI.LT.1.)CCCNOI=SIGNOI                                     004465
01266   601*          IF(SIGNOI.GE.1.)CCCNOI=1.                                         004473
01270   602*          CNOI(N)=CNOI(N)-CCCNOI*CAPNOI/DERC1                               004501
01270   603*    C     NITROGEN ATOM                                                     004501
01271   604*          CN1=CN(N+1)-CN(N-1)                                               004506
01272   605*          CN3=CN(N+1)-2.*CN(N)+CN(N-1)                                      004511
01273   606*          CAPN=WN(N)+(W21+W22)*CN1+W23*CN3                                  004516
01274   607*          SIGN1=ABS(EPSI*DERC*CN(N)/CAPN)                                   004523
01275   608*          IF(SIGN1.LT.1.)CCCN=SIGN1                                         004530
01277   609*          IF(SIGN1.GE.1.)CCCN=1.                                            004536
01301   610*          CN(N)=CN(N)-CCCN*CAPN/DERC                                        004544
01301   611*    C     OXYGEN ATOM                                                       004544
01302   612*          CO1=CO(N+1)-CO(N-1)                                               004551
01303   613*          CO3=CO(N+1)-2.*CO(N)+CO(N-1)                                      004554
01304   614*          CAPO=WO(N)+(W21+W22)*CO1+W23*CO3                                  004561
01305   615*          SIGO=ABS(EPSI*DERC*CO(N)/CAPO)                                    004566
```

1. Report No.	2. Government Accession No.	3. Recipient's Catalog No.
NASA TP-1227		

4. Title and Subtitle	5. Report Date
A Numerical Solution of the Navier-Stokes Equations for Chemically Nonequilibrium, Merged Stagnation Shock Layers on Spheres and Two-Dimensional Cylinders in Air	May 1978
	6. Performing Organization Code
7. Author(s)	8. Performing Organization Report No.
Kenneth D. Johnston and William L. Hendricks*	M-254
	10. Work Unit No.
9. Performing Organization Name and Address	
George C. Marshall Space Flight Center Marshall Space Flight Center, Alabama 35812	11. Contract or Grant No.
	13. Type of Report and Period Covered
12. Sponsoring Agency Name and Address	Technical Paper
National Aeronautics and Space Administration Washington, D.C. 20546	14. Sponsoring Agency Code

15. Supplementary Notes

Prepared by Systems Dynamics Laboratory, Science and Engineering.
*Lockheed Huntsville Research and Engineering Center

16. Abstract

Results of solving the Navier-Stokes equations for chemically nonequilibrium, merged stagnation shock layers on spheres and two-dimensional cylinders are presented. The effects of wall catalysis and slip are also examined. The thin shock layer assumption is not made, and the thick viscous shock is allowed to develop within the computational domain. The results show good comparison with existing data. Due to the more pronounced merging of shock layer and boundary layer for the sphere, the heating rates for spheres become higher than those for cylinders as the altitude is increased.

17. Key Words (Suggested by Author(s))	18. Distribution Statement
	STAR Category 34

19. Security Classif. (of this report)	20. Security Classif. (of this page)	21. No. of Pages	22. Price
Unclassified	Unclassified	102	$6.25

* For sale by the National Technical Information Service, Springfield, Virginia 22161

NASA-Langley, 1978

3 1 1U,D, 042778 S00903DS
DEPT OF THE AIR FORCE
AF WEAPONS LABORATORY
ATTN: TECHNICAL LIBRARY (SUL)
KIRTLAND AFB NM 87117